Amélioration de la Précision Dynamique des Robots Industriels pour desOpérations de Manipulation Robotique

Amine Rahmouni

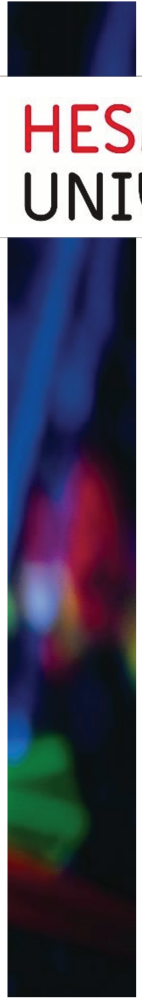

HESAM UNIVERSITÉ

Arts et Métiers Sciences et Technologies

2021-ENSAM-0001

École doctorale n° 432 : Sciences des Métiers de l'ingénieur

Doctorat

T H È S E

pour obtenir le grade de docteur délivré par

l'École Nationale Supérieure d'Arts et Métiers

Spécialité "Automatique"

présentée et soutenue publiquement par

Amine RAHMOUNI

Le 03 MAI 2021

Amélioration de la précision dynamique des robots industriels pour des opérations de manipulation robotique

Improving the dynamic accuracy of industrial robots for robotic manipulation

Directeur de thèse : **Richard BEAREE**

Co-encadrement de la thèse : **Mathieu GROSSARD & Eric LUCET**

Jury

M. Kamal YOUCEF-TOUMI, professeur (HDR), Mechatronics Research Laboratory, MIT, Cambridge, USA	Président
Mme Hélène CHANAL, maître de conférences (HDR), IFMA, Univ. Blaise Pascal, Clermont-Frd, France	Rapportrice
M. Pedro RODRIGUEZ-AYERBE, professeur (HDR), L2S, Centrale Supelec, Paris-Saclay, France	Rapporteur
M. Nazih MECHBAL, professeur (HDR), PIMM/DYSCO, ENSAM, Paris, France	Examinateur
M. Richard BEAREE, professeur (HDR), LISPEN, ENSAM, Lille, France	Examinateur
M. Mathieu GROSSARD, ingénieur-chercheur (HDR), CEA-LIST, Paris-Saclay, France	Examinateur
M. Eric LUCET, ingénieur-chercheur, CEA-LIST, Paris-Saclay, France	Invité
M. Pascal FUGIER, Référent technique, CEA PRTT Haut-de-France, CEA Tech, Lille, France	Invité

T H È S E

Arts et Métiers - Campus de Lille
LISPEN

À mes mères HADDA & MASSOUDA

Remerciements

Ce projet fait l'objet d'un financement de la part du Conseil Régional Hauts-de-France et du Fonds Européen de Développement Régional FEDER. Au titre du ressourcement, ce projet est effectué dans le cadre de la convention partenariale pour la création d'une Plateforme Regionale de Transfert Technologique CEA TECH en région signée par CEA TECH, la Région Hauts-de-France, la Métro-pole Européenne de Lille, la Communauté d'Agglomération de Valenciennes et la Communauté Urbaine de Dunkerque. Cette étude sur «l'amélioration de la précision dynamique des robots industriels pour des opérations de manipulation robotique» est conduite par le CEA TECH PRTT Hauts-de-France. Les travaux de recherche sont réalisés dans les deux laboratoires: LISPEN aux Arts et Métiers Lille & LRI au CEA List Paris-Saclay.

Je tiens à remercier M. **Kamal YOUCEF-TOUMI**, professeur à Massachusetts Institute of Technology (MIT), pour l'honneur qu'il me fait d'avoir présidé le jury de ma soutenance de thèse. Je remercie également Mme **Hélène CHANAL**, maître de conférence à Université Blaise Pascal, et M. **Pedro RODRIGUEZ-AYERBE**, professeur à Centrale Supelec Paris, pour avoir rapporté ma thèse. Je tiens aussi à remercier M. **Nazih MECHBAL**, professeur aux Arts et Métiers Paris, et M. **Pascal FUGIER**, référent technique au CEA Tech, d'avoir pris part à mon jury de thèse.

Je remercie mes encadrants M. **Richard BEAREE**, professeur aux Arts et Métiers Lille, M. **Mathieu GROSSARD**, ingénieur-chercheur au CEA-LIST, et M. **Eric LUCET**, ingénieur-chercheur au CEA-LIST, pour leurs précieux conseils durant ce travail et pour leurs qualités humaines : modestie, bienveillance et moralité qui resteront pour moi un exemple à suivre dans ma vie professionnelle.

Je souhaite également remercier l'ensemble des doctorants des Arts et Métiers Lille, et tous mes amis avec qui j'ai passé trois belles années à Lille. En particulier, je remercie the best qui m'ont aidé dans l'élaboration de cette thèse: **François HÉLÉNON**, **Kristina LAZEBNA**, **Lucie TANTIN**, **Marielle DEBEURRE**, **Michel AULELEY**, **Sara WINTERSOHLE**, **Zelmira ALAYO**. Un grand merci à **Marie COIGNARD** et **Bilyne JOSEPH** pour le gateau de thèse :)

Lamine

Abstract

The modern industry leans on the automation of its factories since human-machine groups are prone to be more efficient than groups wholly comprised of one or the other. Among the latest offering technologies, a new generation of industrial robots that don't need to be walled off from human and they are relied to work side by side in one shared environment. Therefore, largest manufacturers of industrial robots offer optimally designed manipulators which are mechanically flexible. Program the robot what to do is the way for having better improvements on the robotic task and adapt it to any evolution in working conditions.

Research advancements have enabled the robot to handle tasks that till now only human could handle in the factory such as in robotic manipulation context. This later is highly concerned with several industrial process such as assembly operations for loading and unloading parts from an assembly line. When handling flexible load with the robot, the accuracy of previous robotics tasks and sometimes even their feasibility may be significantly limited by undesired motion-induced vibrations and deformations of the manipulated object. These deformations have detrimental effects on the settling time, the accuracy and the integrity of the operational process in a constrained environment. The problem of avoiding the degradation of the flexible loads when they are handled by an industrial robot is addressed in this thesis.

The flexural motion of the robot and the flexible load are the main errors sources in the task positioning and load's shape degradation. The dynamic precision improvement for robotic manipulation tasks may achieved by using control design. On the other hand, the kinematic redundancy is assisted in the control of robots to enhance their performances and maneuverability. However, in the case of the redundant manipulators, we demonstrate that the redundancy resolution can be exploit to compensate for the motion-induced deformations. A feedback control approach based on torque optimization is proposed for accuracy improvement of flexible redundant manipulators in which the self-motion inherent in redundancy feature is exploited to damp out the vibration while maintaining the end-effector posture. In the second part of the present work, the robot's task redundancy is used to handle the undesired deflection of the end-effector and load deformations via a smoothing trajectory approach along with a deformations compensation action which are integrated together in the design of the proposed feedforward control.

Keywords: Industrial Robots, Redundancy Resolution, Vibrations and Deformations Control, Trajectory Shaping, Flexible Loads Manipulation, Flexible Robot Manipulators.

Résumé

L'industrie moderne s'appuie sur l'automatisation de ses usines, car les groupes homme-machine sont plus efficaces que les groupes composés uniquement de l'un ou l'autre. Parmi les dernières technologies proposées, une nouvelle génération de robots industri-els qu'ils travaillent côte à côte dans un environnement commun avec l'homme. C'est pourquoi les plus grands fabricants de robots industriels proposent des manipulateurs conçus de manière optimale et ils sont mécaniquement flexibles. Programmer le robot est le moyen possible d'améliorer la tâche robotique et de l'adapter à toute évolution des conditions de travail.

Les progrès de la recherche ont permis au robot d'accomplir des tâches que seul l'homme pouvait jusqu'à présent accomplir dans l'usine. Par exemple dans un contexte de manipulation robotique. Ce dernier est très concerné par plusieurs processus industriels tels que les opérations d'assemblage : le chargement et le déchargement de pièces d'une line d'assemblage. Lorsque le robot manipule une charge flexible, la précision des tâches robotiques précédentes et parfois même leur faisabilité peuvent être considérablement limitées par des vibrations et des déformations induites par le mouvement de l'objet manipulé. Ces déformations ont des effets néfastes sur le temps d'excution, la précision et l'intégrité du processus opérationnel dans un environnement contraint. Le problème d'éviter la déformation des charges flexibles lorsqu'elles sont manipulées par un robot industriel est abordé dans cette thèse.

La structure flexible du robot et la charge sont les principales sources d'erreurs dans le positionnement et déformation de la charge. L'amélioration de la précision dynamique pour les tâches de manipulation robotique peut être obtenue en utilisant des techniques de contrôle. Cependant, dans le cas des manipulateurs redondants, nous démontrons que la résolution de la redondance peut être exploitée pour compenser les déformations induites par le mouvement de robot. Une approche de contrôle par rétroaction basée sur l'optimisation des couples est proposée pour améliorer la précision des manipulateurs redondants et flexibles, dans laquelle les mouvements internes sont exploités pour amortir les vibrations tout en maintenant la posture de l'effecteur. Dans la deuxième partie de ce travail, la redondance est utilisée pour traiter la déviation indésirable de l'effecteur et les déformations de la charge en utilisant une approche de lissage de la trajectoire ainsi qu'une action de compensation des déformations qui sont intégrées ensemble dans la conception de la commande proposée.
Mots-clés: Robots Industriels, Résolution de Redondance, Contrôle des Vibrations et des Déformations,Planification des Trajectoires, Manipulation de Charges Flexibles, Robots Manipulateurs Flexibles.

Contents

List of Figures

List of Tables

Chapter

1 THESIS CONTEXT

- This project is funded by the Hauts-de-France Regional Council and the European Regional Development Fund. As part of the resourcing, this project is carried out within the framework of the partnership agreement for the creation of a Regional Technology Transfer Platform CEA* TECH signed by CEA TECH, the Hauts-de-France Region, the European Metropolis of Lille, the Valenciennes Agglomeration Community and the Urban Community of Dunkerque. This study on "improving the dynamic accuracy of industrial robots for robotic manipulation" is conducted by CEA TECH PRTT Hauts-de-France. The research works are carried out in the two laboratories: LISPEN at Arts et Métiers Lille & LRI at CEA List Paris-Saclay.

- Ce projet fait l'objet d'un financement de la part du Conseil Régional Hauts-de-France et du Fonds européen de développement régional FEDER. Au titre du ressourcement, ce projet est effectué dans le cadre de la convention partenariale pour la création d'une Plateforme Regionale de Transfert Technologique CEA* TECH en région signée par CEA TECH, la Région Hauts-de-France, la Métropole Européenne de Lille, la Communauté d'Agglomération de Valenciennes et la Communauté Urbaine de Dunkerque. Cette étude sur «l'amélioration de la précision dynamique des robots industriels pour des opérations de manipulation robotique» est conduite par le CEA TECH PRTT Hauts-de-France. Les travaux de recherches sont réalisés dans les deux laboratoires: LISPEN aux Arts et Métiers Lille & LRI au CEA List Paris-Saclay.
  **LE COMMISSARIAT A L'ENERGIE ATOMIQUE ET AUX ENERGIES ALTERNATIVES : établissement public de recherche à caractère scientifique, technique et industriel.*

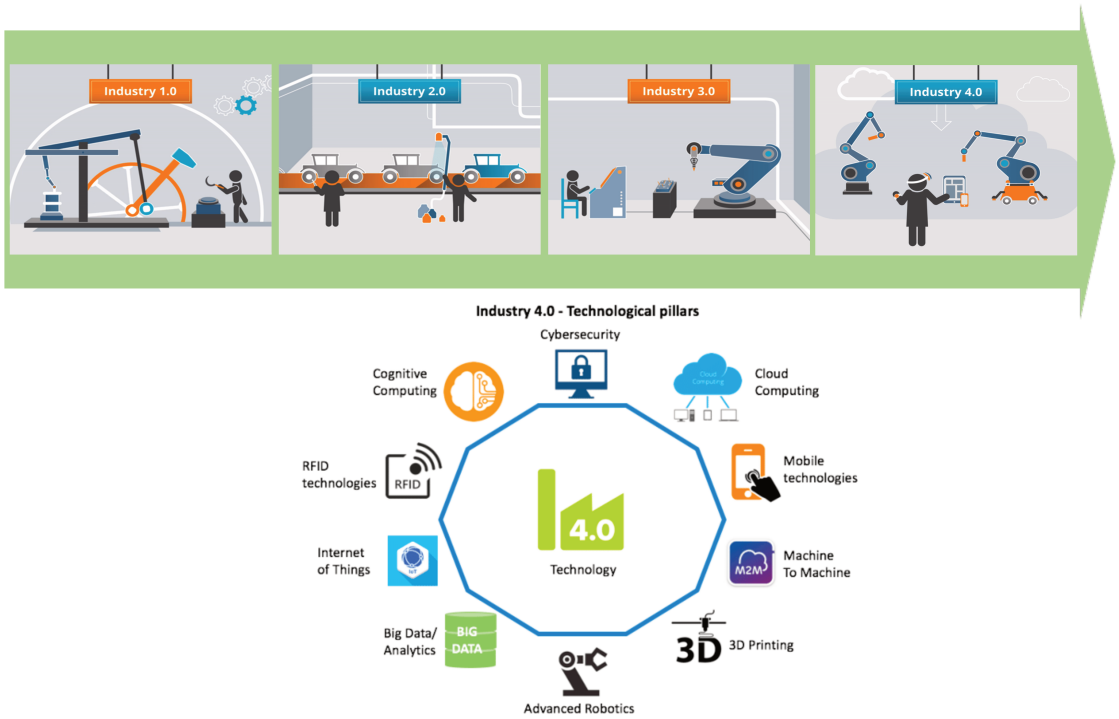

Figure 1.1: Industry evolution: Different technologies for industry 4.0.

1.1 ROBOTIC MANIPULATION SOLUTIONS

Since its introduction to the technology era, the robot invades quickly every active field to respond to human life needs. Such as the manufacturing industry, space, health, and so on. The industrial processes along with their applications requirements, such as time optimal production and reliability, are in need of dynamic systems including robot manipulators with a high level of dexterity to operate in sophisticated environments.

The human-robot interaction is the main challenge for this new industrial era, i.e. the industry 4.0 [1], see figure (1.1). The current development of collaborative robot manipulators which are dedicated to the interaction with humans reveals envisaged operational scenarios for which humans and robots share the same work space. Either in the industrial context for production or in the areas of personal assistance. Many norms and charts have been introduced since, to guarantee the safety of the workers and the quality norms [2].

The robotic manipulation is one of the widely used processes in manufacturing industry, in order to improve the production return on investments. Thus, solutions for mobile robot manipulators (i.e. one or two manipulator arms on a mobile base) find a particular interest. With many different types of robots in the market, the best choice can be based on task specifications along with the cost. For example, the payload capacity, manipulating factor and the applicable force, these factors are presented in figure

				
ROBOT	ABB Roberta 3	FANUC CR-35 iA	UNIVERSAL ROBOT UR10	KUKA LBR IIWA 14
DOFs	6	6	6	7
Payload	12 kg	35 kg	10 kg	14 kg
Reach	1200 mm	1813 mm	1300 mm	820 mm
Repeatability	± 0.1 mm	± 0.04 mm	± 0.1 mm	± 0.15 mm
Weight	30.5 kg	990 kg	28.9 kg	30 kg
Joints Velocity	110 °/s	750 mm/s	1000 mm/s	70-180 °/s

Figure 1.2: Technical specifications for most used industrial robot manipulators.

(1.2) for most used industrial manipulators. One may note that after choosing the robot based on the process characteristics, some specifications should be considered this time to enhance the robot performance, where accuracy is one of the major concerns.

1.2 INACCURACY IN ROBOTIC MANIPULATION

The inaccuracy sources are multiple, but they can be differentiated into two categories, errors due to mechanical design and errors due to the used control. The deformation in a mobile manipulator could be treated separately, by assuming that the manipulator is rigidly attached to a mobile robot, which is the generally considered case in practice. In the following, we present the different potential factors which may affect the robotic task accuracy: flexible structure of robot manipulator, mobile platform and flexible load.

1.2.1 Flexible manipulators

The robotic vision of the future paid more attention to flexible manipulators, which have lightweight structure, low cost, high load to mass ratio and low energy consumption as well as the capability of performing a given task with high speed. In addition to the flexible compliance in human-robot interaction. All of these remarkable advantages of the flexible manipulators compared to those of the conventional rigid robot manipulators

Joints Design

Joints	Torque	Stiffness
1 & 2	200 N	20000 N/m
3 & 4	85 N	12000 N/m
5 & 6 & 7	35 N	6000 N/m

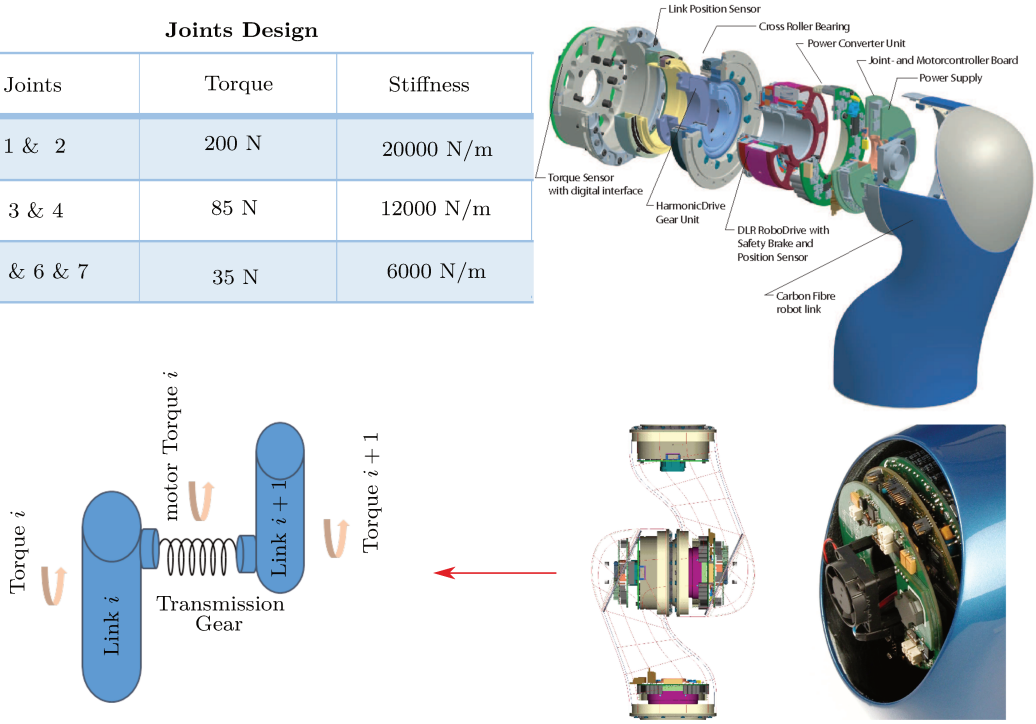

Figure 1.3: Mechanical joint design of DLR lightweight manipulator.

make them the appropriate generation of robot manipulators for the advanced industry.

The robot manipulator consists of series of links connected by joints. However, the presence of the flexible substructures induces an oscillatory behavior at the manipulator end-effector, hence the accuracy deterioration and performance degradation. This error depends on both the robot compliance and the externally applied force at its tool center point (TCP) and/or along with its structure. The deformation is time-varying and mainly differs in the work-space due to the changes in the manipulator configurations. In this case, the TCP motion is influenced by both rigid and flexural motions which are dynamically coupled.

1.2.1.a Flexible joints robot

In the case of flexible joints manipulator, the robot is characterized by rigid links and flexible joints. The elasticity of the motor-to-joint transmission may be represented as a set of simple spring-damper pair systems, where the spring is modeled as torsional for rotational joint and linear for translation one [3, 4, 5]. The assumption on which relies the linear elasticity is due to the small limited deformations in the joint where the contributions of the nonlinear dynamic are neglected.

The motion transmission/reduction components makes the joint mechanically compliant, see figure (1.3). It is preferably used to comply with physically environment

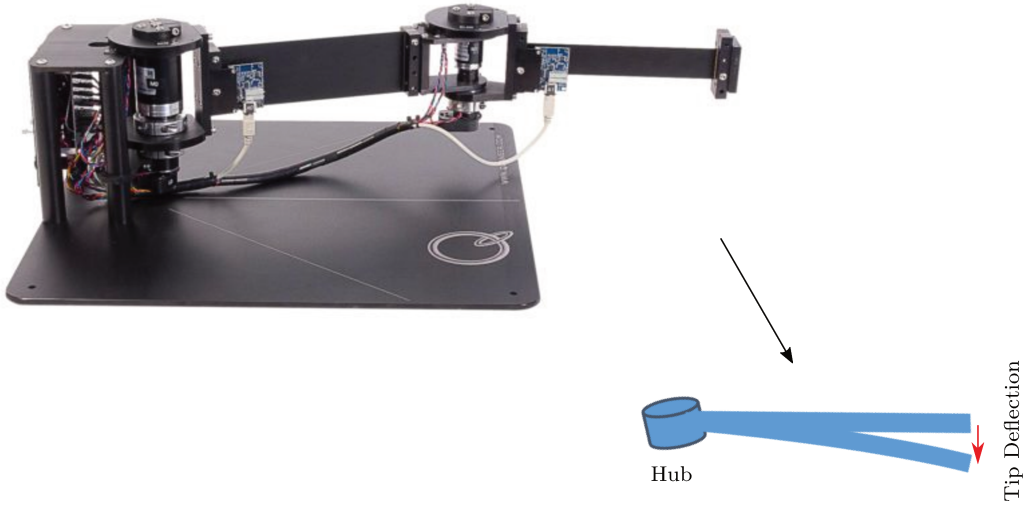

Figure 1.4: QUANSER 2 DOFs flexible link manipulator.

contact for soft interactions. For example, the safe human-robot collaboration context [2]. One may note that the flexible joints are subject to store strain energy due to the energy transformation from kinetic to potential energy between the robot dynamical inertia and the flexible joints. Many robotic tasks require considerably developed joint-torques, which mainly excite the flexible structure in the joint leading to dynamic vibrations at the end-effector.

For each of the flexible joints in the robot, it exists a force compliance between the driven torque of the considered joint and its own oscillatory system. As a result, the vibration could be controlled directly via the joint torques. Notwithstanding, the dynamic system seems highly coupled and nonlinear, a simplified system could be considered by neglecting both the inertial coupling between the links and the motors and the viscous damping to achieve simple control as in [6]. Nevertheless, the nature of the flexible structure holds an infinite number of Degree Of Freedoms (DOFs) which may influence the control efficiency [7].

1.2.1.b Flexible links robot

The flexible links are made from resistant lightweight materials, assumed with uniform properties. This particular structure has an enormous impact on energy saving, since less power energy compared to the robot with heavy rigid structure could drive the resulting

lightweight robot, see figure (1.4). The robot operational speed increases as well as the payload-to-mass ratio [8, 9]. Remarkably, the flexible link manipulators attract many applications in diverse fields. For example, robot with flexible long arms are the best candidate in space applications to achieve a long reach in aim to assist astronauts. In the low gravity environment, the robot may help to collect space debris and maintain the space station and insure the supplying process [10, 11]. Overall, the flexible manipulator is mounted on free floating spacecraft to extend its maneuverability [12]. In the medical field, safe operations are guaranteed due to the robot compliance and the reduced inertia.

Although, the robot has intrinsically low stiffness features which may constrain some of its functionalities. The flexibility distribution along each slender flexible link causes generally positioning deterioration at the end-effector since it is too sensitive to the joints motion. In the motion point of view, it may be resumed essentially in the link bending along its length in transversal direction more than the torsional direction. As a result, the flexible link can be considered as a cantilever beam [13]. Generally, the deflections are negligible in the longitudinal direction of the link [14]. One may note that the external forces introduced by the effect of the load may degrade considerably the manipulator dynamic which inevitably excites more the vibration during the manipulation process [15, 16]. Moreover, the brutally altered vibration provokes irregular movement in robot joints which may eventually deteriorate the dynamical performances [17]. The deflection model of the flexible link has an infinite number of DOFs because of the large flexibility distribution [18]. This leads to under-actuated system since ordinarily a defined number of driven actuators is assigned at each joint to control the end-effector pose. Thus the control complexity of the manipulator increases in case of active damping control.

1.2.2 Mobile platform

The mobile platforms are adapted in large variety of fields depending on the use context. For example, the logistic robots in warehouses, autonomous cars, the wheelchairs for the elderly and disabled. The mobility solution is exploited as well in the manufacturing factories in which the robot manipulator may be installed on the mobile platform for the purpose to expand its work-space and manipulability. The mobility ability allows the mobile robot to operate in different working contexts.

The conventional mobile robots platform, with one/two pair(s) of actuated wheels, have limitation in term of manoeuvrability in order to execute certain tasks under some kinematic constraints, such as obstacles avoidance. On the other hand, the omni-directional mobile platforms offer more kinematic possibilities to the robot work-space due to the special mechanical construction of its mecanum wheels, see for example [19]. Compared to the conventional wheels, the mecanum wheels are independently actuated. They were invented by Ilon in 1975 [20]. The curved rollers are arranged around the circumference of each wheel. The disposition of each roller axis should skew by 45^o to the concerned wheel axis. Thus, the Omni-directional platform has three DOFs in the horizontal motion plane which allows it to move instantaneously in any direction by the simple combination the velocity of the wheels without steering the wheels at all. In addition to motion redundancy, the omni-directional mobile platform offers time-saving

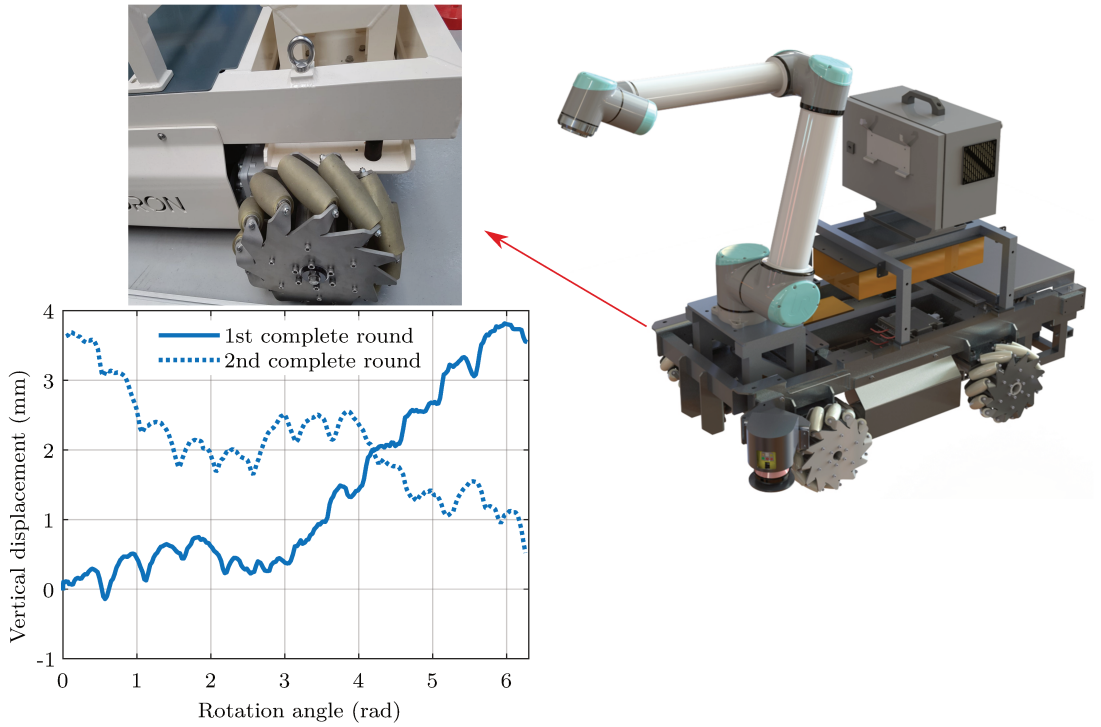

Figure 1.5: TC200 mobile Platform: 12 curved rollers on each wheel. Error quantification is measured for 20% of maximum power. The vertical deviation amplitude due to the mecanum wheels (i.e. gap between inner rollers and outer rollers) is around 1 mm less than the one which is issued from the floor surface (≈ 4 mm).

and less energy-consuming [19].

Commonly in the approach depicted in the literature, the mobile base and the manipulator are independently managed in terms of work-space trajectory. In order to improve the productivity, the motions of the mobile base and the manipulator must be coordinated. As a result, the mobile manipulator can be considered as a single system with a high redundancy degrees. This potential advantage in time over the mobile manipulator motion can be a helpful factor in improving the accuracy of the entire system. However, the rigid motion of the mobile base is likely to deteriorate the dynamic precision of the manipulator end-effector, in particular by causing vibrations, see figure (1.5). Due to the curved structure of the rollers, it is unsuitable to execute smooth motions. The contact point between the wheel and the ground is too small so that it jumps discontinuously from one roller to another during the motion. Thus, the sequential rotation of the mecanum wheel induces periodic vibrations along the motion which may limit the performance of the navigation algorithm [21]. In [22], kinematic simulations on omni-directional wheelchair prototypes reveal that periodic vibrations are noticed during the mobile platform motion along with the perpendicular motion axis, its amplitude is approximately within $1mm$. Moreover, the lateral motion is likely to induce

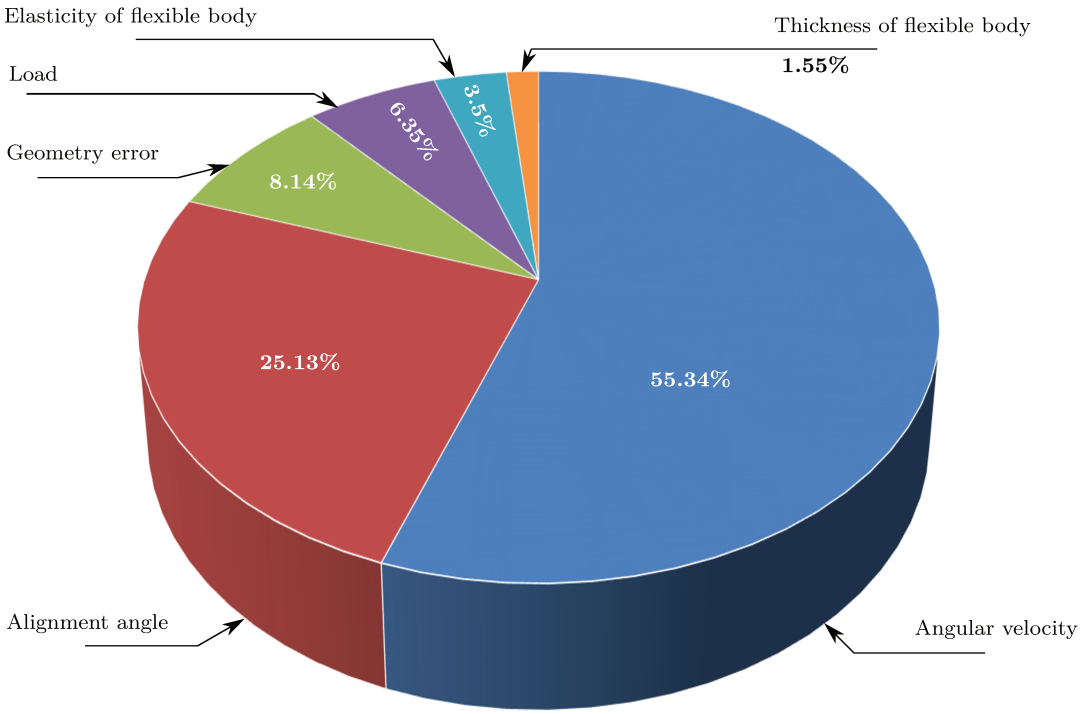

Figure 1.6: Vibration due to the mobile platform structure [24]: the gap/geometry errors are selected as factors related to the design error ;The elasticity and the thickness of the flexible body of the wheels are related to the tire i.e. the urethane rubber wrapped around rollers and its thickness ;Errors in machining and assembly can deform the alignment angle ;The velocity and the load effect are added in navigation process.

most of the vibrations compared to the straight motion. In [23], the author points out that the shifting of the gravity center of the mobile robots may cause error in mobile robot positioning, i.e. slippage error. The wheels velocity and the applied normal force may deviate the platform center of gravity. For example, this may happen during the simultaneously coordinated motion of the robot platform and the robot manipulator. Besides to position errors, it can also lead to energy waste problems [21].

The vertical component of the motion-induced error is critical for mobile robots operations. Therefore, it can bring instability and deformations to the tool/transferred-load at the end-effector of the robot manipulator. Different factors are related to the emergence of these deformations during the mobile platform motion [24]. It is mainly affected by the angular velocity, wheel alignment with the platform-body vertical axis, geometry form including the gap due to the discontinuous contact point, flexible structure of the platform body, see figure (1.6). One may note that the most contributed factor is the contact surface since the mobile platform is so sensitive to the ground irregularities [25]. This error is considerably noticed during the platform motion, see figure (1.5).

Figure 1.7: Example of deformable objects manipulation "car bumper", the motion-induced vibrations can be presented by oscillatory system including the vibration modes.

1.2.3 Flexible load

In manipulation context, the intervention of workers is restricted because of the safety issue or under other constraints. For example handling melted steel containers or any sort of dangerous liquids. Therefore, the robot manipulator is assigned to handle different sorts of loads which have either rigid or flexible body structure. The manipulation of such deformable objects can be found in cars and aerospace industries for assembling operations, such as cables or car bumper, see figure (1.7). Same as in daily life such as for clothes folding. It is not qualified to manipulate flexible loads using algorithms which are developed for manipulating rigid bodies, the deformation constraint should be considered in aim to adjust the grasping and the transportation process for example. Thus, the robot may achieve the desired pose which corresponds to the load tip or any other reference point on the body structure. This includes the orientation for a given angle or the form pose for a specific curvature.

Specific robotic manipulation should be addressed in case of deformable loads. The load structure may be deformed under external actuated forces or those issued from the robot dynamic itself at the gasping point where applied the actuated force. Therefore, time-varying degradation on its shape compared to the original shape may occur. One may note that not all deformed objects can regain their initial form, this feature may

distinguish deformable objects into three main patterns. Based on the dimensional deformation and physical properties, such as linear deformable objects such as beam and rope. Two dimensional deformation, if the object degradation occurs in one plane either on the contour or the surface. For example, the liquid sloshing in case of linear transportation of liquid container. Three dimensional deformation, such as in case of manipulating a piece of meat where the deformation are noticed in three directions of the load. Same as any other flexible structures, the flexible load is an under-actuated system which may inhere infinite DOFs number [26]. Along with the load positioning and orientation control, the undesired deformation should be reasonably retained by keeping the vibration amplitude bounded [27, 28].

1.3 PROBLEM DEFINITION

In the context of the robotic manipulation in factory, either the flexible structure inherent in the flexible manipulators or the manipulated flexible loads are susceptible to induce an oscillatory behavior as long as the load is moved in the free space which causes uncertainty in the end-point position. This is critical in many robotic applications, especially for some tasks with high speed and precision requirements. In view of the previous points, the accuracy of the manipulation task with mobile manipulator can be deteriorated due to three distinguished levels: mobile platform, robot manipulator and deformable load. The impact of each one of these errors is progressively dependent on the other one.

Moreover, the industrial applications especially and other distinct robotic manipulation processes in general are in need of robot manipulators with extra maneuverability and dexterity to operate in the most sophisticated and unstructured varying environments. The redundant manipulator is adapted for such situations, knowing that it is able to execute the same task in several configurations since it has more DOFs than those required to execute a specified task. This redundancy offers additional DOFs to deal with many kinematic and dynamic issues related to the robot manipulators to enhance their performances. Nevertheless, this imply a long chain of robot structure with potential free actuators which increases the robot flexibility.

The aim of this work is to develop control strategies in the context of mobile manipulation in an assembly line environment (supply, positioning, machine loading). These must ensure the dynamic precision of the positioning of the end-effector while minimizing the execution time in order to manipulate potentially flexible objects. On the one hand, the accuracy improvement of the robot depends mainly on the reduction of the end-effector deformations which are induced by the motion of the manipulator and/or by the mobile platform. On the other hand, the manipulated flexible object may be deformed not only by the accumulated deformations from the robot but it can be affected by the TCP trajectory profile as well. The present study aims to resolve two scientific challenges by exploiting the kinematic redundancy of the robot. First, using the redundancy of robot to resolve criteria related to work-space constraints. Secondly, the previous resolutions will be exploited to define a proper trajectory for the robotic task while in-

tegrating functional criteria related to a given task such as deformations reduction and control torques minimization. One may note that the redundancy may have exciting effect on vibration of the robot manipulation task due to the mechanical architecture and the free-moving torques. Thus, the main contribution of this work is to enhance the dynamic precision of the robot in the context of flexible objects manipulation by exploiting these self motions.

In literature, controlling the vibrations turned out to be a practical approach, a vast research on its control for manipulators is deeply analyzed in the state of art for both robot system and robotic manipulation of deformable objects. For example those which rely on force/torque sensors and referred to as state feedback control. Vibrations are integrated in the global control architecture. Either via robot-sensors data to updated the joints torque command [29, 27] or by using numerical estimators to establish the control law such as linear control PID [30], adaptative control [31]. Than the vision system is introduced, the RGB-D camera is used to reinforce the force feedback control in aim to handle complex manipulation contexts [32]. On the other hand, the vibrations control is separated from robot control scheme in open loop architecture. The feedforward action is exploited to deal with vibrations reduction of stable controlled robot system. This can be achieved via 3D environment simulation to predict the deformation for given maneuver [33]. In order to satisfy both the trajectory tracking and vibration damping, the motion planning can be adapted to vibration reduction by exploiting the methods of trajectory planification, such as smoothing trajectory generation using input shaping strategy [34, 35].

With regard to the control approaches proposed in literature, the scientific contribution of this thesis addresses the exploitation of the redundancy resolution to reduce the motion-induced vibrations and deformations for accurate and safe robotic manipulation.

1.4 CONTRIBUTIONS AND THESIS ORGANIZATION

Contribution 1: Vibration reduction control for redundant flexible robot manipulators exploiting redundancy capacities

Both vibration reduction and task accuracy improvement for flexible redundant manipulators, using the resolution of redundancy are addressed in this work. The exciting force of flexural motion which is induced by the motion of the manipulator causes undesired deflection at the end-effector. Based on an elasto-static model of the collaborative robot which is kinematically redundant, the null space inherent in redundancy feature is exploited to damp out the vibration while maintaining the end-effector posture. In order to exploit all the degrees of freedom in the null space, a feedback control design based on torque optimization has been introduced using analytical method for the redundancy resolution.

***Article**: Amine Rahmouni, Richard Bearee, Mathieu Grossard, Eric Lucet "Vibration reduction method for redundant flexible robot manipulators". IFAC 2020, Berlin.*

Contribution 2: Robot trajectory generation for flexible load transfer under deformation reduction constraints

In this study we address the problem of reducing the elastic deformations and the residual vibrations of flexible loads when they are handled by a robot manipulator. During the manipulation of the low-stiffness load, such as bumper or exhaust system in automotive industry, large motion-induced deformations and vibrations may be induced. These deformations will have detrimental effects on the settling time, on the accuracy and on the integrity of the operational process in a constrained environment. The trajectory shaping approaches, i.e smoothing filter or input shaping method are well-known solutions for the suppression of the residual vibrations at the end of a rest-to-rest motion. However, using trajectory shaping technique alone may not be sufficient to suppress the static elastic deformations during the transfer phase of the object. Thus, the main contribution of this work is to propose a two stages feedforward based approach that combines trajectory shaping technique for vibrations reduction, with a deformation compensation trajectory. The latter exploits the rotation space of the manipulator to mitigate the flexural motion of the flexible load.
***Article**: Amine Rahmouni, Richard Bearee, Adel Olabi, Mathieu Grossard, Eric Lucet "Robot trajectory generation for three-dimensional flexible load transfer". IECON 2019, Lisbone.*

Contribution 3: Trajectory tracking with vibration constraints for multi-axis motion

In the context of trajectory planning we propose a technique to improve the accuracy of robot manipulators for multi-axis composed motion. As mentioned previously, the manipulation of flexible loads and/or the inherent flexible structure of the manipulator induce undesirable vibration at the load/end-effector level which result in motion inaccuracy. The addressed study gives better insight into the ability of the jerk-limited profile along the time synchronization to reduce the residual vibration and guarantee a precise tracking of the prescribed trajectories. For online filtering shaper, a proper compensation scheme has been put forwards in order to achieve a consistent synchronization between the different axis trajectories of the manipulator. The effectiveness and the feasibility of different approaches for industrial robot applications are evaluated.
***Article**: Amine Rahmouni, Richard Bearee, Mathieu Grossard, Eric Lucet "Jerk-limited trajectory tracking with vibration constraints for multi-axis manipulators". S-mart 2019, Les karellis, Montricher Albanne.*

Thesis organization

The thesis is organized according to the main contributions which are mentioned above, see figure (1.8):

- **Chapter 2** introduces the use of the redundancy resolution for precision improvement of the robot manipulator with inherent flexible structure. First, the dynamic

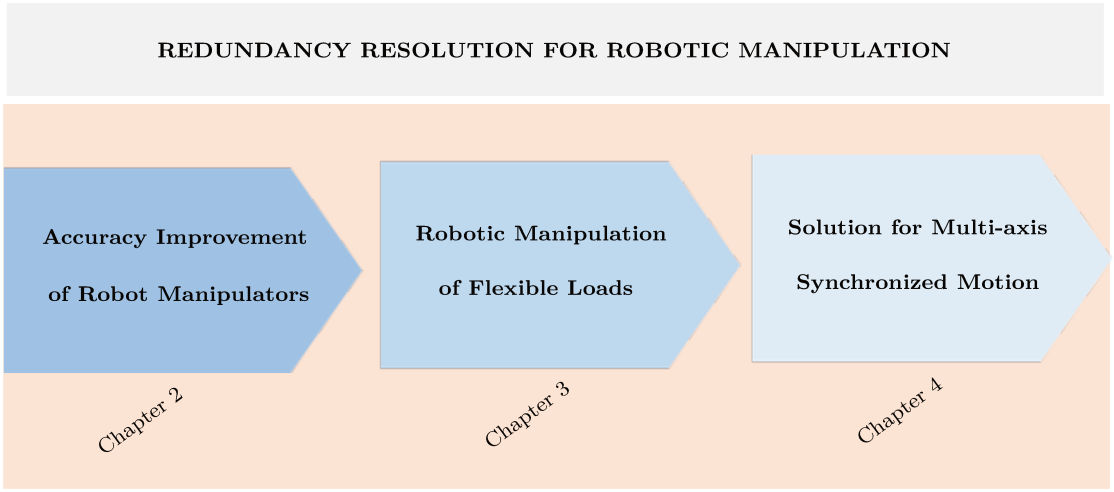

Figure 1.8: Thesis organization.

compliance between flexural motion and the robot control DOFs is analyzed to quantify the dynamic error. The redundancy solution helps to damp out the time-varying vibration in meanwhile the nominal trajectory is tracked precisely. This solution reveals optimal configurations where the robot energy is minimized since the torque optimization constraint is considered in redundancy resolution.

- **Chapter 3** quantifies all sources of deformations of the mobile robot manipulator and flexible load at the end-point of the manipulated object. The elastic deformation and the residual vibrations are controlled via trajectory planning approach using a feedforward scheme which is the combination of both smoothing shaping filter and robot redundancy resolution. The approach robustness is considered and discussed for accurate robotic manipulation in industrial applications.

- **Chapter 4** focuses on issues about trajectory degradation for multi-axis motion where the time delay of the shaping filter induces an asynchronized motion. The feedforward scheme is adjusted by adding a compensation action on the filtered trajectories. The main categories for synchronized motion are proposed depending on the transitional error and the nature of trajectory planning, i.e. online or offline scheme.

Chapter

2 VIBRATION CONTROL OF REDUNDANT ROBOT MANIPULATORS

A robot manipulator is a spatial structure which consists of n links connected by n joints which are either revolute and/or prismatic. The joints are more likely to contain flexible mechanism due to the compliant elements that form the motion transmission chain. The links could be either rigid or flexible depending on the elasticity of the material. As highlighted in the previous chapter 1 despite the advantages of using lightweight manipulators in modern industry, the robot flexibility is subject to deteriorate the positioning accuracy and add more constraints on the robotic task.

The exciting force of flexural motion, which is induced by the manipulator joint motion, eventually causes deflection at the end-effector. In section 2.2, the dynamic interdependency between the manipulator motion and the flexural dynamic system is analyzed to better explain this phenomenon. For the sake of better performance, the vibration control should be achieved without degrading the robotic task precision. In this chapter, both vibration reduction and task accuracy improvement for flexible redundant manipulators is addressed using the resolution of redundancy.

The kinetic redundancy allows the manipulator to achieve additional performances. The fact that it is offering more DOFs compared with those which are required to execute a given task leads to infinite configurations in joint-space to hold the same Cartesian posture of the end-effector. In order to exploit all the degrees of freedom in the null space, a feedback control design based on torque optimization is introduced in section 2.3 using analytical method for redundancy resolution. In section 2.4, the null-space motion inherent in redundancy feature is beneficially exploited to damp out the vibrations while maintaining the nominal trajectory of the manipulator end-effector.

2.1 REVIEW ON VIBRATIONS CONTROL

Adjusting the mechanical structure of the flexible manipulator by stiffening its flexible elements may overcome its flexibility at the cost of a lightweight manipulator. This process eventually yields a high-inertia or complex rigid manipulator by increasing, for example, the non-linearity in the physical model. Therefore, since controlling the vibrations turned out to be a practical approach, a vast research and deep analysis on control of the flexible manipulators is in progress to date.

In control design, the control of motion-induced vibrations should be considered in addition to the control of manipulator motion. Depending on how the vibrations are controlled, in general, two main approaches are distinguished in case of flexible redundant robots. The first category integrates the vibrations analysis into the main control algorithm of the robot motion. Characteristically, this combination works either for linear or nonlinear control design. The second category uses the redundancy resolution feature to carefully select the optimal configuration of the robot manipulator among all other available solutions, so that the vibrations are optimally reduced during the motion and along the planned path. In the following sections, each category is underlined through relevant examples in literature and illustrative control schemes.

2.1.1 Control-based approach

The control algorithm is designed in order to compute the input torques in the allowed interval limits of the robot actuators to drive the flexible manipulator in a predefined path whilst try to minimize the deformation of the end-effector. The specific structure of the manipulator induces an unsteady motion along the end-effector path which results from nonlinearly-coupled dynamic between the rigid body motion and the flexural motion due to the elasticity of the flexible structure. Therefore, a compromise should be made between the precision, or trajectory tracking, and steady motion preservation (vibration reduction). The feasibility of this control is guaranteed by adopting the control theory of linear and non-linear dynamic systems to extend it to the case of the flexible manipulator in general.

The active control schemes are established based on nonlinear and linear control design theory for dynamic systems, such as PID control [36], singular perturbation control [37], stable inversion control [38], adaptive control [39], intelligent control algorithms [40], and so on. These control systems rely on the manipulator dynamic system and/or are in need of feedback information from the system output signals which are provided by sensors and/or numerical estimator, see figure (2.1). The linear control theory, such as PID control, is used mainly for trajectory tracking while state feedback is implemented in order to reduce the tip vibration. In [36], two control actions are merged, where H_∞ enfolds the PID controller to increase the robustness against the estimation uncertainty of the identified system. An enhanced version is adapted to get comply with manipulator configuration changes and stabilizes vibrations via adaptive sliding-mode, see [39]. The computed torques control, which are deduced from the inverse dynamics, are exploited to build the feedback linearization scheme, see [41, 42, 43, 44]. The state measurement

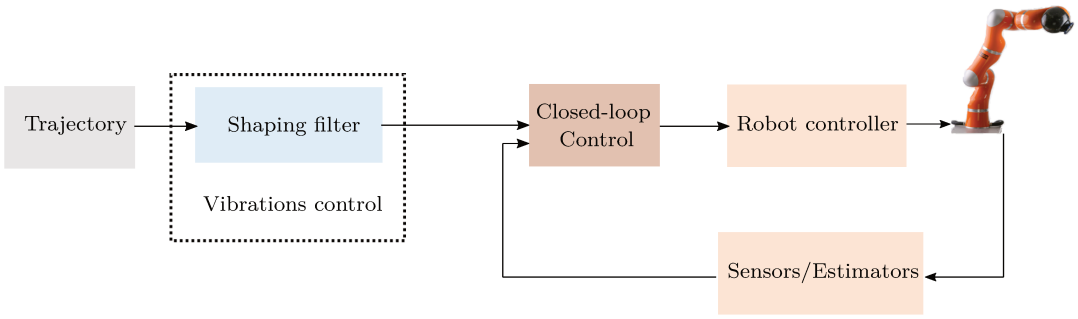

(a) Open-loop approach

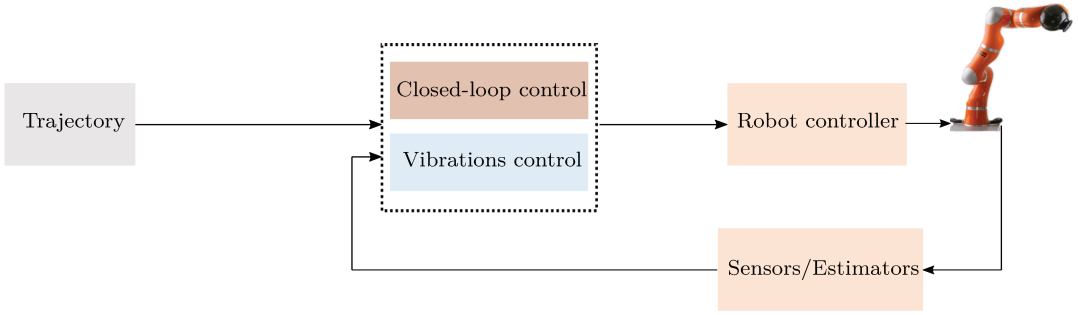

(b) Feed-back approach

Figure 2.1: Vibrations control schemes.

data are collected using sensors (accelerometers, and optical sensors) and/or by implementing state estimator such as Kalman's filter, Which is used to construct optimal motion control, such as linear quadratic regulator (LQR) or linear quadratic Gaussian (LQG) structures to actively control the vibration [45]. It guarantees the stability and robustness in the presence of bounded uncertainty. The inverse-dynamics-based control has been extended to the case of flexible manipulators, and so for the combination of rigid and flexible states, by considering the constraint of minimizing the vibrations to guarantee the system stability [46]. In [47], the control law is based on trained neural networks for the friction compensation, this ultimately has non-negligible impact on the actuation energy-wasting.

On the other hand, the open loop control generates a smooth trajectory from the reference trajectory, which is modulated by pre-estimated frequencies of the flexural motion, in order to minimize the residual vibrations. The classical input-shaping technique, which is introduced in [35], is designed for rest-to-rest motion within a previously-defined time interval, with the aim of suppressing the residual vibrations by filtering the reference input. In [48], the trajectory is shaped by inverse dynamic analysis within optimum speed, and the robustness is effectively approved by the sensitivity analysis for slightly

damped dynamics. Since then, different shaping filters are developed and updated for overall mechanical systems. For example, the damped jerk-limited profile in [49] is adapted to the case of under-damped flexible systems. In addition, the exponential filter in [50] increases the smoothness of the motion profiles regarding the injected trajectory. The filter modulates/shapes the input signal without feedback measurement data from the system dynamic. It avoids any complex calculation, since only specific parameters of the flexural motion are required. The approach-proceeding relies on solving only a set of linear equations. One may note that the system parameters' variation and uncertainties are handled by the closed loop block, which guarantees the trajectory tracking, see figure (2.1). Therefore, the input shaping filter is generally combined with the closed loop based control scheme to achieve positioning control and reduce vibrations of flexible manipulators. The filter parameterization relies exclusively on the system dominant mode and eventually depends on the robot configuration since the vibrations vary in different motion directions. In [51], an adaptative algorithm is proposed to continuously update the shaping filter parameters depending on the robot actual configuration. In [52], linear control is combined with input shaping to increase the robustness of the system. In [53], the input shaping is combined with feedback controller in such a way as to monitor and improve the control performance, and insures the system stability in front of unknown disturbances. Output-based shaping filter is proposed in [54] to cope with the force reaction for different scale payloads. The robustness along with the trajectory tracking is compared for two optimal linear controllers, LQR and PID. Since the frequency characterisation of the flexural motion is unsteady, in [55], the adaptative shaping filter is put forward to take over the variation of natural frequency by deriving an algebraic identification after proceeding to the estimation step. Computing approach is used in order to avoid any complexity related to the use of the dynamic model to construct the control law, for example the genetic algorithm, the optimization algorithms which employ tools such as fuzzy logic [40] and neural networks [56]. These algorithms are adapted to fix suitable gains in feedforward block, feedback scheme or both.

2.1.2 Redundancy-based approach

The kinematic redundancy of redundant robots is highly investigated. In literature, this internal motion is referred to as self-motion or null-space. The redundancy is used to deal with different kinematic and dynamic issues related to robot manipulators, in order to enhance their performances. For instance, in [57] and [58], the redundancy is used to deal with obstacle avoidance and joints constraints respectively.

The conventional control schemes above were developed to be applied to both redundant and non-redundant flexible manipulators. Little attention has been paid to take advantage of the redundancy of flexible manipulators either for vibrations suppression or for designing simple controller. Therefore, the redundancy application in the control design is rare and few works have investigated this ability. For instance, in [59], a control design in dynamic level for multi-priority control in redundancy space is analyzed. In [60], the operational space control design is proposed for the redundant manipulators, in velocity and acceleration levels.

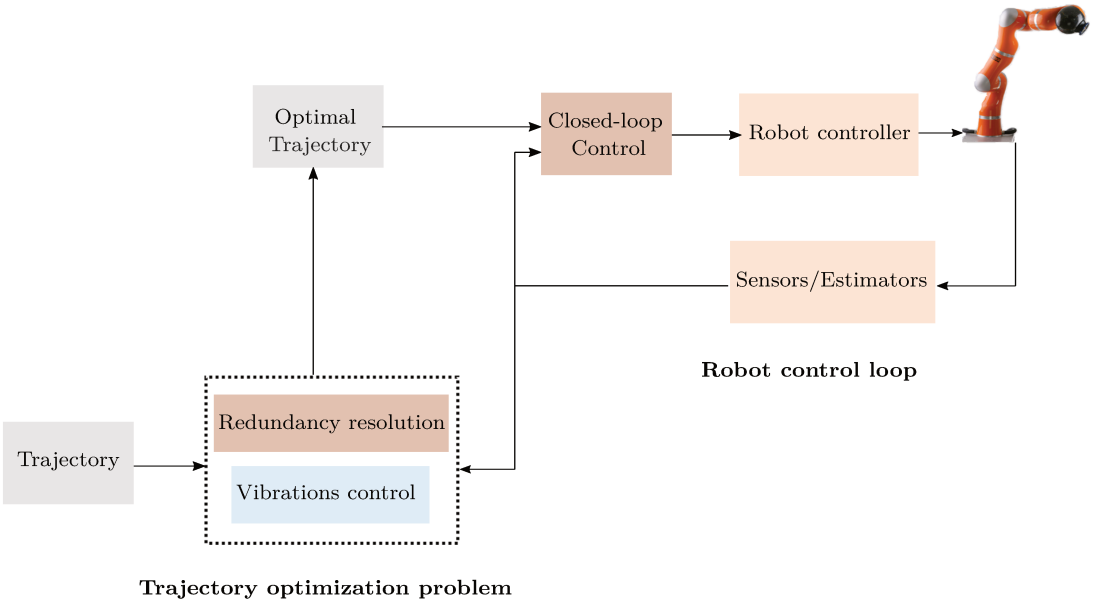

Figure 2.2: Vibrations control via redundancy resolution.

The joint motion is capable of affecting the vibrations since the dynamic of the rigid body and the flexible parts of the flexible manipulator are highly coupled. This ability may be used efficiently to achieve smooth motion without exciting the vibration modes. The redundancy ability affecting the manipulator flexibility has been introduced and examined in few works. The figure (2.2) depicts the general scheme of vibration control via redundancy resolution for flexible redundant manipulators, in aim to find optimal trajectory with minimal vibrations. In[58] and [17], the null-space of the joint acceleration has been used to achieve an optimal joints motion so that the vibrations are reduced. Nevertheless, the optimization algorithm consumes a considerable amount of time and discussions regarding the potential impact of the configuration initialisation case have not been presented. The self-motions switching are prone to result in unstable joint motion, and in some cases the optimal solution for joints motion is irregular and difficult to execute online due to the numerical complexity of large amounts of calculation at every discrete point. In [62] and [63], authors have established a control design based on the Jacobian null-space, which is used explicitly to damp out the vibration dominant modes. It has been proven that the self-motion gets rid of the manipulator flexibility effects only when the number of redundancy degrees is the same as the number of selected

modes to be controlled. It maintains precise tracking of the end-effector trajectory, and this is guaranteed as long as the the flexible redundant manipulator is not in a singular configuration. Similarly, in [64], a flexural state estimator using force/torque sensor is beneficially added this time to the control design to reduced the induced vibration of flexible appendage in space robot. A numerical approximation on the redundancy resolution has been made for simplification in practical implementation, which may decrease the effectiveness of vibrations suppression and implies additional uncertainties. In [65], the resonance-ratio control is designed to suppress the vibrations. The work space observer is used to estimate the flexural reactive force, which is injected afterward in the Jacobian null-space in addition to the joint local control. In spite of that, assuming that the joints velocities are considerably small could be admissible only for low dynamical maneuvers. Otherwise, it is not advantageous for other common motion ranges which restrains the application of this approach, especially that the flexible manipulators are chosen for their higher speed. In [66], the vibration reduction is guaranteed by resolving the kinematic redundancy with the help of an additional constraint which is obtained from vibration dynamics. This technique takes advantage of the task-space augmentation approach which relies on the augmented Jacobian, where the flexural dynamics of the induced vibration is considered as an optimisation problem. In this case, the joint's motion solution may become unfeasible surrounding the algorithm singularity of the augmented optimization problem.

2.2 GENERALIZED DYNAMIC MODEL FOR FLEXIBLE MANIPULATOR

2.2.1 Overview

Generally, most of control approaches rely on dynamic models of the considered manipulator. Therefore, the important step towards optimal performances and effective control is to provide an accurate and practical model. For the flexible manipulator modelling, three formulations are commonly used: Newton-Euler formulation, Lagrange formulation and Kane's formulation. The presence of flexible elements in the manipulator structure inevitably implies highly nonlinear coupled dynamic models. The flexural motion is explicitly dependent on the robot set-up configuration and therefore the rigid body motion of the manipulator joints. In the case of the flexible-link manipulator, the joints are supposed to be rigidly stable motion transmitters, where the link elasticity is important.

The flexural displacement of the flexible link and the dynamic model of the manipulator could be derived simultaneously using a set of techniques depending on the dynamic vibration theories, such as Euler-Bernoulli beam theory, and on the way in which the continuous dynamic model is discretized. The flexibility distribution along the link modeling leads to a complex, non-minimal system with infinite DOFs. Thus, the idea of achieving an exact solution seems to be impossible since the robot manipulator generally provides a few DOFs. This issue could be solved by discretizing the

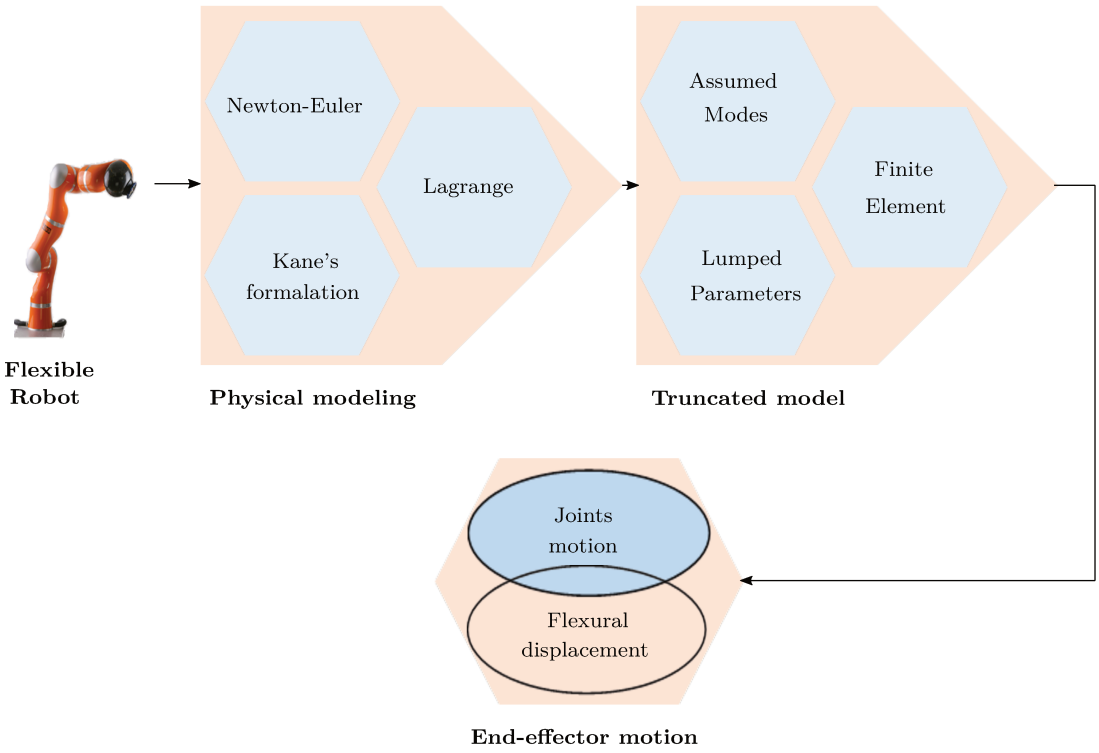

Figure 2.3: Flexible manipulator Robot modeling.

continuous system to a reduced-order model using truncated methods, such as assumed mode, finite element technique and lumped-parameter, which are presented below. The figure (2.3) presents a diagram which illustrates the modeling process for the flexible manipulator. For more details about the existing approaches and their analysis, the reader is recommended to refer back to general reviews presented in [67, 68, 69] and the references therein.

- **Assumed mode:** this method discretises the dynamic equations into a sum of truncated sets of assumed modes to represent the link deflection with regular cross-section [70]. The method provides a low order representative system where its accuracy is proportional to the number of the considered modes. Therefore, it should be a compromise between the accuracy and the complexity of the model. However, the modal analysis is an interesting method when it comes to describing the flexibility of the system, since it makes it possible to achieve good control based on the reduced-order model. For example, in [71], the dynamic model of a two-link flexible manipulator is reduced to a set of discretized subsystems using assumed mode method for feedback control combined with neural network.

- **Finite element technique:** it is widely used to numerically analyse the mechanical structure. The order of the discretized model depends mainly on the number of finite elements which used to discretise the flexible link; generally, the required number is considerably huge. In this case the real time implementation for control purpose is restricted, for which the reduction of the modal order is indispensable, see [72]. For instance, in [73], the equivalent rigid-link system dynamic formulation is combined with the finite element method to both considerably reduce the number of system DOFs and optimize the computational time. The finite-dimensional system kept the motion of the robot smooth and fine. In [74], an established comparison study between the finite element method and assumed modes for flexible manipulator modeling using Lagrange dynamic formalism is proposed. An additional number of differential equations is required to better approximate the flexural dynamics which extend the calculation time. The linear method, i.e assumed modes method, which relies on time-varying frequencies, is suitable for links with uniform cross-sections. In contrast, the finite elements can handle easily single or multi link with complex geometries using nodal analysis which is convenient for no-uniform cross-sections.

- **Lumped-parameter:** this formulation assumes basically the flexible link to be equivalent to kinematic chain of virtual joints, where at the tip of each one a lumped mass is attached with massless linear spring for elasticity modeling [75, 76]. The nonlinear lumped parameters are suitable for modeling the nonlinear regime within spatial discretization of the flexible elements and can additionally ensure proper optimal numerical solution. For instance an optimal pre-shaping input and joint angles feedback for closed loop control is proposed for highly flexible manipulator manipulation in [77]. The process requires less complex numerical calculation compared to the finite-element approach. The lumped method is adequate for simple model presentation and numerical simulations. This advantage can be exploited to design robust controllers. For example, in [78], the PD control is proven to achieve better control performance with comparison to the singular perturbation controller. The bounded input and bounded output stability is guaranteed regarding the payload variation. In [79], the Lyaponov criteria ensures the sliding surface stability of the PID sliding mode controller which avoids the chattering phenomena and achieve precise trajectory tracking.

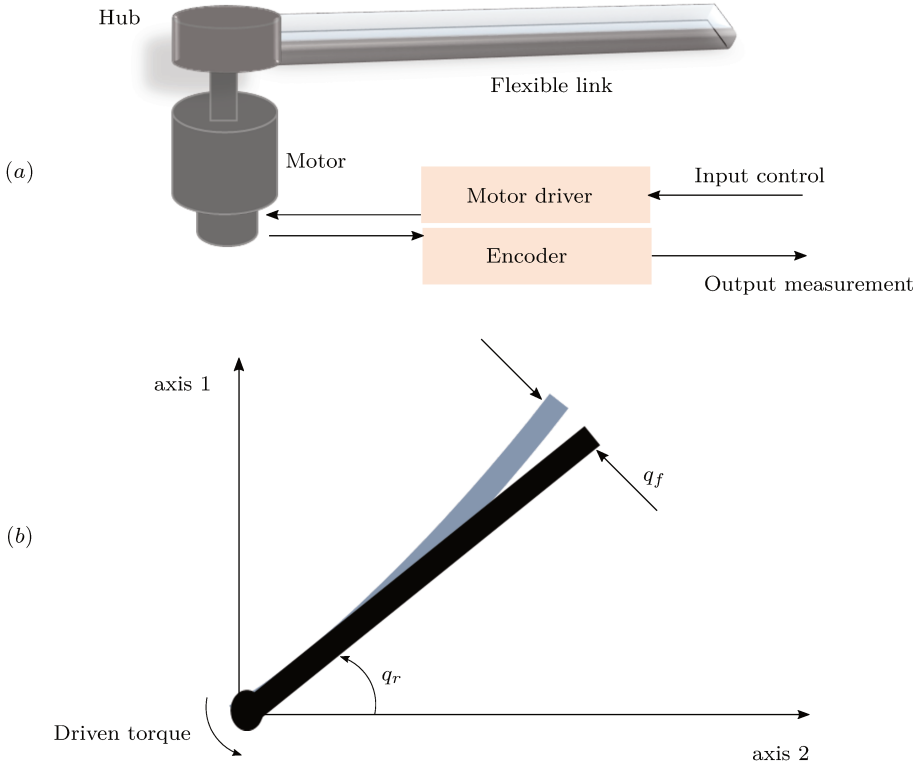

Figure 2.4: Schematic drew of single flexible link: (a) a simplified diagram, (b) planar representation

2.2.2 Dynamic analysis

The dynamic structure of the flexible manipulator is the combination of both the joints motion, i.e the motion of the rigid body, and the flexural motion, i.e the elastic deformation in the flexible elements, which is depicted by n_r rigid DOFs and n_f flexural DOFs respectively. The figure (2.4) exhibits the planar definition of the single flexible link case, where the deformations are considered at the tip of arm.

Based on Lagrange's formulation and assumed modes method, see for instance [17] and [80], the dynamic model of the flexible manipulator with flexible links is generally described by n dynamic equations of motion, where $n = n_r + n_f$ is the total DOFs of the system,

$$M(\Theta)\ \ddot{\Theta} + D(\dot{\Theta}, \Theta)\ \dot{\Theta} + K(\Theta)\ \Theta = \Gamma + \tilde{\Gamma} \tag{2.1}$$

where

- $\Theta = [q_r^T\ q_f^T]^T \in \mathbb{R}^n$ is the generalized coordinates vector, $q_r \in \mathbb{R}^{n_r}$ and $q_f \in \mathbb{R}^{n_f}$ are respectively the joint coordinates vector and the elastic displacement coordin-

ates vector;

- $M(\Theta) \in \mathbb{R}^{n \times n}$ is the global mass matrix;
- $D(\dot{\Theta}, \Theta) \in \mathbb{R}^{n \times n}$ denotes the global damping matrix;
- $K(\Theta) \in \mathbb{R}^{n \times n}$ is the global stiffness matrix;
- $\Gamma \in \mathbb{R}^{n}$ is the generalized torques vector, which depends on the control torques;
- $\tilde{\Gamma} \in \mathbb{R}^{n}$ is the vector which aggregates the Coriolis, gravitational and centripetal forces in addition to other nonlinear dynamics including the externally applied forces and the non-conservative forces such as friction forces.

One may note that the flexible links of the flexible manipulator are modeled as clamped base beams [80]. The dynamic model of the flexible manipulator is supposed to be estimated by a numerical estimator or practically identified, see for instance [65].

In the process of Lagrange formalism, the dynamic of the flexible manipulator is derived from the kinetic and potential energy balance and formulated into two set of time-varying equations, which are differentiated via partial derivatives. They are related to the rigid variables and the flexural variables of the conservative form of Lagrange's equation [81]. Therefore, the dynamics of both rigid and flexural motion may be described separately from (2.1) as follows

$$M_{rr}\ \ddot{q}_r + \tilde{\Gamma}_r = \tau \tag{2.2}$$

$$M_{fr}\ \ddot{q}_r + M_{ff}\ \ddot{q}_f + D_f\ \dot{q}_f + K_f\ q_f = \tilde{\Gamma}_f \tag{2.3}$$

where

- $M_{rr} \in \mathbb{R}^{n_r \times n_r}$, $M_{fr} \in \mathbb{R}^{n_f \times n_r}$ and $M_{ff} \in \mathbb{R}^{n_f \times n_f}$ are block matrices of the global mass matrix, where the subscript "r" indicates rigid variables dependency and the subscript "f" indicates flexural variables dependency, or mixed dependency which is depicted by indices "rf" and "fr";
- $\tau \in \mathbb{R}^{n_r}$ is the control torques vector applied to the manipulator joints;
- $\tilde{\Gamma}_r \in \mathbb{R}^{n_r}$ is the non-linear dynamics in the rigid motion;
- $\tilde{\Gamma}_f \in \mathbb{R}^{n_f}$ is the nonlinear force which is applied to the flexural dynamics;
- $D_f \in \mathbb{R}^{n_f \times n_f}$ and $K_f \in \mathbb{R}^{n_f \times n_f}$ are respectively the damping and the stiffness matrices of the flexural motion.

The equation (2.3) shows that the joint dynamic influence the flexural motion dynamic. As the flexural dynamic is not explicitly dependent on the control torques τ, it is not possible to directly control the motion-induced vibrations. Thus, the deformation may be handled through the implication of adapted profiles for joints trajectory. The

distributed flexibility is non-minimum phase system where the number of flexural DOFs is relatively bigger than the actuated joints, which algebraically implies that the matrix M_{fr} does not have full rank. The reactive force which is aroused from the flexural efforts is absorbed in the non-linear dynamics $\tilde{\Gamma}_r$ of the rigid motion depicted by (2.2). The contribution of the reactive force is negligible compared to the algebric sum of other forces in the manipulator dynamic.

In order to achieve a given optimal performance, the dynamic of flexible elements is included in the generalised dynamic model of the flexible manipulator, and used to design various controllers algorithms [8]. The control stability and the precision are the main topic to handle in this case. To sum up, the flexural dynamics should be neutralized without affecting the manipulator's nominal motion.

2.2.3 Kinematic analysis

The end-effector position of the flexible manipulator, which is operating in n_t dimensional work space, is a function of both joint-angles coordinates and elastic displacement coordinates as follows

$$x = f(q_r, q_f) \tag{2.4}$$

where $x \in \mathbb{R}^{n_t}$ is the Cartesian position.

The kinematic model can be derived from (2.4) by time differentiation

$$\dot{x} = J_r \dot{q}_r + J_f \dot{q}_f \tag{2.5}$$

$$\ddot{x} = J_r \ddot{q}_r + \dot{J}_r \dot{q}_r + J_f \ddot{q}_f + \dot{J}_f \dot{q}_f \tag{2.6}$$

where $J_r \in \mathbb{R}^{n_t \times n_r}$ and $J_f \in \mathbb{R}^{n_t \times n_f}$ are the rigid and the flexible Jacobian matrices respectively.

From (2.3), one may notice that the flexural displacement cannot be controlled directly by usual inputs the joints torques. Therefore, in the motion-planning process only the nominal joints motion is considered to generate the desired trajectory for the flexible robot manipulators, see [65] and [**?**]. In this case, the term $(J_f \ddot{q}_f + \dot{J}_f \dot{q}_f)$ in (2.6) is not considered in redundancy resolution. From (2.6), the dynamical resolution of redundancy for motion planning in joint space is given by

$$\ddot{x} = J_r \ddot{q}_r + \dot{J}_r \dot{q}_r \tag{2.7}$$

The flexible manipulator is called kinematically redundant if and only if the number of actuated rigid joints n_r is greater than the dimension of the operational work-space, which is denoted here by n_t. The degree of redundancy m in this case is defined as $m = n_r - n_t$.

The relation in (2.7) is exploited to determine the joints trajectory for input reference. Due to the kinematic redundancy, an infinite configurations of the manipulator are valid for one given task positioning. Among all the possible configurations, one optimal solution is carefully retained depending on the selection criteria. This is referred to as

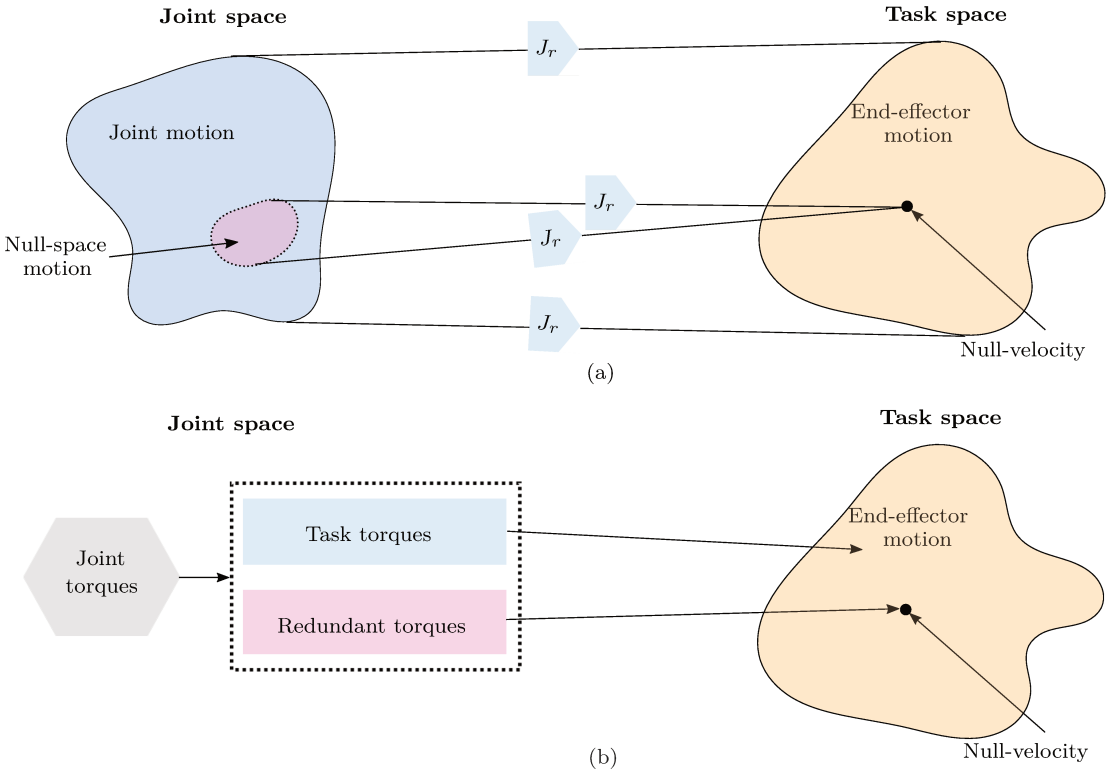

Figure 2.5: Redundancy resolution: (a) Classical definition in motion space, (b) Redundancy resolution using torque partition.

redundancy resolution. The kinematic redundancy has been resolved differently through various theories. The motion of the redundant manipulator is optimally mapped in response to the performance requirements on top of the primary task.

In general, most existent methods for inverse kinematic computation are derived from the pseudo-inverse Jacobian-based redundancy resolution [82, 83, 84, 85, 86, 87, 88, 89]. This tendency of using redundancy is found in most works in literature since it is a universally algebraic approach for defining the joint coordinates from the Cartesian trajectory using the pseudo-inverse Jacobian matrix, i.e Moore–Penrose generalized inverse of the Jacobian, for both non-redundant manipulator and redundant manipulator respectively. The redundant DOFs of the null-space are integrally allocated to the secondary task after executing the primary task.

The numerical solution for the inverse kinematic is introduced to obtain an approximate solution from non-linearity forward kinematic. A comparison between the pseudo-inverse Jacobian method and different numerical approach is conducted in [82] to evaluate the computational complexity in the solution of the iterative process, cost and speed convergence, which are important factors for practical implementation. Weighted

Pseudo-Inverse [84, 85, 89, 90] using inertia mass matrix is a promising approach to obtain optimal task kinematics regarding the dynamic characteristics.

Contrarily to the inverse kinematic methodologies, the dynamic analysis in [91] is very useful since it allows one to employ all the free redundancy DOFs without recalling the pseudo-inverse Jacobian matrix. The driven torques are explicitly selected in accordance with a given Cartesian trajectory acceleration. The factorisation calculation of input torques are highly preferred in the real time implementation and motion control design, where the torques are directly mapped to the driven actuators. Moreover, this approach is valid for both flexible and rigid redundant manipulators. The figure (2.5) depicts the diagram definition of the kinematic redundancy resolution for both conventional general concept and the one which is based on the torques distribution which will be described in the following section.

2.3 CONTROL DESIGN VIA REDUNDANCY RESOLUTION

2.3.1 Redundancy resolution

In the context of flexible manipulator control, the resolution of redundancy based on the pseudo-inverse of the Jacobian matrix is usually used to determinate the reference trajectory of joints acceleration. For example, in [17], the projected joints dynamic in the Jacobian null-space is only devoted to damp out the vibrations. In this case, having extra degrees of redundancy will be used to damp out effectively the vibration, i.e p redundant DOFs to compensate for p flexural DOFs, but not to fulfil any additional secondary task.

In this study, we investigate the use of the extra number of redundancy DOFs in aim to perform more than one second task simultaneously. Therefore, another method for resolution of redundancy, which is based on the manipulator dynamic analysis, has been considered in the development of the proposed strategy to exploit all the available degrees of redundancy, which is thoroughly analyzed in [91]. The joint torques are used in the redundancy resolution, which is advantageous since they are the main input variables to the manipulator controller.

Substituting (2.2) into (2.7), the end-effector acceleration can be rewritten as

$$\ddot{x} = J_r M_{rr}^{-1}(\tau - \tilde{\Gamma}_r) + \dot{J}_r \dot{q}_r \tag{2.8}$$

The following terms are defined for the convenience of the further study development,

$$\vartheta = J_r M_{rr}^{-1} \tag{2.9}$$

$$\chi = \dot{J}_r \dot{q}_r - J_r M_{rr}^{-1} \tilde{\Gamma}_r \tag{2.10}$$

The equation (2.8) then becomes

$$\ddot{x} = \vartheta_{\tau_t} \tau_t + \vartheta_{\tau_r} \tau_r + \chi \tag{2.11}$$

where the joint torques are decomposed into two sets, $\tau_t \in \mathbb{R}^{n_t}$, the task torques to perform a given task, and $\tau_r \in \mathbb{R}^{m}$, the redundant torques which are extra torques regarding the task. $\vartheta_{\tau_t} \in \mathbb{R}^{n_t \times n_t}$ and $\vartheta_{\tau_r} \in \mathbb{R}^{n_t \times m}$ are matrices that form the matrix ϑ, where the ith task torque $\tau_{t,i}$ (respectively the jth redundant torque $\tau_{r,j}$) is associated with the ith column of the matrix ϑ_{τ_t} (respectively jth column of the matrix ϑ_{τ_r}), $(i = 1, 2, ..., n_t)$ and $(j = 1, 2, ..., m)$. The term $\chi \in \mathbb{R}^{n_t}$ aggregates all non-linear dynamics.

At time instant t^*, the joint coordinates $(\dot{q}_r(t^*), q_r(t^*))$ are generally known, as a result the vector χ can be determined, as a consequence, the mapping h given by

$$h : \tau \longmapsto \ddot{x} \tag{2.12}$$

is affine and the admissible acceleration in this case are $\ddot{x}_{ac} \in D_\tau$, where $D_\tau = \{\ddot{x} = h(\tau),\ s.c\ \ \tau_{min,i} \leq \tau_i \leq \tau_{max,i},\ i = 1, 2, .., n_r\}$ where $\tau_{min,i}$ and $\tau_{max,i}$ are, respectively, the lower and the upper limit of the ith joint torque.

The analytical redundancy resolution at acceleration level is used to set up the proposed approach. The algorithm combines both an alternative control design to feedback linearization and a method for reducing the vibrations, in aim to improve the end-effector accuracy.

2.3.2 Feedback linearization via redundancy resolution

The feedback linearization control approach is the combination of two imbricated control loops. First, the inner-loop is constructed to ensure the system linearization. Then, the outer-loop is designed to guarantee the control of the resulting linear system. This control strategy is one of the robust schema for the manipulator control. The free m redundant joint torques $\tau_{r,i}, (i = 1, 2, ...m)$ in the mapping (2.11) are used to cancel the nonlinear dynamics, unlike the traditional feedback linearization control which exploits all the manipulator torques for the same process. Analytically, that can be reached by setting

$$\vartheta_{\tau_r}\tau_r + \chi = 0 \tag{2.13}$$

Since the vector χ is in $\mathbb{R}^{n_t}$, only n_t torques from m available redundant torques are sufficient to cancel completely the nonlinear term χ. But if the redundant DOFs number is less than the task dimension, i.e $(m < n_t)$, we can cancel χ in only m preferential directions. Furthermore, in the cases where there is an excess of redundant degrees of freedom, i.e $(n_t < m)$, an infinite of the redundant torques combination can cancel completely the nonlinear term χ. In this study, the last case is analyzed. The forward analyses have demonstrated that the additional $(m - n_t)$ redundant degrees are useful to affect the flexural motion and eventually damp out the induced vibrations.

Considering the last case, the general solution for redundant torques that satisfies the cancellation of the non-linear dynamics χ is given by

$$\tau_r = -\vartheta^+_{\tau_r}\chi + (I_m - \vartheta^+_{\tau_r}\vartheta_{\tau_r})\tau_\epsilon \tag{2.14}$$

where $\vartheta^{+}_{\tau_r} \in \mathbb{R}^{\mathrm{m}\times \mathrm{n_t}}$ is the generalized inverse matrix of ϑ_{τ_r}, the resulting vector $(I_m - \vartheta^{+}_{\tau_r}\vartheta_{\tau_r})\tau_\epsilon \in N(\vartheta_{\tau_r})$, where $N(\vartheta_{\tau_r})$ is the null-space of ϑ_{τ_r}, $\tau_\epsilon \in \mathbb{R}^{\mathrm{m}}$ is an arbitrary vector, $I_m \in \mathbb{R}^{\mathrm{m}\times \mathrm{m}}$ is the unit matrix.

After the linearization process has been achieved, the joint torques τ_t and τ_r, which guarantee the system linearization, are determined by solving the equations in (2.11) and (2.14) for a given end-effector acceleration $\ddot{x}^d$, providing that the matrix ϑ_{τ_t} is not singular. One may note that the choice of torque sets τ_t and τ_r depends on various factors, such as torque magnitude limits, for more details see [91]. After that, a conventional linear controller can be used to guarantee the end-effector tracking.

The equation (2.14) is parameterized directly in arbitrary term, which represents the torque null-space. This characteristic implies that the torques τ_r has multiple solutions depending on the projected self-motion. In the following analysis, we investigate the possibility of the additional self-motion to reduce the deformations due to the flexural motion.

2.4 METHOD FOR VIBRATIONS REDUCTION

2.4.1 Analysis of the flexural motion

The presence of the arbitrary vector τ_ϵ in (2.14) may generate an infinite number of solutions for the redundant torques τ_r. This self-motion ability, which does not influence the end-effector motion, may be used to adjust the joint motions and the flexural motion.

Substituting the joints acceleration $\ddot{q}_r$ value from (2.2) into (2.3) yields to

$$M_{ff}\ \ddot{q}_f + D_f\ \dot{q}_f + K_f\ q_f = F_f \tag{2.15}$$

$$F_f = \tilde{\Gamma}_f + M_{fr}\ M_{rr}^{-1}\tilde{\Gamma}_r - \mu_{\tau_t}\tau_t - \mu_{\tau_r}\tau_r \tag{2.16}$$

where $F_f \in \mathbb{R}^{\mathrm{n_f}}$ is the exciting force of the flexural motion, $\mu_{\tau_t} \in \mathbb{R}^{\mathrm{n_f}\times \mathrm{n_t}}$ and $\mu_{\tau_r} \in \mathbb{R}^{\mathrm{n_f}\times \mathrm{m}}$ are blocks matrices of the matrix $\mu \in \mathbb{R}^{\mathrm{n_f}\times \mathrm{n_r}}$, where $\mu = M_{fr}M_{rr}^{-1}$.

The extended expression of the exciting force F_f, which includes the arbitrary vector τ_ϵ, is obtained by combining the two equations (2.14) and (2.16),

$$\begin{aligned} F_f = &-\mu_{\tau_r}(I - \vartheta^{+}_{\tau_r}\vartheta_{\tau_r})\tau_\epsilon + \tilde{\Gamma}_f + M_{fr}\ M_{rr}^{-1}\tilde{\Gamma}_r \\ &- \mu_{\tau_t}\tau_t + \mu_{\tau_r}\vartheta^{+}_{\tau_r}\chi \end{aligned} \tag{2.17}$$

Let's consider that the damping matrix D_f is diagonalizable, then the modal analysis of (2.15) will provide n_f independent equations as follows

$$\ddot{\phi}_f + D_\phi\ \dot{\phi}_f + K_\phi\ \phi_f = F_M \tag{2.18}$$

where $D_\phi = diag(2\xi_i\omega_i) \in \mathbb{R}^{\mathrm{n_f}\times \mathrm{n_f}}$, $K_\phi = diag(\omega_i^2) \in \mathbb{R}^{\mathrm{n_f}\times \mathrm{n_f}}$, ξ_i and ω_i are the ith modal damping term and the ith natural frequency for $(i = 1, 2, ...n_f)$. $\phi_f = M_m^{-1}q_f \in \mathbb{R}^{\mathrm{n_f}}$ is a vector that contains the mode coordinates, where $M_m \in \mathbb{R}^{\mathrm{n_f}\times \mathrm{n_f}}$ is the mode

shape matrix. $F_M = M_\phi^{-1} M_m^T F_f$, $F_M \in \mathbb{R}^{n_f}$ is the modal generalized force, where $M_\phi \in \mathbb{R}^{n_f \times n_f}$ is the modal mass matrix, $M_\phi = M_m^T M_{ff} M_m$.

The arbitrary vector τ_ϵ is considered as a control optimization term that can be used to damp out the flexural motion. The modal generalized force is a controllable force via self-motion and it contains two terms: nonlinear term $F_{M,n}$ and control term $F_{M,c}$ which depends on the arbitrary vector τ_ϵ

$$F_{M,n} = M_\phi^{-1} M_m^T \cdot \left[\tilde{\Gamma}_f + M_{fr} M_{rr}^{-1} \tilde{\Gamma}_r - \mu_{\tau_t} \tau_t + \mu_{\tau_r} \vartheta_{\tau_r}^+ \chi \right] \tag{2.19}$$

$$F_{M,c} = -M_\phi^{-1} M_m^T \mu_{\tau_r} (I - \vartheta_{\tau_r}^+ \vartheta_{\tau_r}) \tau_\epsilon \tag{2.20}$$

2.4.2 Flexural motion damping

To damp out the vibrations of the oscillatory system, the exciting force should be eliminated, and more than this, the system damping should be increased as well. Since the self-motion can directly affect the vibration responses of the flexible redundant manipulator as shown in (2.20), the arbitrary vector τ_ϵ could be chosen properly to increase the damping of the manipulator vibration modes and suppress the exciting force, while the desired end-effector position is tracked. The value of the control term $F_{M,c}$ in the modal generalized force which satisfies the vibrations damping is given by

$$F_{M,c} = -D_\phi^d \, \dot{\phi}_f + D_\phi \, \dot{\phi}_f - F_{M,n} \tag{2.21}$$

substituting this chosen term into the equation (2.18), the flexural motion system becomes

$$\ddot{\phi}_f + D_\phi^d \, \dot{\phi}_f + K_\phi \, \phi_f = 0_{nf} \tag{2.22}$$

where, $D_\phi^d = diag(2\xi_i^d \omega_i) \in \mathbb{R}^{n_f \times n_f}$ is the desired modal damping matrix, $\xi_i$is the ith desired modal damping, $(i = 1, 2, ...n_f)$. In practice, the damping ratio D_ϕ is negligible, a numerical estimator using torque/force sensors may be used to obtain the flexural reactive force. Furthermore, the numerical differential value of ϕ_f, $\dot{\phi}_f$, may be determined as well, see [64].

The value of the arbitrary vector τ_ϵ which satisfies the vibration reduction is the solution of the following equation and that by substituting (2.19) and (2.20) into (2.21)

$$A\tau_\epsilon = B \tag{2.23}$$

where,

$$A = -M_\phi^{-1} M_m^T \mu_{\tau_r} (I - \vartheta_{\tau_r}^+ \vartheta_{\tau_r}) \tag{2.24}$$

$$\begin{aligned} B = &- M_\phi^{-1} M_m^T \cdot \left[\tilde{\Gamma}_f + M_{fr} M_{rr}^{-1} \tilde{\Gamma}_r - \mu_{\tau_t} \tau_t + \mu_{\tau_r} \vartheta_{\tau_r}^+ \chi \right] \\ &+ (D_\phi - D_\phi^d) \dot{\phi}_f \end{aligned} \tag{2.25}$$

Finally, by extracting the damping action, the general control algorithm for the flexible robot plant is completed. The diagram of the proposed control method is presented

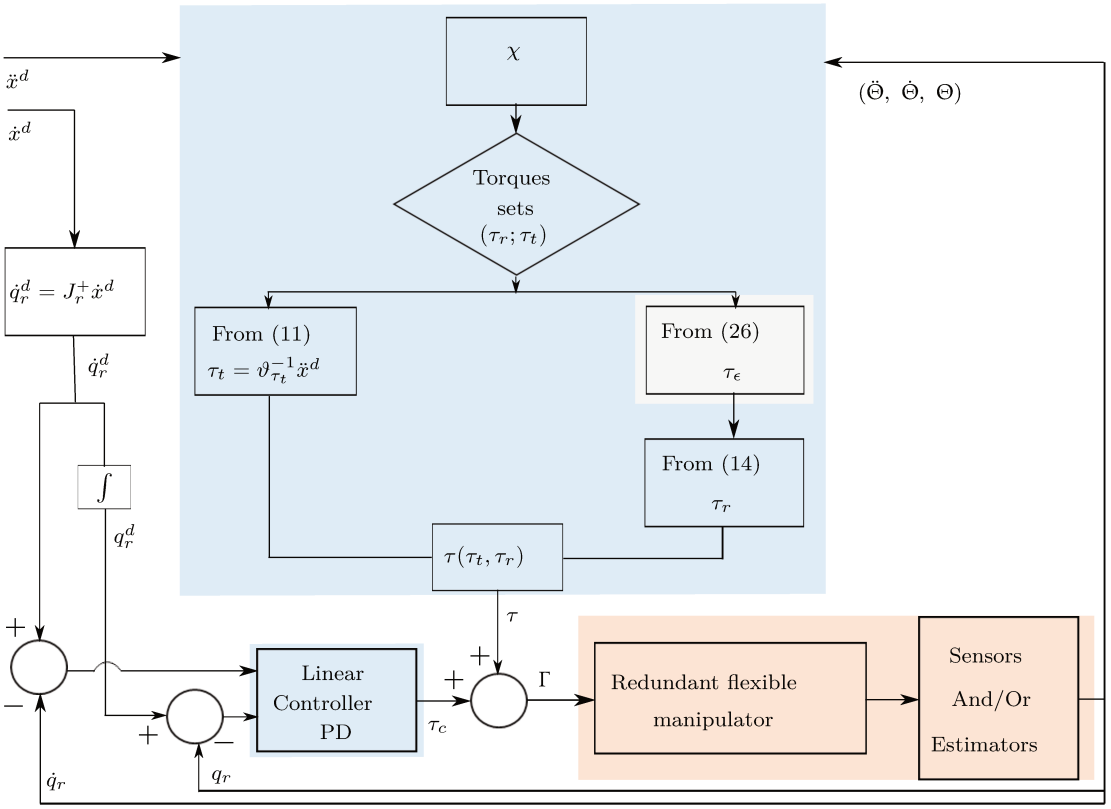

Figure 2.6: Diagram of the proposed feedback control (blue zone) with vibration reduction action (gray zone) for flexible redundant manipulator (red zone). Where $\tau(\tau_t, \tau_r)$ is a torque vector which is composed by components combination of τ_t and τ_r. τ_c is the control torque for the linearized system.

in the Fig. 2.6. The linearization action is going to reduce the control problem complexity by using factorized analysis. Meanwhile, the feedback measurement could be easily synchronized. The linear control is put forward to establish the plant stability and keep continuously precise tracking.

2.4.3 Analysis of self-motion solution

In the relation (2.23), there are m unknown components of τ_ϵ with n_f equations. The solution of this system of equations depends on the rank (ρ) of the matrix A and the augmented matrix $[A\ B]$. When the manipulator is not in singular configuration, $\rho((I - \vartheta_{\tau_r}^+\vartheta_{\tau_r})) = m - n_t$. In general, the matrix μ_{τ_r} is full rank, $\rho(\mu_{\tau_r}) = min(n_f, m)$. Since the matrix M_m^T is full rank, $\rho(M_m^T\mu_{\tau_r}) = \rho(\mu_{\tau_r}) = min(n_f, m)$. The rank of matrix A depends on the number of both the flexural degrees n_f and the difference between the redundant degrees and the task dimension $m - n_t$. The first case considers $(m - n_t) \geq n_f$, the redundant degrees are more than the flexural DOFs and $\rho([A\ B]) = n_f$, there

are infinite solutions τ_ϵ that can damp out the vibration effectively. The second case considers $(m - n_t) < n_f$, either $m < n_f$ or $m > n_f$, we have $\rho(A) = m - n_t$, if $\rho([A\ B]) > \rho(A)$ there are no solutions to the system of equations. But, on the other hand, there are infinite solutions that minimize $||A\tau_\epsilon - B||_2$ when $\rho([A\ B]) = \rho(A)$, the general solution τ_ϵ^* is given by

$$\tau_\epsilon^* = A^+ B + (I - A^+ A)\tau_{\epsilon,0} \tag{2.26}$$

where $\tau_{\epsilon,0} \in \mathbb{R}^{\mathrm{m}}$ is arbitrary vector, $A^+ \in \mathbb{R}^{\mathrm{m}\times\mathrm{n_f}}$ is the generalized inverse matrix of A. The self-motion solution τ_ϵ^* can damp out effectively the flexural motion. The equation (2.26) shows that the solution of τ_ϵ^* still depends on another arbitrary vector $\tau_{\epsilon,0}$, which means that there are many solutions that satisfy the vibration reduction. Thus, the arbitrary vector $\tau_{\epsilon,0}$ may be exploited to design a secondary task for ensuring additional performance criteria. In this case, generally, the additional ability can be used to avoid singularities or obstacles, on promise of accuracy improvement for the flexible redundant manipulator.

2.5 SIMULATION RESULTS

2.5.1 System description

To test and demonstrate the effectiveness of control strategy presented in this paper, $5R$ planar flexible manipulator is used in numerical simulations, see Fig. 2.7. The first 4 links are supposed to be rigid and the last link is flexible. Since the planar manipulator has five rigid DOFs $n_r = 5$ and $n_t = 2$ (since the end-effector rotation is considered to be free), three degrees of redundancy are available, $m = 3$. The motion of the end-effector is expressed in the origin reference frame (XY). In practice, the first mode has the most contribution to the flexural motion than the other vibration modes. In the following analysis, only the two first vibration modes of the flexural motion are retained, $n_f = 2$.

The parameters of $5R$ planar manipulator are given as follows: the length of each 5 links is $1m$. The rigid links have square cross-sections of $0.00045m^2$ and density of $8000Kg/m^3$. The flexible link has a square cross-section of $0.000225m^2$ with elastic modulus of $69GPa$ and density of $2700Kg/m^3$. All terms due to gravity in the dynamical equations are null as long as the manipulator moves in a horizontal plane (XY). Without considering any external forces, only the Coriolis force is retained in the non-linear term, $\tilde{\Gamma}_r = C(\dot{\Theta}, \Theta)$. In this example, we set the two first actuators as task torques $\tau_{t,1} = \tau_1$ and $\tau_{t,2} = \tau_2$. The last 3 torques are considered to be the redundant torques ($\tau_{r,1} = \tau_3$, $\tau_{r,2} = \tau_4$, $\tau_{r,3} = \tau_5$). In addition, no limits on the joint torques have been taken into account. The initial joint angles are $q_r(0) = (80\ \ -145\ 120\ \ -60\ \ -30)^T$ degrees, with null initial velocities $\dot{q}_r(0) = (0\ 0\ 0\ 0\ 0)^T rad/s$. The desired velocity of the end-effector is set to be null at the beginning and the end of the motion. The end-effector was

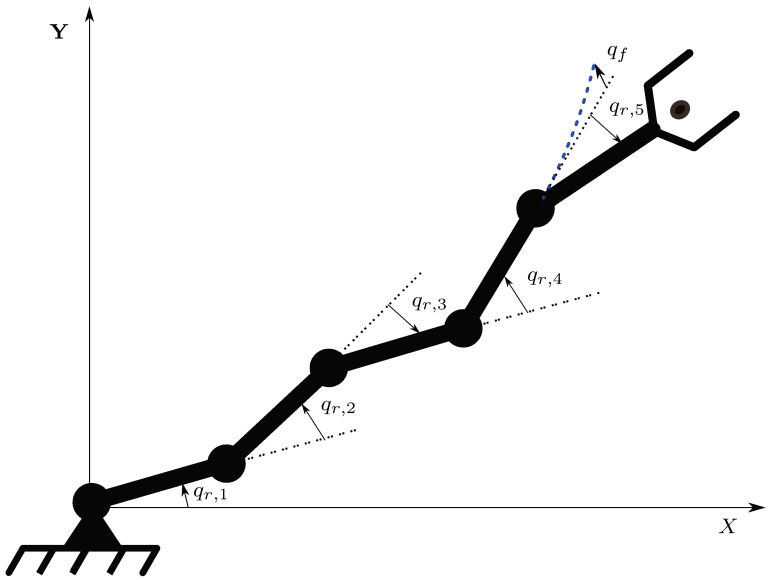

Figure 2.7: Redundant 5R planar flexible manipulator.

controlled to follow a desired accelerations which has Bang-bang profile as follows

$$\ddot{x}_d(t) = \begin{cases} \begin{bmatrix} 0.1 & 0.45 \end{bmatrix}^T \ m/s^2 & 0s \leq t \leq 1.5s \\ \begin{bmatrix} 0 & 0 \end{bmatrix}^T \ m/s^2 & 1.5s < t \leq 3s \\ \begin{bmatrix} -0.1 & -0.45 \end{bmatrix}^T \ m/s^2 & 3s < t \leq 4.5s \end{cases} \tag{2.27}$$

2.5.2 Results analysis

In the following, we analyze the effect of the agitating acceleration profile on the flexural dynamic of the manipulator. The results have shown the responses of the system to the proposed control approach for the two cases, i.e. with and without the utilization of torque's self-motion to damp out the induced vibration. In both cases, the feedback linearization action is active, where the extra set of the torques is devoted to countervail the nonlinear dynamics in the system.

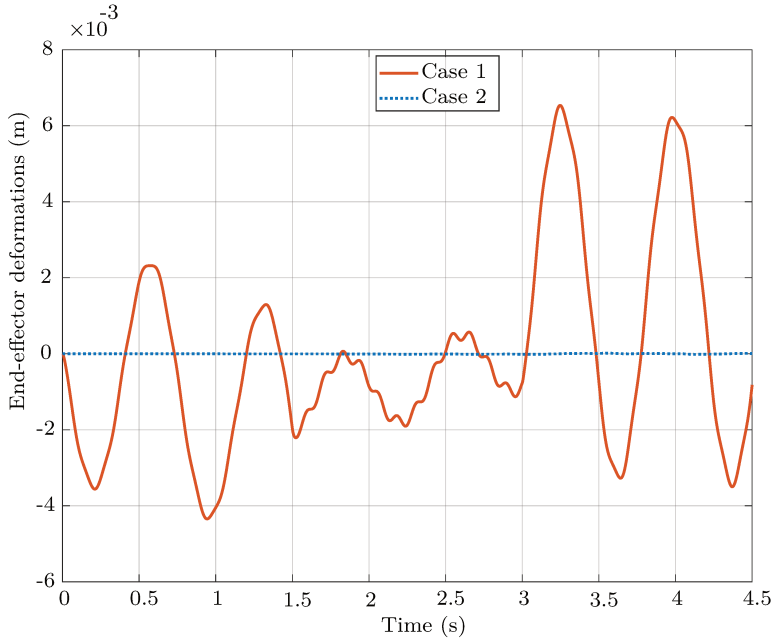

Figure 2.8: End-effector deformations for both cases.

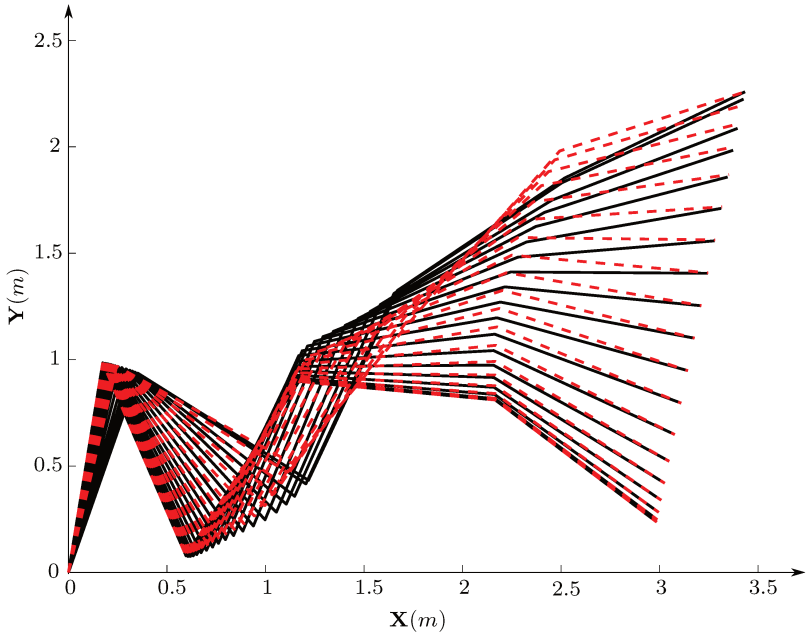

Figure 2.9: Motion configurations of the planar manipulator (solid black line: case1, dashed red line: case2).

Case 1 (τ_ϵ is null):

In this case, the self-motion is only computed to cancel the system non-linearity in (2.13). It is possible to apply the proposed control algorithm because the degree of the redundancy is greater than the work-space dimension. Besides, a conventional PD controller at joint level is designed and then applied to the resulting linear system for maintaining the end-effector position tracking. On the other hand, it is shown in Fig. (2.8) that the end-effector deformations are non-negligible, since the end-effector vibrations have not been reduced. The end-effector follows the desired trajectory with vibrations of maximum amplitude equals to $6.6mm$.

Case 2 (τ_ϵ is not null):

In this case, τ_ϵ is calculated from (2.26). Taking into account the relation (2.26), the self-motion is recalculated to get rid of the non-linearity, and to damp out the vibration modes of the resulting flexural motion simultaneously. One may note that, the torque magnitude of τ_r may become very large as the end-effector approaches singularity. As shown in Fig. (2.8), the deformations of the end-effector are well reduced via self-motion. Comparing the Fig.(2.10) with Fig.(2.11), it can be clearly seen that the self-motion has been changed to take into account the additional task of reducing the vibration deformations, see Fig. (2.9). The end-effector follows the desired trajectory with small deformations (around $0.02mm$ of maximum amplitude).

The torque profiles are shown in Fig. (2.10) and Fig. (2.11). The actuator torques of the two first actuators (τ_1 and τ_2) are significantly larger than the other actuator torques. This depends on which actuator torques are chosen as τ_t or τ_r. Therefore, it is preferable to have a large limit for the first two torques to develop sufficient energy during the manipulator motion. The resulting torques in actuators τ_3, τ_4 and τ_5 in Fig. (2.10) are slightly different to those in Fig. (2.11). This is due to the changing in the self-motion solution with the purpose of damping out the vibrations.

The real time implementation of the proposed algorithm is feasible. Since the robot state such as joint coordinates are generally measurable via implemented sensors, the main challenge is to measure the flexural motion states. Nevertheless, that may be resolved using information derived from torque/force sensors to estimate both the flexural reactive force and the modal coordinates following the estimation approach in [64]. Thus, the discretization and the synchronization problem of data is avoided. Afterwards, the robot model can be simultaneously linearized since the calculation can be factorized.

In the all previous methods presented in [17, 62, 63, 64, 65], the redundancy resolution is used for vibration reduction only and none see the advantage of having more redundant degrees specially in the case of the hyper-redundant flexible manipulator. The proposed algorithm takes advantage of all redundant DOFs, first for controlling the manipulator (feedback linearisation via redundancy resolution), and secondly to suppress the induced vibrations of the flexible links. Moreover, no model simplifications are needed for control design which ensures the reliability of the proposed algorithm. The vibration behaviour is well treated compared to the previous articles, through the analysis, one can see

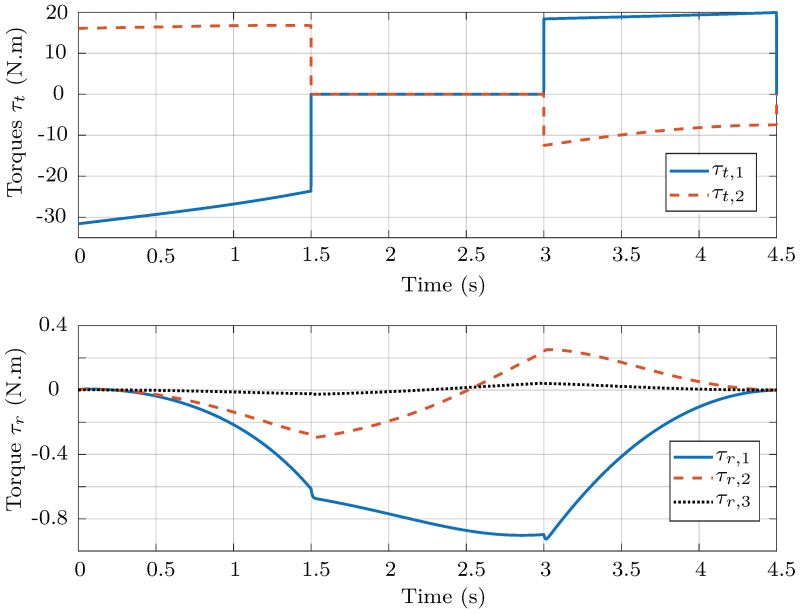

Figure 2.10: Control torque profiles- case 1.

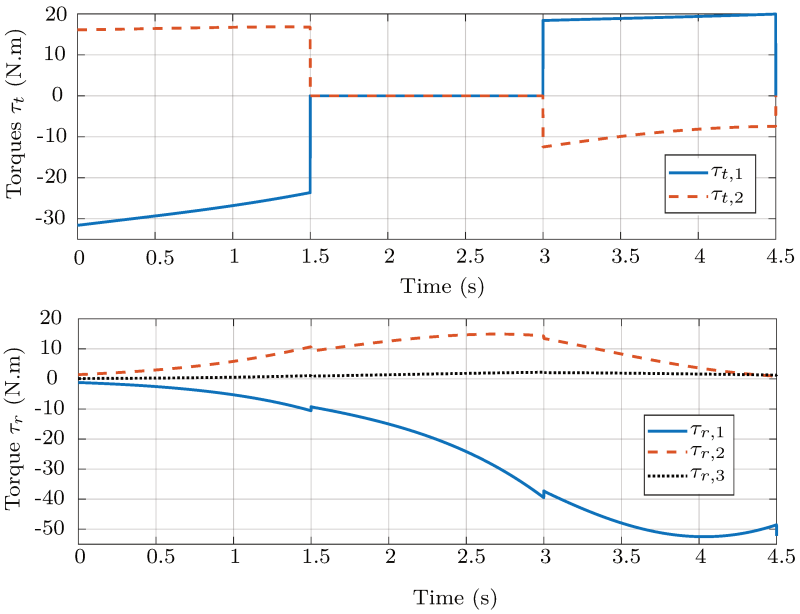

Figure 2.11: Control torque profiles- case 2.

clearly how the vibration are damped. The simulation result shows the effectiveness of the proposed approach.

2.6 CONCLUSION

In this chapter, the self-motions of redundant flexible manipulators are exploited for both designing a control algorithm and establishing a novel method for vibrations reduction of its end-effector while tracking a given trajectory. The feedback control design takes advantage of the extra torques to linearize the plant by eliminating the nonlinear term in the motion dynamic as shown in section 2.3. In section 2.4, the damping action is implemented through the modal analysis of the flexural motion. The self-motion adequately helps to transform the vibration system to free over-damped system. The main contribution is to combine the two control actions in one algorithm using the redundancy resolution of the flexible redundant manipulator. This is a useful result of interest and highly advantageous since the redundancy feature reinforces the optimal functionality of the flexible robot to overcome its positioning limitation.

The effectiveness of this approach has been validated by the results of numerical simulations in section 2.5. It has been shown that the self-motions have cancelled the undesirable dynamics, besides, through the dynamic coupling between the rigid and the flexural motions the vibrations of the end-effector have been reduced as well. The redundant torques can compensate the nonlinear dynamic in preferential directions, i.e three torques are needed to get completely rid of the nonlinear dynamic in three translational directions of robot motion. Only one extra redundant torque is able to damp out the fundamental mode of the flexural motion. In practical applications, only the fundamental mode is retained for frequency analysis of the flexural motion, and at most the second contributed mode could be added if the vibration magnitude are really considerable. We may conclude that by adding additional redundancy DOFs the vibration reduction may become more significant. The analysis of the self-motions satisfying the vibration reduction revealed an additional ability which may be used on promise of improving the kinematic and/or dynamic performances of flexible redundant manipulators.

The robustness of the control approach relies on an accurate dynamic model of the manipulator, and effective measurement and/or estimation benchmark to avoid any sensitivity or dysfunctionality. Indeed, the practical implementation seems challenging but some simplifications are feasible for real time manipulation. However, our interest in this study is to exhibit the core of the problem investigation. In some cases the frequency of the vibration could be out of the plant bandwidth frequencies limits, i.e the vibrations oscillate too fast regarding the manipulator time response. The controller may be unable to synchronise the control signals and thus unable to damp out the vibrations. Nevertheless, the results of the numerical simulations are considered for further development on real manipulator.

Once the deformations are accumulated and quantified for the whole mobile robot manipulator system (mobile platform, manipulator, load), in chapter 3, we design a

practical approach for accurate robotic manipulation in industrial application. The open-loop vibration control is preferably chosen over the feed-back action in this chapter for practical limitation.

Chapter

3 REDUNDANCY EXPLOITATION FOR THE ROBOTIC MANIPULATION OF FLEXIBLE LOADS

During the manipulation of a low-stiffness load, such as a bumper or an exhaust system in the automotive industry, large motion-induced deformations and vibrations may occurred. These deformations will have detrimental effects on the settling time, on the accuracy and on the integrity of the operational process in a constrained environment. In addition to the quality degradation of the manipulated assembly parts which is eventually going to increase the production cost, any mishandling may endanger the security condition of the employees near the robot within the context of human-robot collaboration.

This chapter addresses the problem of the robotic manipulation of deformable objects to guarantee both soft robotic manipulation and safe collaborative environment. The errors of the robot can be quantified along with the load deformation as concluded in the chapter 2. Therefore, the main aim of the present work is to reduce the elastic deformations and the residual vibrations of flexible loads when they are handled by a robot manipulator. In section 3.1, we introduce the related works and the main control strategies to handle the load deformation during the robotic manipulation. Section 3.2 introduces the formalism of this present work and the mathematical modeling.

The trajectory shaping approaches, i.e. the smoothing filter or the input shaping methods, are well-known solutions for the suppression of residual vibrations at the end of a rest-to-rest motion. It is the outcome of the study previously given in section 3.3 to conclude on the influence of the trajectory shape on the motion-induced deformations. However, using trajectory shaping technique alone may not be sufficient to suppress the static elastic deformations during the transfer phase of the object. Thus, in section 3.4 we propose a two stages feedforward-based approach that combines trajectory shaping technique for vibrations reduction with deformation compensation trajectory. The latter exploits the null-space of the manipulator to mitigate the flexural motion of the flexible

load. The effectiveness of the proposed algorithm has been verified analytically in section 3.5 via the sensitivity analysis of the control design and then conducted experimentally on industrial robot in section 3.6.

3.1 INTRODUCTION

3.1.1 Related works on robotic manipulations of flexible objects

The robotic manipulation is highly concerned by an exigent production process with several industrial tasks including assembly operations, loading and unloading parts from an assembly line or a machine, and the safe manipulation more specifically in the physical human-robot interaction. These factors should be respected in aim to build a reliable and a flexible new generation of factories to satisfy the highly demanding consumption-markets. The optimal profits could be reached not only by reducing the consumed energy but also by respecting the quality standards of the products. The final product is mainly the outcome of multiple production processes, starting from the designing and then the manufacturing of the product until the assembling and the packaging stages. The robot tends to manipulate a large selection of pieces and parts in different production stages. One may note that some specifications should be concerned due to the mechanical structure of the manipulated objects, which can be physically rigid or flexible. When handling a flexible load at the robot tip, the accuracy of the previous robotic tasks, sometimes even their feasibility, may be significantly limited by undesired motion-induced vibrations and deformations of the manipulated object.

Many works on flexible objects manipulation have been done in different industrial contexts. The flexible objects may be categorized into separated sets based on their mechanical properties, such as compliance, strain and compression strength. For example three different sets are proposed in [92, 93]: linear, thin and lump objects. The flexible objects with highly deformed structure are referred to as soft object. In other point of view, they can be classified based on their shape and dimensional deformations (beam-like, planar, 3-D volumetric objects) [94]. The industrial robotic manipulation is totally different from human-like manipulation [95]. For example, the clothes manipulation is a critical case because of their thin-shell and non-linear deformations which are issued from imposed geometric and kinematic constraints [96, 97, 98]. In [98], the mesh of 3-D models is used to collect the necessary database in aim to predict the optimal trajectories to fold/unfold garments from/to a desired pose. The manipulation pipeline includes the visual recognition for the pose estimation at first stage before performing the robotic manipulation. The performance of the approach depends mainly on the quality and the analysis of the database. Therefore, the optimization algorithm such as deep learning may enhance significantly the manipulation scenario in practice. For example the ropes and clothes manipulation [99]. The mobile manipulation of flexible objects is introduced as well for domestic service robots within the context of human-robot co-operative manipulation [100]. Similarly the human-like movements in the manipulation of flexible objects is adapted, see [101]. The transportation of the liquid container is

Figure 3.1: Industrial context of mobile robot manipulating a flexible car bumper.

susceptible to provoke oscillations and irregularities on its surface which is referred to as sloshing effect, see for instance [102, 103]. The sloshing waves are caused by the force resultant of the acceleration profile and the gravity. In [103], the liquid surface behaviour is depicted by spherical pendulum system to construct an adapted trajectory for the transfer of liquid containers with minimal sloshing.

In automotive and aerospace industries, the robotic manipulation of the manufactured parts in assembly plants and production lines involves flexible materials, such as a bumper and plane-wing panels, see figure (3.1). These particular parts are essentially made from light weight materials such as aluminium, plastic and carbon fiber panels. Their deformation behaviour according to one motion plane is presented by the first modes of the vibrations (the most sensitive during displacement) which are preponderant, and classically can be denoted by an equivalent mass-spring system [104]. This case of study is practically less complex compared to soft objects with high non-linearity due to the friction, hysteresis and unpredictable parameters variation. For example in [105], the stiffness of large-structure parts in aircraft manufacturers may induce posture uncertainties during the assembly process due to the non-uniformly contact force, which is distributed over the panel surface. Such flexible parts with unchanged shape in the

natural and recovering states integrate generally specific and uniform stiffness properties. Thus, the modeling becomes effectively simple and coherent, and the deformations control may conduct to better results in practical applications.

3.1.2 Review on deformations control

In practice, the positioning and the manipulation of flexible objects is restrained by the issues related, for a major part, to the sophisticated modeling and eventually the deformations control complexity. The physical contact resulting from the interaction of the manipulated object with its environment adds more geometric constraints to the system, i.e. the applied force at the end-effector and the external forces applied on the object such as gravity and friction. The existing methods can be coarsely divided into three main categories: physics-based model control such as the state feedback approach, vision-based techniques, and empirical approach such as the open-loop.

3.1.2.a Feedback control

The state feedback approach is generally based on the use of extra force/torque sensors to measure the vibrations of the flexible object. In [29], a vibration control scheme is synthesized based on the feedback of vibration which is measured by the force sensor. The control is established by integrating the vibration control into the controller of the robot wrist joint. In [27], authors proposed a velocity field tracking-control scheme using proportional integral force feedback to transport and manipulate a deformable material with the mobile manipulator. The object-state feedback aims to set the deformations in tolerable range. In [106], an example of path planning in biomedical applications is treated, where the visual feedback based control is used to adjust the cells orientation in fluid flow via micro-pipette and to optimally compensate for external applied forces. In [105], the robot system integrates the data processing of the force sensor in the closed loop to establish an admittance control of large flexible panels, the end-effector force of the manipulator is adapted to comply with the applied force along the contact surface of the panel during the assembly process of the aircraft wing. The high-speed robot motion can be exploited to reduce the dynamic complexity of flexible objects to an equivalent linear model in aim to simply generate a feasible and optimal motion profile [107]. The rope dynamic is simplified under high constant robot speed, where the model-based deformation control is practically achieved regarding the dynamic constraint and the neglected dynamics [108]. In [109], the nonlinear dynamic is firstly descritized and then linearized it around the origin which allows to build a robust controller for the linear system. This is helped to design the linear controller for deformable objects positioning, such as PID [30]. In [110], a fuzzy control is proposed and compared with PID controller based on the force/torque data acquisition to reduce the vibrations due to the manipulation of flexible linear object. Nevertheless, the variation of the elasticity proprieties is inevitable and mainly depends on the trajectory form and the object hysteresis mechanism properties which are underlined in [111]. In [31], an adaptative control algorithm is proposed for manipulating flexible rubber objects, included the robust control law based

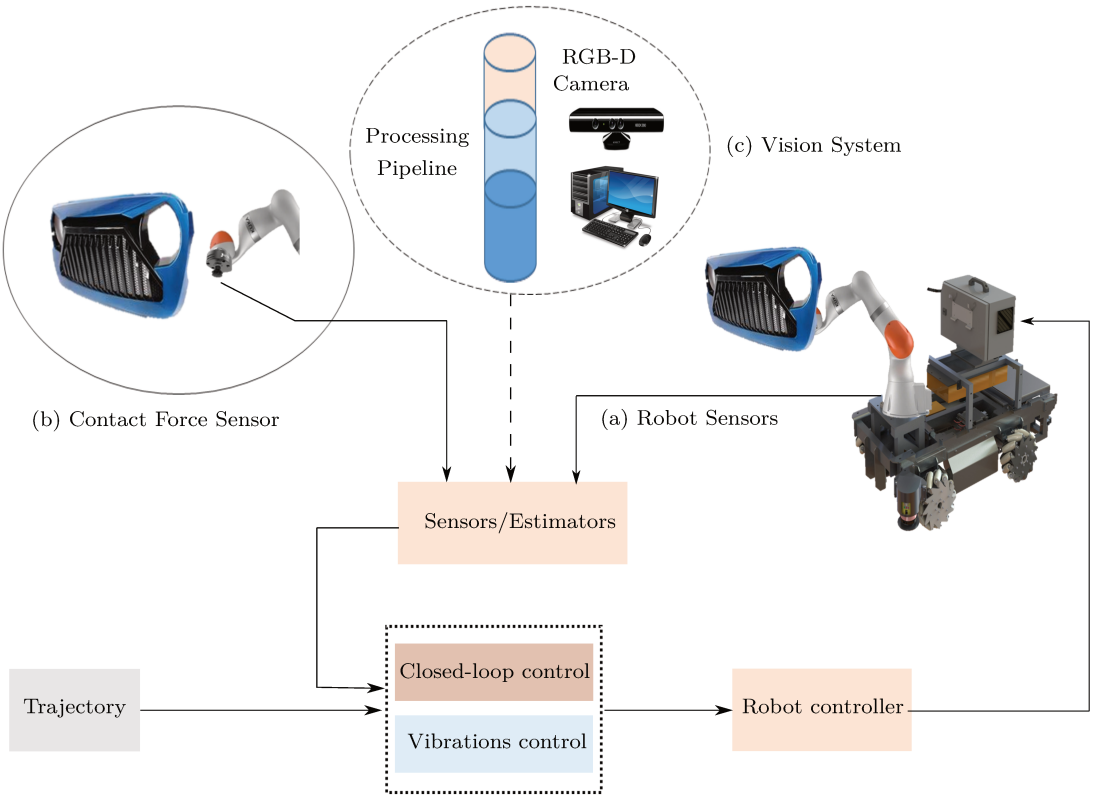

Figure 3.2: Flexible load manipulation: (a) robot joint sensor which are required to establish robot control ;(b) force feedback ;(c) vision based control.

on sliding mode approach and Lyapnov function guaranteed the stability performance and the robustness against impedance parameters switching. Advantageously, the adaptative sliding mode is used for the position-based control to damp the vibrations of deformable linear objects in [112]. The dynamic model is divided into actuated and under-actuated sub-systems using linear transformation. In [113], author proposed an approach for cooperative manipulation of a complex pendulum-like objects. The acceleration and torque signals are used in the closed-loop control via measured contact forces. The proposed adaptive control for energy injection is based on the estimated natural frequencies. In the other hand, the motion control algorithm with minimum energy manipulation can be achieved by resolving an optimization problem by taking into account the deformations and the collision avoidance in the the cost function as in [114]. In [115], the kinematic of a flexible object is decoupled into a rigid body motion and a flexible motion which represents the deformations using clamped-free model, where the PD controller is used in the close-loop control for vibrations suppression. As shown in figure (3.2), the necessary information to build the control algorithm can be obtained from different feedback signals, such as force sensors, torque sensors and vision system.

3.1.2.b Vision-based control

The fusion of vision and force feedback for the control of highly deformable objects is sometimes necessary for complex system manipulation [32]. In [116], the motion dynamic model of flexible object is predicted using deep neural network which is based on RGB-D camera as the sensor data feedback. The time-series torques are introduced in the backpropagation algorithm to generate the input torques command for flexible objects manipulation, see figure (3.2). This strategy is referred to as the vision-based manipulation [117]. The flexible object manipulation can rely on the vision system without using any physical simulations or modeling, only by employing an optimal post-processing and recovering phases [118]. In [119], a model-based vision system for robotic manipulation of ropes is presented. The self-supervising learning algorithm is used to estimate the object dynamic model. For practical applications, a method which produces training data for aim to plan a trajectory with reduced state spaces is presented in [120]. It is used forward for neural network architecture construction of deformable objects [121] such as force control based on neural networks for vibration damping [122]. In [123], visual-servo control for the position and shape of a deformable object with unknown compliance parameters is proposed. The data are collected from the both end-effector motion and object's deformation measures, then Gaussian process regression is used for learning object model. A comparison study which is conducted on different methods of reinforcement learning methods is presented in [124, 125], and similarly for deep neural networks in [126]. In [127], authors proposed a mass-spring modeling technique to construct a two-dimensional quadra-angular mesh of cloth, where the particles are connected by one or more different virtual springs: structural, shear and bending spring. The first stage simulation is conducted to compute the change of the particle position for predicting the deformation and finally estimate an optimal path for the robot manipulator. In [128], authors tend to embed the mesh of the clothes structure to reduce the model order based on admissible solution of physical loss terms. Through the robotic manipulation, the mass-spring modeling approach is implemented to identify the stiffness properties of the flexible structure similar to living plants [129]. In [130], an adaptable system of a combined pipeline is proposed including vision, physical modeling, prediction and learning for an optimal real-time manipulation of flexible objects, such as peg-in-hole and putting-down on flat surface actions. The object recognition and localization problems with a new hybrid pipeline are handled in [131]. In case of mobile robotic manipulation of deformable objects, in [132], the deformation cost function is estimated using Gaussian process regression, while the force sensing identifies the parameters for the compliance model by acquiring the contact force to predict the upcoming object pose.

In general, the flexible objects have complex and non-uniform properties which could make it hard to use the systematic-modeling approaches [133, 134, 135]. In addition, the numerical or analytical modeling approaches such as finite elements are suitable for numerical simulations but difficult to incorporate into the robot controller in practical tests. The efficiency of the state feedback approach may be primarily limited by the technical and economic viability of adding extra sensors.

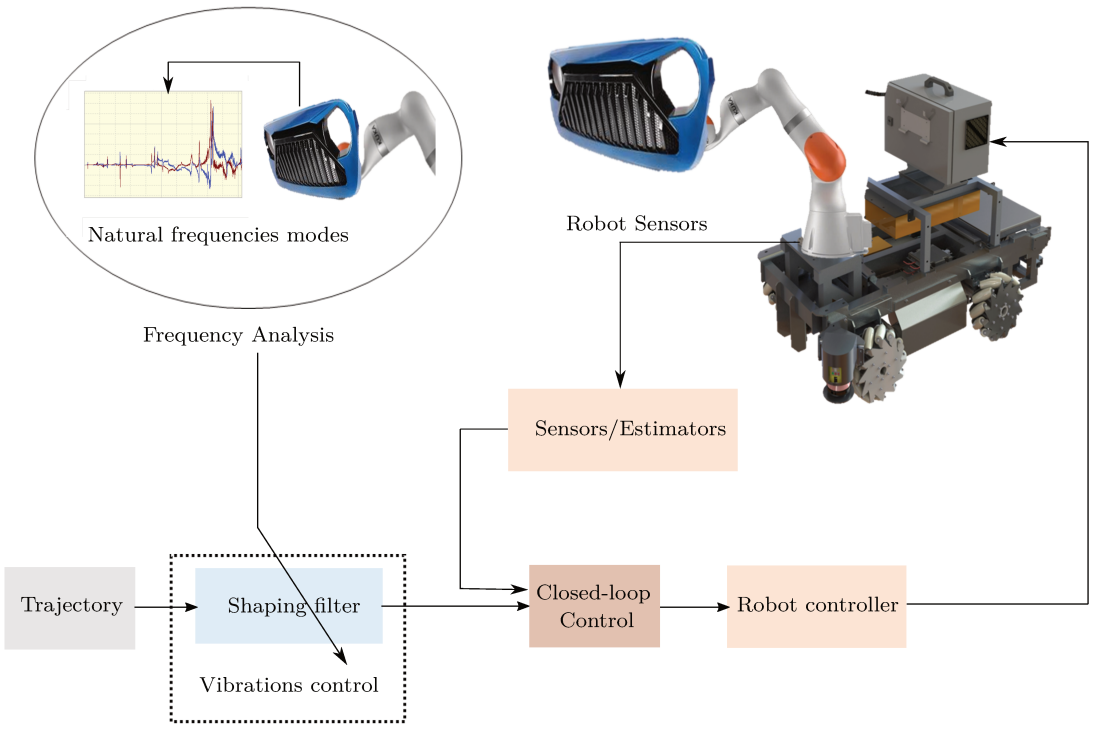

Figure 3.3: Open loop control approach: input shaping technique illustration.

3.1.2.c Open-loop control

From an open-loop point of view, the feedforward control is mainly designed to predict an optimal trajectory based on the pre-acquired information on deformation proprieties. In [33], the vision-based technique takes advantage of the 3D environment simulation to physically make prediction for the manipulation of deformable linear objects. In [98], the deformations minimization problem is resolved using vision system to build an optimal trajectory from a given cloth pose. Before proceeding to the manipulator motion planning, the model-driven is used in feedforward control for pose/object recognition, i.e. to find the match between the actual object pose and one from formerly existing database. The auto-regressive with the exogenous stochastic is introduced in [136] to simply model the robot-beam system. The control algorithm is consisted of a feedforward block which integrates an adaptative PID controller and a feedback control for the robot system to optimize the force applied to the flexible metallic beam and reduce the residual vibrations. The study shows low sensitivity to the measurement noise and the parameters uncertainties. In [137], the feedforward control which is based on the object parameters' identification is used along with the high-speed visual feedback control by which the order of dynamic model is reduced in aim to easily generate an adequate smooth trajectory.

The input shaping technique is a well-established method to suppress motion-induced residual vibrations, see for instance [34, 35]. This technique turned to be a robust and effective algorithm in practical applications, where only the natural frequency and the damping ratio of the contributed flexural modes are required [138]. The deformations of the flexible objects body with uniform properties can be characterised by set of dominant vibratory modes, which may be used afterwards for the open loop control, see figure (3.3). For example to design appropriate filter shaping [133, 139, 140, 141]. In [139, 140, 141], the oscillatory behavior of a liquid container during motion is interpreted as a spherical pendulum. Shaping filter is used to suppress the oscillatory behavior of the liquid, and the trajectory of the robot is adapted by introducing a tilting compensation value to compensate for the deformation during the motion. The simplicity of such control is advantageous for the industrial applications. It is feasible to apply such a control only when considering a finite number of natural modes such in the case of beam-like deformed objects.

3.2 LOAD DEFORMATIONS MODELING

In this work, the manipulation of flexible object with the shape-recovering property is considered. The soft objects are excluded in this case. The translational displacement task of a flexible object with n DOFs serial manipulator ($n \geq 6$) is retained for the following development. The robot manipulator is kinematically redundant for the previous 3D task and among the remaining extra DOFs, the orientation in 3D space will be used in the proposed methodology for the elastic deformation compensation. In the case of linear transfer, the deformations due to twisting and extension of the load are ignored, only bending deflection is maintained for the geometrical representation of the load-shape curvature. Thus, the modeling passes from complex to linear model formalism. This can be reached by regrouping the system vibration modes in the modal representation.

The flexible object to be manipulated is assumed to be submitted to dominating modal deformations. In practice, the flexural motion of a near-linear object, i.e. with a main deformity axis, is dominated by the first bending natural frequency in the two transverse directions. For the sake of simplicity, figure 3.4 demonstrates the planar definition of the problem for one bending deformation. One may note that the flexural motion in the other plane can be handled using the same approach. The flexible load is supposed to be rigidly grasped by the robot gripper at the robot Tool Center Point (TCP). Its position is noted $\mathbf{P}_{tcp}$. The contact point robot-load undergoes, permanently during the motion, the resulting force from robot driven torques.

In the following, the elastic deformation of the object is considered. The pure flexural motion of the object tip, noted $w(t)$, is assumed to occur in robot motion direction only, i.e. Y_{tcp} axis, where no axial deformation is considered. Hence, the coordinates of the object tip, noted $\mathbf{P}_{ob}$, can be expressed in the TCP frame R_{tcp} with the origin point $\mathbf{P}_{tcp}$

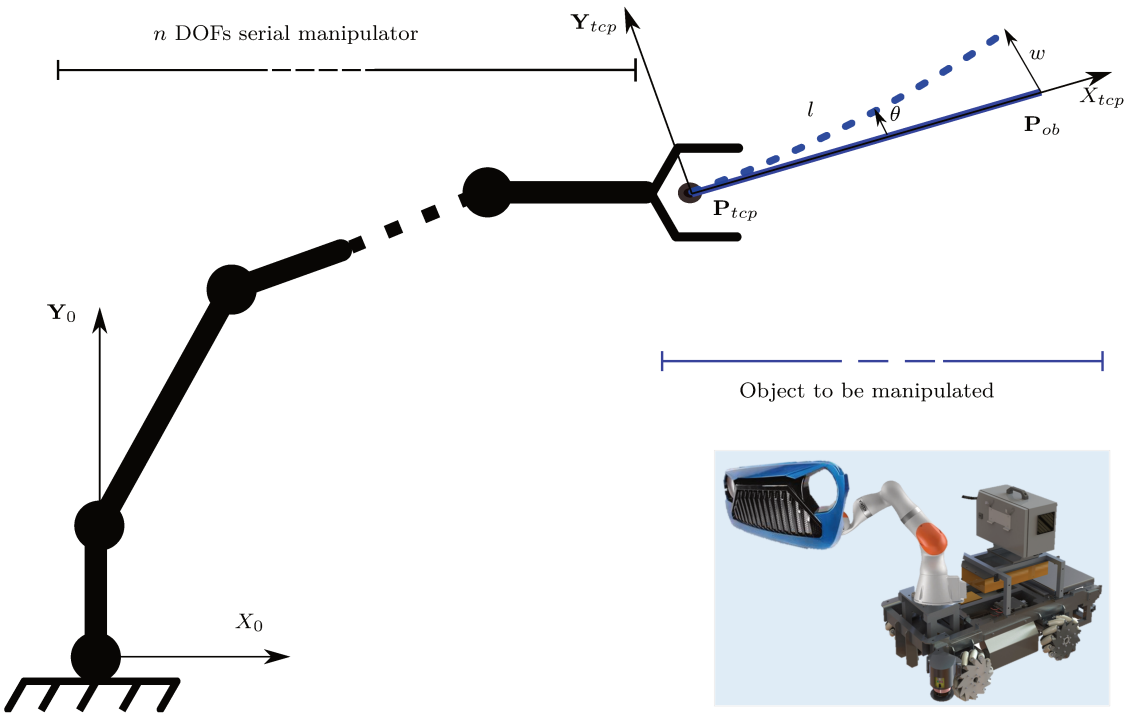

Figure 3.4: Parameters definition: robotic manipulation of a cantilevered object with one dominating bending motion.

as follows

$$\mathbf{P}_{ob} = \left\{ \begin{array}{c} l \\ \\ w \end{array} \right\}_{R_{tcp}} \tag{3.1}$$

with l and w are respectively the length and the flexural deformation of the object.

The dynamics of the points $\mathbf{P}_{tcp}$ and $\mathbf{P}_{ob}$ in the fixed absolute frame are submitted to the same rigid-body motion imposed by the robot TCP trajectory. The evolution of the position $\mathbf{P}_{ob}$ results from the sum of the previous rigid mode with the elastic deformation $w(t)$. Noting $y_{tcp}(t)$ and $y_{ob}(t)$ respectively the position of the points $\mathbf{P}_{tcp}$ and $\mathbf{P}_{ob}$ in Y_{tcp} direction, the deformation $w(t)$ can be written as

$$w(t) = y_{ob}(t) - y_{tcp}(t) \tag{3.2}$$

Considering now small variations of the deflection angle, noted θ in figure 3.4, the

approximated deflection angle of the object can be expressed by the following expression

$$\theta(t) \sim \frac{w(t)}{l} \tag{3.3}$$

The dynamic vibration of the object tip, which occurs only in Y_{tcp} direction, can be modeled by the following general second order equation in continuous Laplace domain

$$\frac{y_{ob}(s)}{y_{tcp}(s)} = \frac{\omega^2}{\omega^2 + 2 \cdot \xi \cdot \omega \cdot s + s^2} \tag{3.4}$$

with s is the Laplace operator, ω and ξ are respectively the natural frequency and the damping ratio of the considered bending mode. Substituting (3.2) and (3.4) into (3.3), the dynamics of the deflection angle θ can be written

$$\theta(s) = -\frac{1}{l} \cdot \frac{2 \cdot \xi \cdot \omega \cdot s + s^2}{\omega^2 + 2 \cdot \xi \cdot \omega \cdot s + s^2} \cdot y_{tcp}(s) \tag{3.5}$$

which leads in time domain to the differential equation

$$\theta(t) + \frac{2 \cdot \xi}{\omega} \cdot \dot{\theta}(t) + \frac{1}{\omega^2} \cdot \ddot{\theta}(t) = -\frac{2 \cdot \xi}{l \cdot \omega} \cdot \dot{y}_{tcp}(t) - \frac{1}{l \cdot \omega^2} \cdot \ddot{y}_{tcp}(t) \tag{3.6}$$

As a consequence, the deflection angle for the considered bending mode will be driven by the acceleration and the velocity of the robot TCP in motion direction (Y_{tcp} axis in the example above). In the same way, the TCP acceleration along Z_{ob} direction may induce vibrations of the first bending mode around Y_{tcp} axis.

The shaping filter approach can practically be the privileged solution to get rid of the vibrations in (3.6) over the feedback state technique, since the states signal reconstruction requires complex architecture. Thereafter, the relation between the trajectory form and its impact on the induced vibrations is discussed in the next section. The conventional limited-acceleration profile is used as referential for the comparison study.

3.3 TRAJECTORY PLANNING FOR VIBRATIONS REDUCTION

3.3.1 Motion laws and motion-induced vibrations

The trajectory can be interpreted as the admissible solution for a mathematical problem with kinematic constraints (on position, velocity, acceleration, jerk, ...) which is defined in time interval $[t_j \quad t_{j+1}]$, see (3.7). The trajectory is mainly constructed from one of the two principle categories: polynomial and trigonometric or it can be a combination of both, see for instance figure (3.5). Each law is characterized by its acceleration and deceleration phase.

$$Q = Q(t) \qquad\qquad t \in [t_j \quad t_{j+1}], j \in \mathbb{N} \tag{3.7}$$

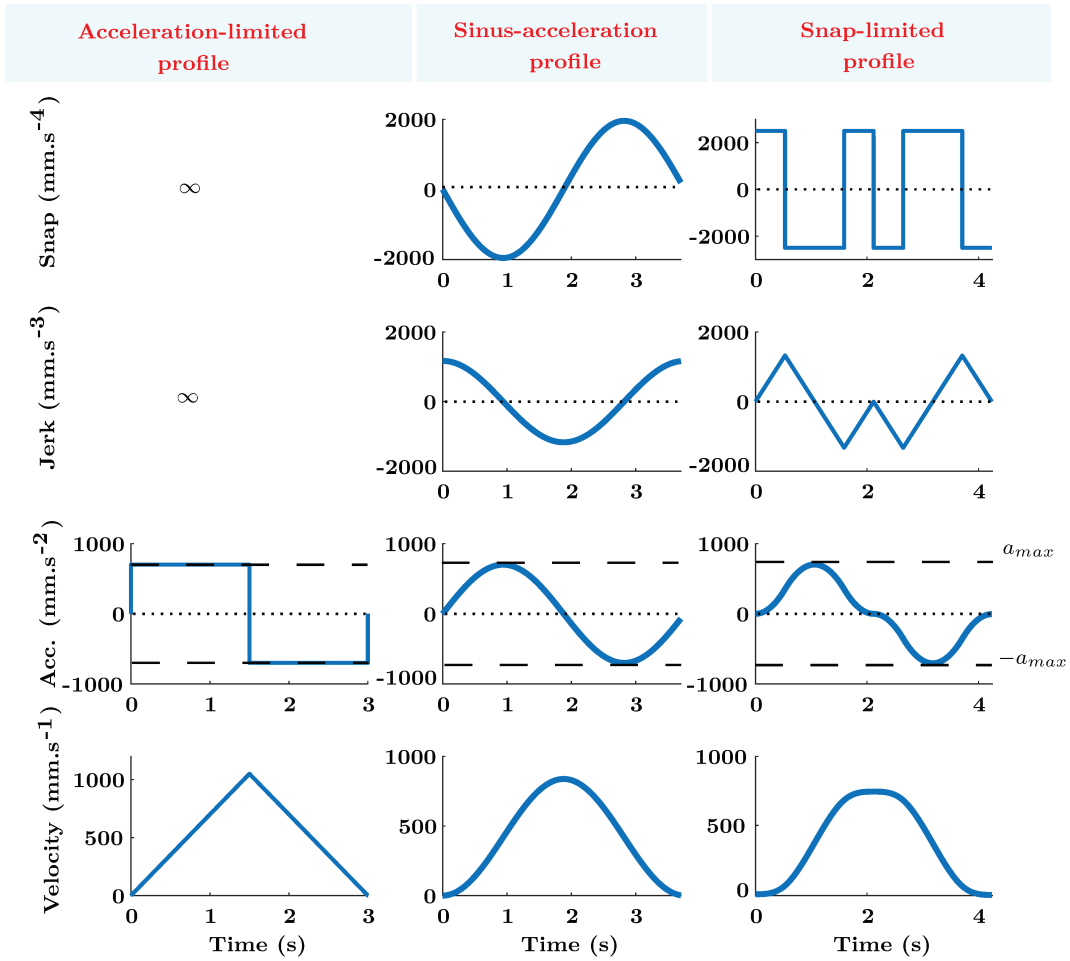

Figure 3.5: Motion profiles: polynomial (acceleration-limited profile and snap-limited profile) ;trigonometric (sinus-acceleration profile).

1. **Polynomial**: the problem expressed in (3.7) can be numerically resolved using a polynomial with $(n_p + 1)$ terms, n_p is the highest power which is also equivalent to the number of the kinematic constraints. Moreover, it defines the degree of smoothness regarding the induced vibrations from the injected trajectory.

$$Q(t) = c_0 + c_1 \cdot t + \cdots + c_{n_p} \cdot t^{n_p} \tag{3.8}$$

where $c_i \in \mathbb{R}$ for $i \in \mathbb{N}$, i.e. $i = 0, 1, ..., n_p$, are the polynomial coefficients.

Many trajectories can be driven based on the polynomial degree. For example, the linear trajectory for constant velocity, the curved trajectory for constant acceleration or constant jerk and so on for snap and higher derivatives. The acceleration and snap limited trajectories are presented in figure (3.5). In [142], optimization techniques are presented and analysed their impact on the robot's kinematics and

dynamics, the distinguished criterion arising from the system itself or imposed by the task are considered such as minimum time and low energy consumption. One may note that the degree of the smoothness is increasingly proportional to the polynomial degree. The higher-degree polynomial allows to consider additional constraints. Practically, it is coherent to minimize the amplitudes of the derivatives of the position profile throughout the movement for better homogeneous motion. The simple linear trajectory with discontinuous velocity could not be favorable for practice applications owing to the fact that the impulsive acceleration are not supportable by the robot actuator. One may note that the discontinuous acceleration profile may induce deformations along the executed trajectory for systems with mechanical elasticity, such as in the case of flexible robot and/or flexible transported-load. Such an effect is more noticeable for minimum-time motion execution, where the required acceleration and the velocity values are considerably high. In [143], for smoothing purpose, the time-optimal constrained trajectory is constructed by controlling the jerk profile where the cubic splines are exploited for parameterization. Obstacles avoidance, joint limits and motion-duration are included in the cost function as well. In [144], roots multiplicity are employed to determine the coefficients of higher-degree polynomial in aim to build smoother acceleration profiles with minimum jerk. Nevertheless, numerical difficulties for coefficients identification are inevitable. Moreover, the algorithm consumed-time should be considered. In [145], a dynamic approach for cubic polynomial curve is optimized using the Golden-Section method and under the pseudo-velocity consideration. The trajectory is implemented online in industrial robots for the experimental validation. In [146], the multi-points trajectory generation is addressed. A numerical polynomial interpolation is used in between the adjacent path points to insure a continuous connection. On the other hand, the numerical computation between two successive points are more susceptible to influence the smooth motion quality compared to trigonometric functions.

2. **Trigonometric**: the trajectory is constructed in this case from trigonometric functions (sine, cosine, $\cdots$) which has the propriety of non-null continuous time-derivatives in the time interval $[t_j \;\; t_{j+1}]$, algebraically this class of functions belong to C^{∞} class. For example, the harmonic trajectory in which the acceleration and the position profile are proportional but with priorly inverted sign, see for instance the sinus-acceleration profile in figure (3.5). The acceleration profile is discontinuous at the time interval limits t_j and t_{j+1}. Therefore, the cycloidal and elliptic trajectory are proposed, which present a continuous jerk profile to insure smoother motion.

$$Q(t) = f(sin(t), cos(t), t) \tag{3.9}$$

This kind of trajectory has an infinite continuity out of the commutation points. In [147], a synchronized and jerk-bounded trigonometric S-curve profile is built in joint space, where the jerk takes sine wave form. In [148, 149], a trigonometric splines trajectory generator for robotic arms is proposed in the joint's space traject-

ories using fourth-order trigonometric splines. Smooth and time-optimal S-curve trajectory using polynomial and trigonometric model combination is proposed in [150]. The trigonometric and Polynomial functions combination are also used for mobile robot application [151]. In [152], an algebraic and trigonometric splines are merged to generate a continuous trajectory for robot manipulators.

3. **Other trajectory profiles**

   The trajectory profile essentially depends on the chosen application which can be a combination of the elementary trajectories presented above. In [153, 154, 155], an offline planning is suggested to handle the case of multiple constraints including those of the payload. In [156], the weighted sum of jerk and the execution time terms are considered in the cost function. The resulted trajectory is optimally minimized and then validated experimentally on an industrial robot in [157]. An optimal trajectory is assigned by properly selecting the desired criteria such as continuous function with continuous derivatives and optimally minimum values for the acceleration or jerk. In [158], the quintic and cubic polynomial equations are merged to provide smooth and continuous motion trajectory to drive the knee joint in aim to replicate the walking cycle of normal human walking on an exoskeleton prototype. In [159], the global minimum-jerk is solved in a minimax optimization problem via the interval analysis. The proposed cubic splines trajectory converges with considerable precision. Some motion laws are surely less complicated to implement in real time applications. For example, the minimum execution-time trajectory is preferred in point-to-point motion such as pick-and-place task [160]. The bang-bang profile is suitably assigned for this purpose. The linear motion, i.e. trapezoidal velocity, is supported by parabolic/polynomial blends for more smoothness. On the other hand, the polynomial trajectory is privileged for precise trajectory tracking satisfying smoothness criterion. In addition, it is convenient to reduce as much as possible the amplitude of the acceleration to avoid significant stress efforts that may trigger the vibrations. Therefore, smooth acceleration profile should be considered in the limit of the system frequency bandwidth. Other methods can be found in literature, such as trajectory planning based on radial basis functions [161]. One may check the general reviews for more detailed explanation of the existing optimization algorithm for the trajectory planning in [162, 163].

Comparison study

There is an evident interaction between the motion law and the induced vibrations, the effective motion-duration is also affected by the trajectory form. The two main comparisons are the following:

1. **Motion-induced vibrations:** The impact of the motion law on the vibrations for a given system can be quantified via the temporal representation or by analyzing

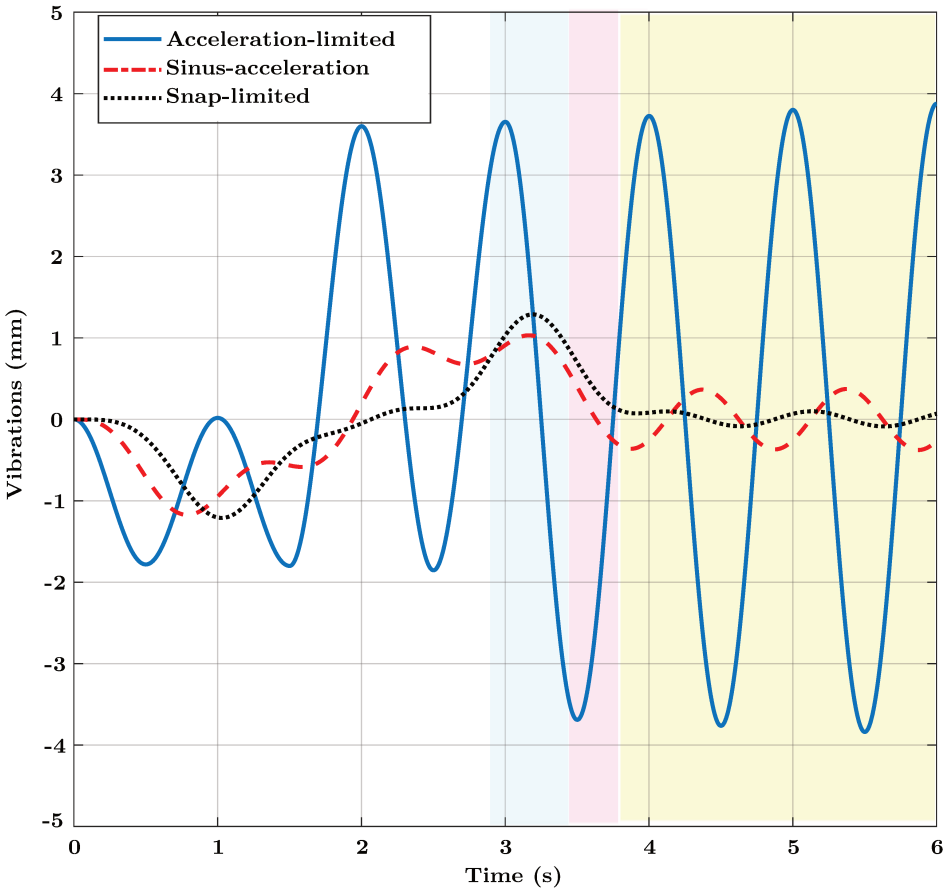

Figure 3.6: Graph of motion-induced vibrations, i.e dynamic error $(Q_{ref}(t) - Q(t))$, of polynomial and trigonometric trajectories

the frequency spectrum. For this aim, the induced vibrations during and after the displacement time are compared to reference profile, i.e. the standard bang-bang profile, see figure (3.6). The dynamic error is given by $w(t)$ in (3.2). One of the first things one may notice is that the vibration maximum amplitude is proportional to the acceleration profile, and it is important after abrupt variations in discontinuous points. Discontinuous acceleration profile induces larger vibration compared to smoother profile which is the case for the bang-bang acceleration. The polynomial acceleration form of the snap-limited profile is smoother than the sinus-acceleration profile, where the residual vibrations which are induced by this later are considerably larger compared to those of the polynomial trajectory. The vibration behaviour is more notable in the acceleration, i.e. inertial level. This

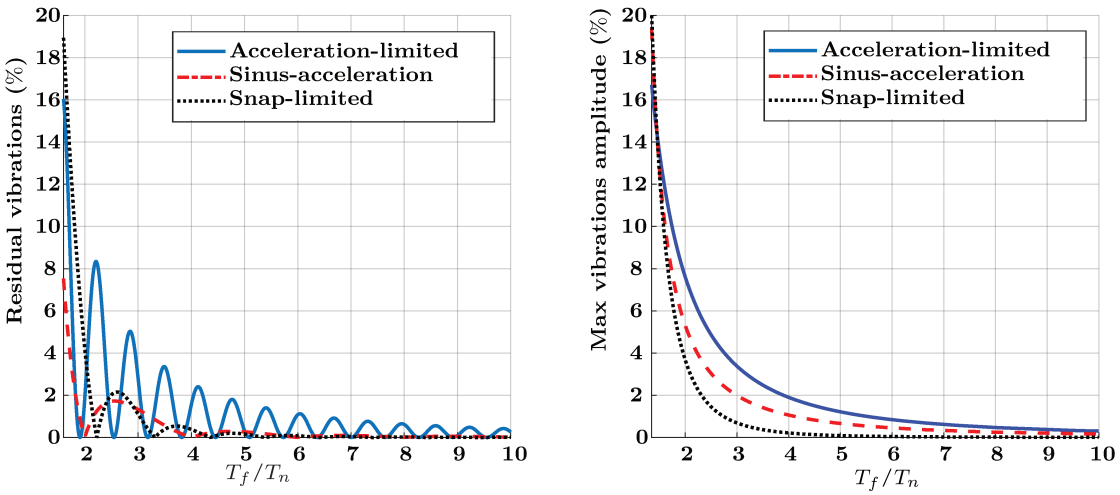

Figure 3.7: Residual vibrations graph of polynomial and trigonometric trajectories in function of the dimensionless time ($\frac{T_f}{T_n}$), where T_f is the motion duration and T_n is the vibration time period.

can be explained by the fact that the velocity and the position are obtained by means of integrator. This low-pass filter tends to eliminate the modes with high frequencies, where less high frequencies modes implies smoother motion. Figure (3.7) shows the vibrations analysis for a given reference trajectory Q_{ref}, where the vibrations percentage rate is calculated as follows

$$\begin{aligned} &\frac{\max\limits_{t\geq T_f}(w(t))}{Q_{ref}} && \text{Residual vibrations percentage.} \\ &\frac{\max\limits_{t<T_f}(w(t))}{Q_{ref}} && \text{Maximum vibrations rate during the motion.} \end{aligned} \tag{3.10}$$

The vibration percentage is given with respect to the width of the displacement, i.e. as function of dimensionless time which is determined by the ratio between the final time and the vibration time period ($\frac{T_f}{T_n}$), see [164]. This representation offers a better insight to the comparative study on the performance of the different motion laws. The dimensionless time-ratio is fixed by both the covered distance and the acceleration limitations because of the system and the actuators limits. The bang-bang profile presents a small acceleration module despite the discontinuities, i.e. induced-vibrations. On the contrary, continuous profile is tend to have a larger amplitude of the acceleration such as a high order polynomial and cycloidal trajectories, see figure (3.5). It can be seen that the residual vibrations are significantly reduced for movements of a duration greater than 3 or 4 times the time period of the preponderant vibratory mode (T_n). The vibrations spectrum

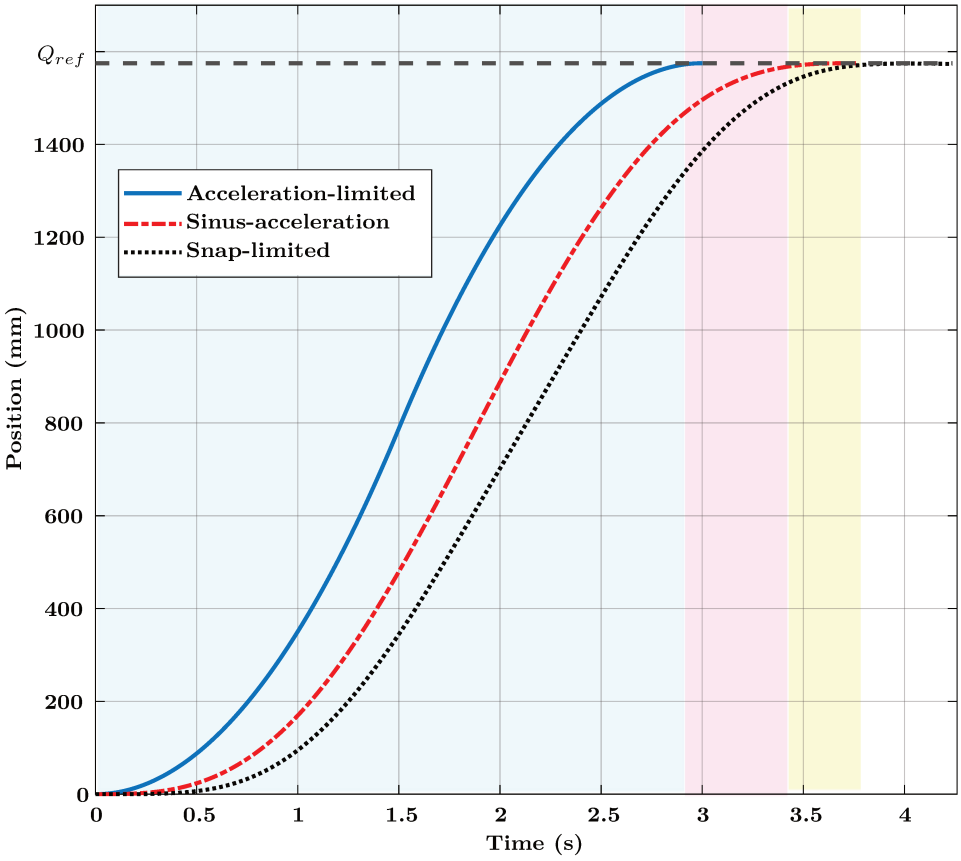

Figure 3.8: Position trajectories which are issued from polynomial law (acceleration-limited profile and snap-limited profile) ;trigonometric law (sinus-acceleration profile).

is notably mitigated using the motion law of harmonic type, and it is nearly vanished for a displacement of 4 times T_n in case of the snap-limited trajectory input. This confirms the fact that the higher polynomial order trajectory is the less residual vibrations are induced. In literature, the trajectories which are derived from Fourier expansion are developed for a better compromise between the minimum vibrations and minimum acceleration amplitude optimization problem, nevertheless the numerical solution is complex and not practical for real-time implementation.

2. **Kinematic constraints:** The form of the trajectory significantly determines the motion duration and the induced-vibrations. However, keep in mind that the softer the motion law is, the longer the movement becomes. This phenomenon is demonstrated in figure (3.8) where the colored zones indicate the necessary time to achieve the reference position Q_{ref}: the faster one is the acceleration-limited profile

(blue zone) followed by the sinus-acceleration profile (additional red zone) and the snap-limited profile (additional yellow zone). The profile with large terms implies a motion profile with minimum acceleration amplitude. On the other hand, the smoothness criterion will be more privileged despite the augmented kinetic energy. It may be of interest to consider the compromise between different optimisation criteria.

To sum up, the continuous trajectory inevitably affects the motion duration and the induced-vibrations. One may note that the chosen motion law should respect the actuator limitations, such as thermal conditions and kinematic restriction. Therefore, it should be tested first on simulation before eventual implementation since the computed trajectory risks to be inadmissible by considering several optimization criteria on robot kinematics. The vibrations can be reduced if only if the system energetic spectrum is low at the natural frequencies. For this reason, the trajectory can be adapted in case of polynomial trajectory via the polynomial degree and via the natural period in case of the trigonometric trajectory. The jerk/snap profiles offer the possibility to achieve a better compromise, respectively, to reduce the residual vibrations and optimally minimize the motion-duration compared to the bang-bang acceleration profile. The discontinuities in the bang-bang acceleration profile are undesirable for mechanical system with elasticity, while the jerk constant profile has low acceleration and continuous profiles. However, a proper filter such as input shaping technique may be designed to smooth the motion of a given acceleration profile. The jerk-limited profile is a well known shaped profile for industrial applications. Its performances can be adjusted to intend significant vibrations reduction by adjusting the jerk-time to be equivalent to the time period of the dominant vibration mode. Consequently, if the frequency changes its performance will be degraded. Nevertheless, the duration of the effective motion is reduced, independently on the frequency variation.

3.3.2 Jerk-limited trajectory

The input shaping scheme [34] can be explained as a sequence of impulses such as finite impulse response (FIR), called shaper, which are convolved with the desired trajectory to suppress or reduce the residual vibrations at the end of point-to-point motion, see figures (3.3) and (3.10). Some of the vibration suppression properties of input shaping technique can be directly found in some trajectory patterns. The input shaping method has been extended into multiple approaches to accommodate parameters uncertainty for more robustness, and to minimize some cost functions as well as to respect the dynamic constraints of the system [165]. For instance, in [166], authors propose a finite impulse filter-based trajectory generation for vibration reduction. The jerk-limited profile is obtained by convolving acceleration-limited profile with a moving average filter FIR [167]. This type of trajectories is mainly used to compute optimal trajectory profiles for industrial robots [167, 49]. The jerk time, i.e. the acceleration slope time, can be explicitly linked to the vibration caused by a dominating flexural mode. Hence, the jerk-limited profile can be seen as special combination of the smoothness property of

polynomial profiles and the vibration reduction property of basic input shaping. In [168], an algorithm is suggested to generate motion law with a jerk-limited trajectory profile in aim to damp out the vibration based on the FIR filter-based approach. Bearee, in [49], has introduced the damped jerk-limited profile to take into account the damping coefficient of the flexible motion, which is critical parameter in many dynamic systems. The author improved the conventional jerk-limited profile by introducing asymmetry segments, and that by defining non-equal FIR filter coefficients. Biagiotti, in [50], has generalized the previous approach to exponential online-filter profile and thus a new adapted FIR filter coefficients have been determined to suppress the induced vibration for under-damped flexible motion.

We recall that the dynamic model of the manipulated object in the previous example is a second order system, which is presented in (3.6). Its excitation input force F_u is an affine combination of the robot kinematics (TCP acceleration and velocity) along (Y_{ob}) axis as follows

$$\theta(t) + \frac{2 \cdot \xi}{\omega} \cdot \dot{\theta}(t) + \frac{1}{\omega^2} \cdot \ddot{\theta}(t) = F_u \tag{3.11}$$

The trajectory shaping approach for vibration compensation of such an oscillatory system is well established method. In this context, the vibration reduction can be achieved by several types of shaping filters. In this study, the jerk-limited profile, which is available in most robot controllers, is used for the joints trajectory. Moreover, since the robot manipulators have been the main subject for the modern industry, we investigate the feasibility and the consistence of the jerk-limited profile to enhance the motion and the accuracy of the robotic tasks. The figure 3.9 describes the acceleration profile for a rest-to-rest motion using jerk-limited pattern compared to the motion with simple acceleration-limited pattern. The jerk-limited profile implies a trapezoidal or a triangular acceleration profile and that depends on the chosen time intervals. If the jerk time is less than the half of the acceleration time interval than it generates trapezoidal velocity, else it can be triangular velocity. As in the bang-bang acceleration profile, the kinematic constraints, initial and final values of the trajectory have to be considered to shape the acceleration-limited profile for a suitable rest-to-rest trajectory, see for instance [49].

As depicted in figure 3.10, a jerk-limited trajectory can be easily and efficiently synthesized by applying a moving averaging Finite Impulse Response (FIR) filter to an acceleration limited profile, with a filter time equals to T_J. The FIR filter F_{JL} can be described in continuous time domain by the function (3.12), where s is the Laplace domain operator and A_i are the impulse amplitudes for the equivalent shaper.

$$F_{JL} = \frac{1}{s}(A_1 + A_2\ e^{-sT_J}) \tag{3.12}$$

The extra motion duration T_J compared to the acceleration-limited solution is equal to the jerk time. It is fixed by the relation between the maximum acceleration value and the maximum jerk value given by

$$T_j = \frac{a_{max}}{J_{max}} \tag{3.13}$$

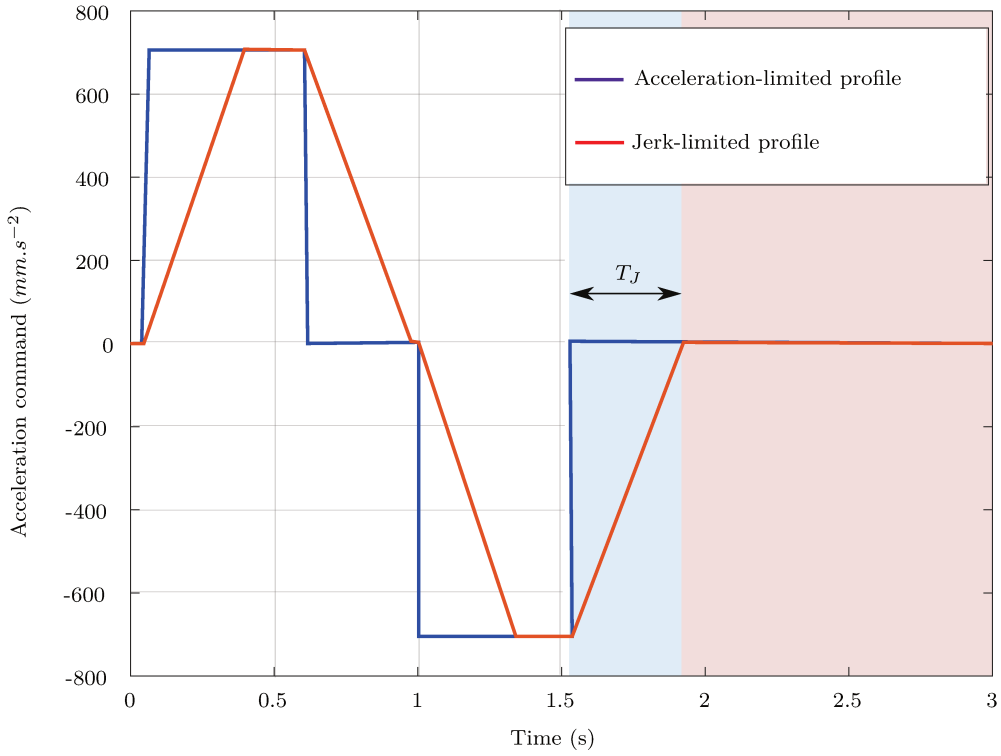

Figure 3.9: Example of a jerk-limited profile. The blue zone indicates the time delay due to the shaping filter.

Consequentially, the resulted acceleration profile has a rampe part with slope equals to a_{max}/T_j. The choice of the jerk time which correspond to the filter delay time is still a critical situation [168]. The generator of trajectories handles non-zero velocity and acceleration as well as non-symmetric acceleration bounds. Time-optimal and time-fixed solutions for different shapes of jerk profile.

As described in [49], the filter F_{JL} has some common properties with classical shapers. Considering an undamped vibration with a given natural frequency ω_n, the cancellation of the residual vibration by the jerk-limited profile is equivalent to the zeros placement at the undamped flexible poles locations, i.e. at $s = \pm j\omega_n$. Applying this principle to the previous jerk shaper given by (3.12), the resulting equation to be solved becomes

$$F_{JL}(s)|_{s=\pm j\omega_n} = 0 \tag{3.14}$$

This expression can be rewritten as a system of trigonometric equations

$$\begin{aligned} A_1 + A_2\ cos(\omega_n T_j) &= 0 \\ A_1\ sin(\omega_n T_j) &= 0 \end{aligned} \tag{3.15}$$

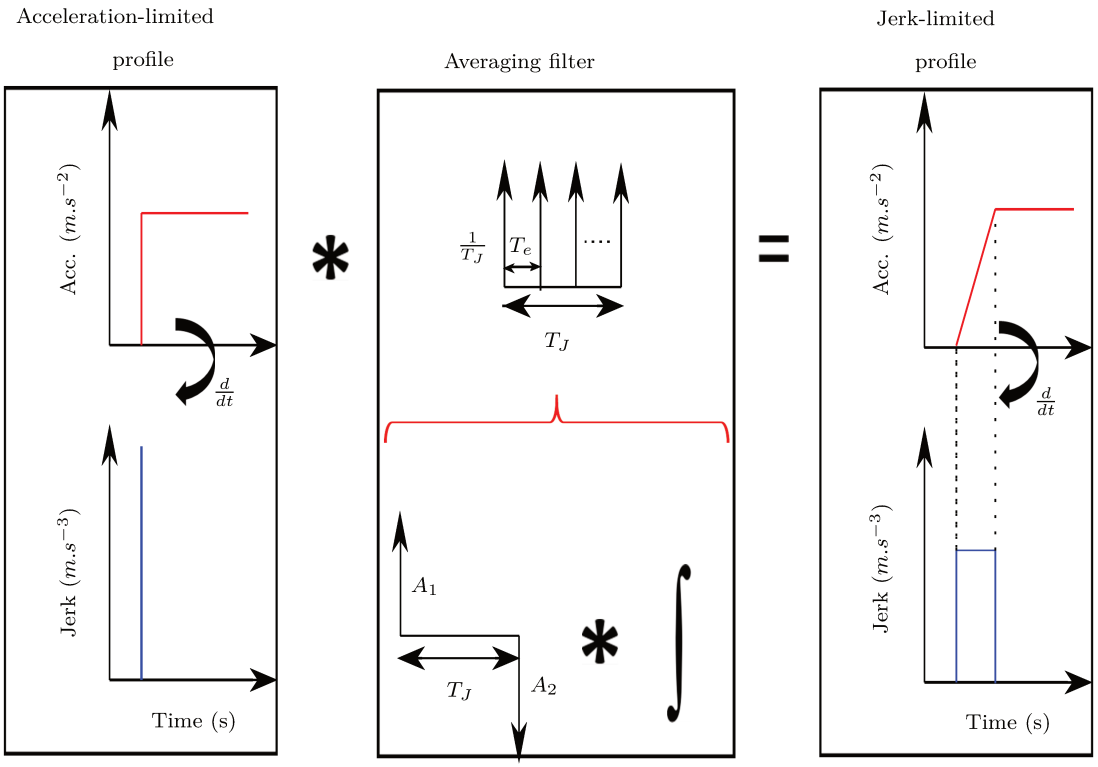

Figure 3.10: FIR filtering scheme equivalent to jerk-limited profile. T_J is the filter time (equivalent to the jerk time) and T_e is the sampling time of the controller.

By setting the filter time T_J equals to the natural time period of the vibration, the residual vibrations are suppressed. This simple tuning methodology of the FIR filter F_{JL} can be expressed as follows

$$\begin{aligned} T_J &= k\frac{2\pi}{\omega_n} \\ A_1 &= -A_2 = \frac{1}{T_J} \end{aligned} \tag{3.16}$$

where k is a positive integer. The jerk time can be taken equal to a multiple integer of the vibration period. k classically is set to one for time saving, as consequence, the jerk time is equivalent in this case to the natural period of the dominating flexible mode. Based on the input shaping formalism, the previous result concludes the explanation about the capacity of jerk-limited approach to cancel the residual vibrations for an undamped flexible mode. Using this tuning methodology the maximum jerk value will be imposed by both the jerk time and the maximum acceleration value according to the relation (3.13). A detailed analysis and the adaptation of such a method for the damped vibrations case can be found in[49, 50].

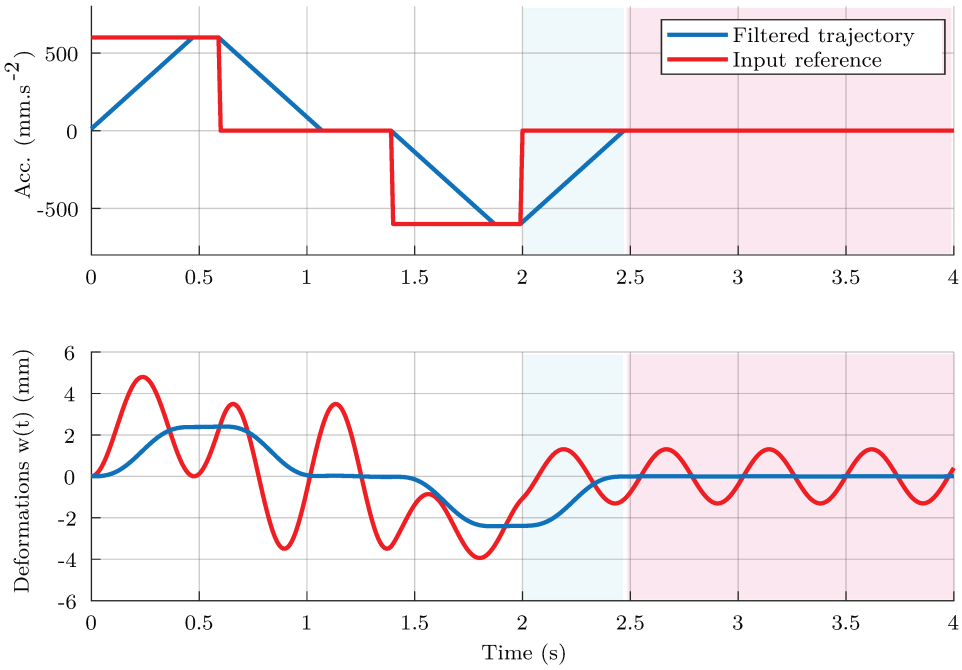

Figure 3.11: The deformation before and after applied shaping filter on the reference trajectory. The deformations are composed from vibrations (in red line) and elastic-motion deformation (in blue line). The simulations have been done on Matlab for bang-bang trajectory input. The vibration frequency is tooken equal to 2.3 Hz.

Since the exciting force of the vibration system contains a linear combination of the acceleration and the velocity of the end-effector kinematics, the two input signals should be injected into the same shaping filtered. The cascade of successive filter may be employed to compensate for more than one vibratory mode. The total vibration suppression is feasible only in case that the dominant mode is perfectly identified, analytically and/or experimentally. Otherwise, the vibrations can be reduced within certain effectiveness rate, which can be priory defined by analyzing the sensitivity effect on the residual vibrations in section 3.5. The time delay of the filtered signal should be considered to synchronize the robot motion specially when the 3D motion has different vibration modes on each axes and hence different time delay.

Hence, using the previous feedforward action, the residual vibrations and most of the vibrations occurring during the motion are suppressed, as shown in figure (3.11). Although, the presence of a dynamic compliance between the TCP acceleration and the flexural motion leads to large amplitude deformations that stand along the TCP motion. The next stage of this study consists in suppressing the deformations of the load tip during and after the motion.

3.4 METHODOLOGY FOR VIBRATION AND DEFORMATION COMPENSATION

3.4.1 Residual deformation compensation

The deformation in the motion duration is relatively proportional to the acceleration profile, with opposite sign to this latter. It occurs as a reaction to the TCP inertial force, which is totally independent from the system resonance. Therefore, the feedback control can be proposed as solution to instantaneously correct the tracking error between the principle axis of the transported-object and the reference frame of the end-effector. Although, it is not practical solution since the dynamic of the deformation angle $\theta(t)$ is relatively faster than the time response of the robotic system in general case. In order to optimize the process time and exploit all the DoFs of the robot as well, we present a technique that benefits of the rotation degrees of the end-effector which are offered by the kinematic redundancy as additional optimisation parameters to eliminate the static component in the flexible motion.

Assuming that the load vibration can be canceled or reduced, i.e. the oscillatory system given by (3.6) vanishes and $\ddot{\theta} = \dot{\theta} = 0$, the remaining deflection angle would be dominated by the static contribution of (3.6),

$$\theta(t) = -\frac{2 \cdot \xi}{l \cdot \omega} \cdot \dot{y}_{tcp}(t) - \frac{1}{l \cdot \omega^2} \cdot \ddot{y}_{tcp}(t) \tag{3.17}$$

Thus, the angle θ can be determined via input kinematics. Algebraically, limits on θ can be fixed with the respect to the kinematic constraints of the end-effector, in this case $0 \leq |\theta| \leq 2\pi$. The equation (3.17) establishes the relationship between the static deformation during the motion and the instantaneous acceleration/velocity of the robot TCP.

Let's suppose that the load vibration is suppressed by the trajectory shaping method, the residual deflection angle θ will be given by (3.17). This remaining motion-induced deformation during the motion can be mitigated by a proper compensation scheme of the deflection angle using the rotational space of the robot TCP, i.e. by adjusting the orientation of the load tip during the motion. This action is added to the design of the feedforward action and can be written as follows

$$Rot_{tcp}^{new}(\theta(t)) = Rot_{tcp} \cdot Rot_{comp}(-\theta(t)) \tag{3.18}$$

where Rot_{tcp} and Rot_{comp} are, respectively, the predefined TCP rotation matrix in base frame and the added rotation matrix which counteracts for the estimated deflection angle. The angle θ is used to control the relative motion between the load and the robot end-effector.

From (3.17) it is noticed that the angle θ depends eventually on the TCP acceleration and, to a lesser extent, on the TCP velocity (if the damping is sensitive). One may note that the continuity of the trajectory after the compensation action relies on the continuity of the angle θ. Thus, the desired trajectory has to be continuous in such a way to do

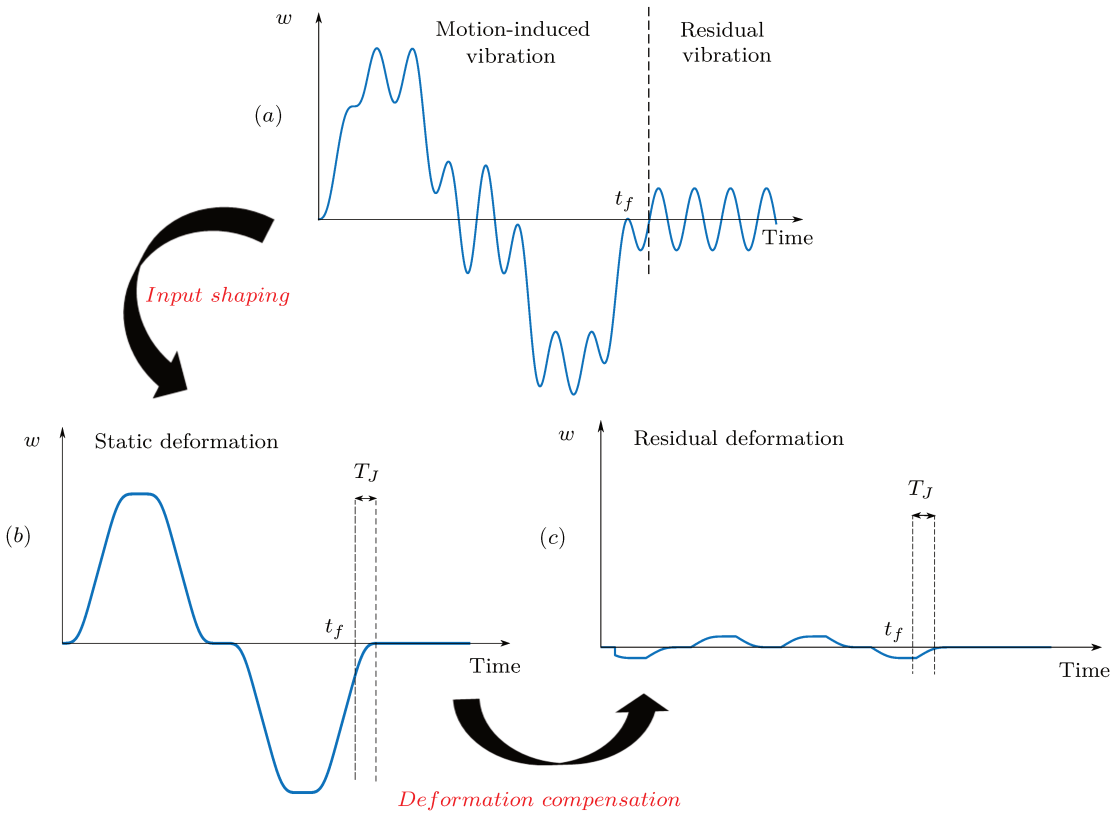

Figure 3.12: Deformation w: (a) initial deformation and vibration. (b) deformation with shaping trajectory for vibration compensation. (c) residual deformation with shaping trajectory and deformation compensation. T_J depicts the time delay due to the shaping filter.

not excite the vibration system. In the proposed approach, the vibration reduction properties which are introduced in the TCP trajectory via the shaping method will be extended to the added TCP rotational motion, which will not introduce new vibrations to the load. In other word, the smoothness property passes from the robot kinematics to the orientation eventually.

3.4.2 Proposed feedforward scheme

The input shaping aims to filter the injected reference trajectory in order to suppress the vibration modes of the flexural motion. The main limitation of the open-loop vibration control is that the vibration can be suppressed at the end of the motion, but the elastic deformation of the flexible object during the motion, which is depicted by (3.17), still exists. The proposed methodology which is depicted in figure 3.12 is a two stages feedforward-based approach. The first stage consists in compensating for the motion-induced vibration via trajectory shaping. The second stage aims at suppressing

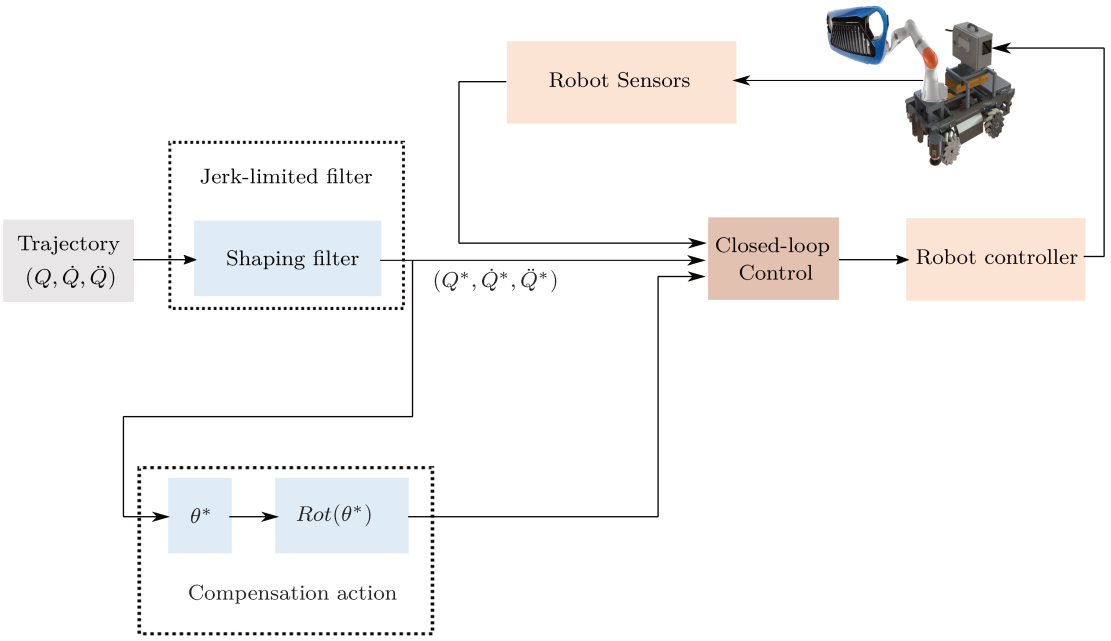

Figure 3.13: Control diagram of the proposed feed-forward control design. The low-level robot control is supposed already done which is the case of the most industrial robots.

the remaining static component of the tracking error during the motion, i.e. the static deformation of the load tip, using the rotational DOFs of the robot TCP.

The end-point of the manipulated-object is determined from the robot trajectory $Q(t)$, see figure (3.13). The TCP trajectory is filtered by the jerk-limited in the first stage to obtain smooth motion $Q^*(t), \dot{Q}^*(t), \ddot{Q}^*(t)$. Consequently, the object orientation is filter as well by implication $\theta^*(t)$. The rotational compensation action is then defined for the end-effector orientation $Rot(\theta^*(t))$. The optimal trajectory is injected to the robot controller as the joint coordinates are assigned to each of the robot actuators.

Based on two stages combination in feedforward control, this study proposes a trajectory generation method for industrial robot manipulators, so that the deformations during three dimensional motion and the residual vibrations of the flexible load are suppressed. The simplicity in the design and its independence from any real-time feedback signals, make it a robust control approach to be efficiently implemented in industrial devices. The angular θ is the constructive DOF for the flexural motion. This parameter can be controlled via the Cartesian position of the robot TCP. For that reason, the robot trajectory may be adapted to hold the manipulated object in its steady pose. The

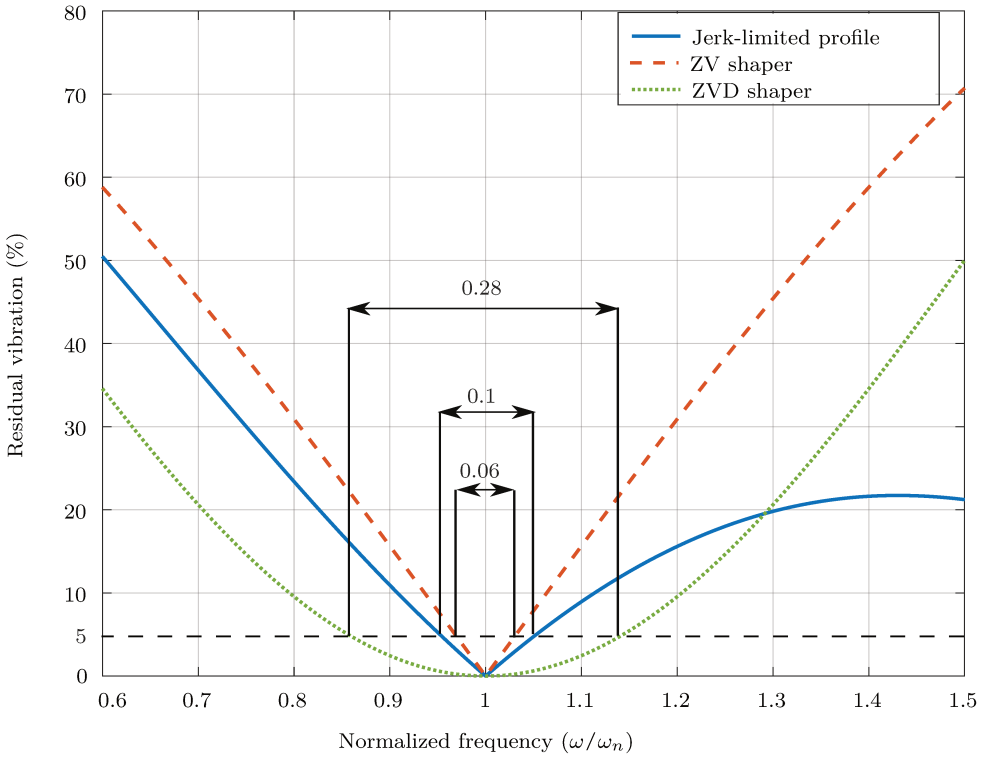

Figure 3.14: Sensitivity of the residual vibration suppression action [49].

redundancy of the robot is exploited in aim to align the flexible object so that the static deviation will be compensated.

3.5 SENSITIVITY ANALYSIS

3.5.1 On vibrations reduction

The proposed feedforward method is inherently sensitive to parameters estimation and variation. Naturally, the main parameter for the vibration and deformation compensation is the value of each modal frequency to be canceled. In the input shaping framework, it is customary to define the sensitivity plot, i.e. the percent of residual vibration amplitudes as function of the normalised frequency variation (ω/ω_n), with ω and ω_n are respectively the estimated and the real value of the natural frequency. Such a sensitivity plot is depicted in figure 3.14 for the jerk-limited profile which is used in this study and for two well-known shapers, the Zero-Vibration (ZV) shaper and the Zero-Vibration-Derivative (ZVD) shaper (see [35]). Here, 100% residual vibration corresponds to the vibration which is induced by an acceleration step command, and robustness or sens-

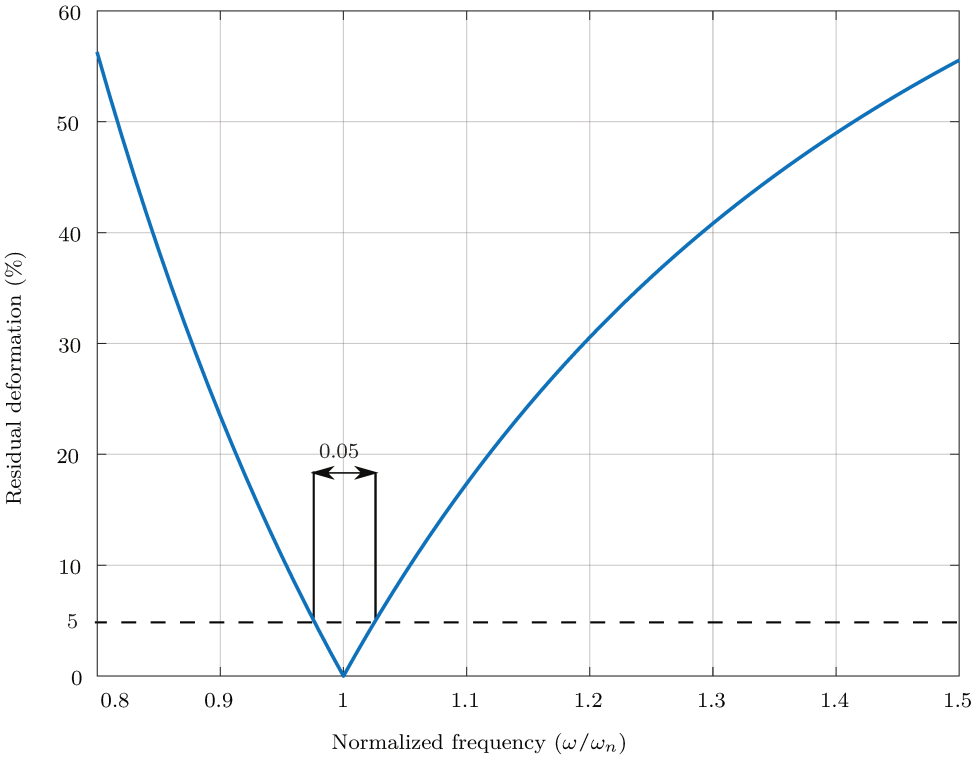

Figure 3.15: Sensitivity of the deformation compensation action.

itivity is classically defined as the frequency range over which a command induces less than 5% vibration. These sensitivity curves reveal how much residual vibration will exist when there is an error in the estimation of the system frequency. Hence, the jerk-limited trajectory tune to cancel the residual vibration of one flexible mode will be around 40% more robust than a ZV shaper. Moreover, the low-pass filtering property which is introduced by the integrator is effective to reduce significantly the impact of the neglected high frequency modes without any required frequency identification, which is practical for the industrial applications.

3.5.2 On deformations compensation

The same methodology can be followed to express the sensitivity plot for the deformation compensation. The deformation is affected by the variation of the angle compensation θ given by (3.17) and can be expressed as

$$w_n = l\theta = -\frac{2\xi_n}{\omega_n}\dot{y}_{tcp} - \frac{1}{\omega_n^2}\ddot{y}_{tcp} \tag{3.19}$$

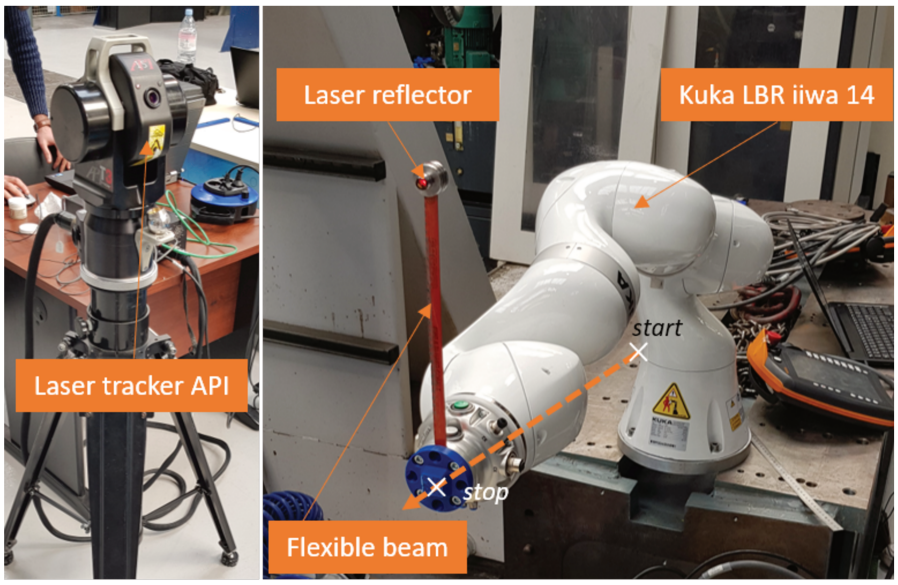

Figure 3.16: The experimental setup.

where ω_n and ξ_n are respectively the frequency and the damping values of the dominant mode in the load vibration. Considering a compensation action with the estimated frequency and damping value ω and ξ, the remaining residual deformation can be evaluated as follows

$$\frac{\Delta w}{w_n} = \frac{w_n - w}{w_n} = 1 - \left(\frac{\omega_n}{\omega}\right)^2 \cdot \frac{a \cdot (\frac{\omega}{\omega_n}) + b}{a + b} \tag{3.20}$$

where $a = -2 \cdot \xi \cdot \dot{y}_{ob}$, $b = -\ddot{y}_{ob}/\omega_n$. Assuming now that the damping can be neglected for the dominating deformations, the sensitivity of the deformation compensation is given by

$$\frac{\Delta w}{w_n} = 1 - \left(\frac{\omega_n}{\omega}\right)^2 \tag{3.21}$$

Figure 3.15 represents the sensitivity of the deformation compensation according to the normalized frequency. 100% residual deformation corresponds to the initial deformation without compensation. One can note that the sensitivity to keep the residual deformation below 5% is almost half the sensitivity of the vibration compensation action. However, in a more practical manner, an error of 10% for the estimated vibration frequency still allows to reduce the deformation by 80%.

3.6 EXPERIMENTAL VALIDATION

3.6.1 Experimental setup

To validate the proposed methodology and evaluate its effectiveness, an experimental validation has been done with a 7 DOFs robot manipulator kuka iiwa 14, which holds a

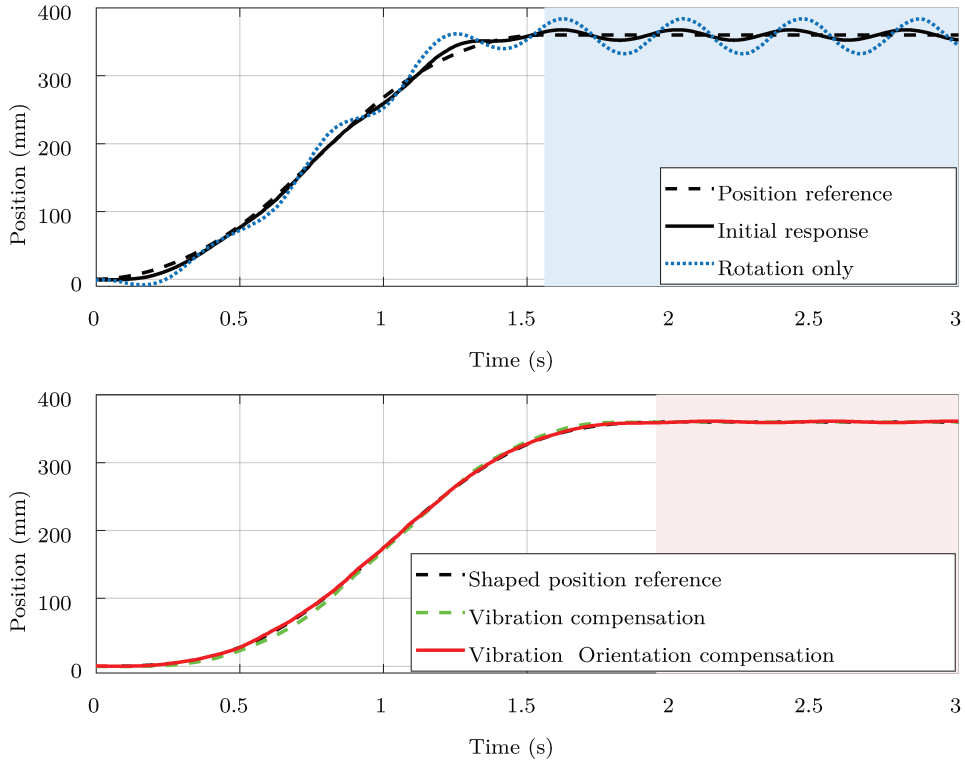

Figure 3.17: The load tip position for different cases. The after-motion state of the no-shaped (acceleration-limited) and shaped (jerk-limited) trajectory cases is depicted by the blue and the red zones respectively.

flexible beam (see figure 3.16). A laser tracker from API is used to measure the beam tip displacement along a predefined linear trajectory of the robot TCP. Only the first vibration mode of the flexural motion is considered in the motion direction. The Laser-tracker API is used to extract the flexural motion characteristics. The system parameters have been identified as follows: the natural frequency is $\omega = 2.2Hz$ $(0.038rad/s)$; the beam length is $l = 0.25m$; the value of the damping ratio is close to $\xi = 0.001$, and therefore the damping can be reasonably neglected for the considered beam.

Four different cases are presented in the following. The first case corresponds to the initial response of the beam with no vibration and deformation compensation. The second experiment consists in adding the deformation compensation action (static compensation) only. In the third case, only the vibration compensation is used and the last case combines the vibration and deformation compensation actions. The different robot TCP trajectories have been generated off-line and then sent to the robot joint controller with a sampling time equal to $4ms$.

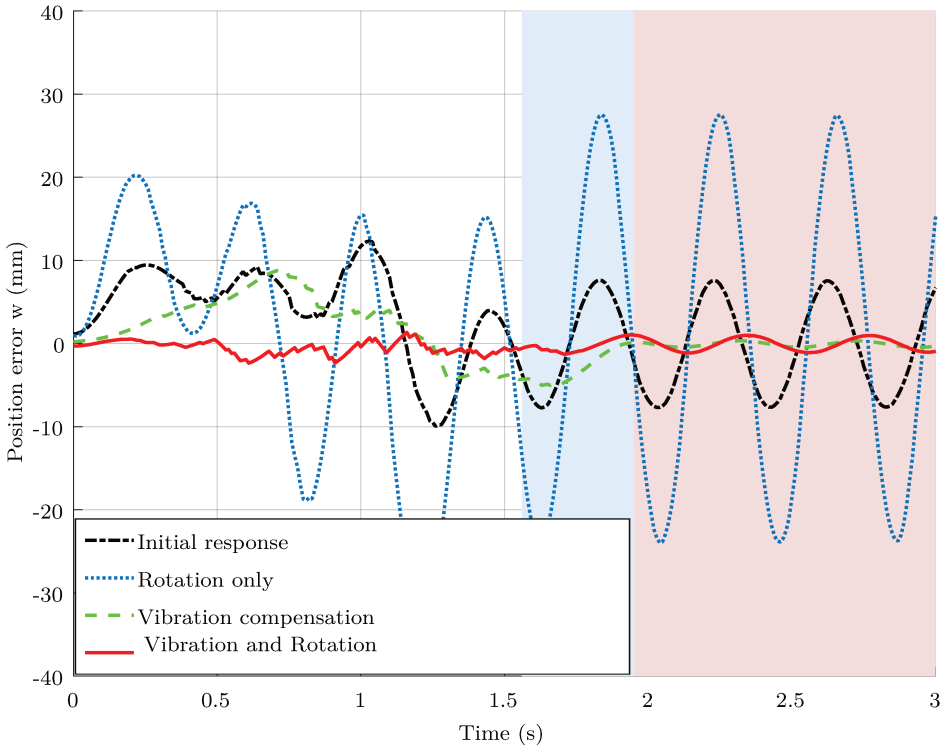

Figure 3.18: The load tip tracking error before and after motion. The blue zone indicates the time delay due to the shaping filter for the jerk-limited trajectory.

3.6.2 Discussions

Figure 3.17 shows the evolution of the measured load tip position and figure 3.18 shows the measured position tracking error of the load tip for the different trajectories. Table 3.1 gives the main quantitative results for the different trajectories. For the initial measured response and for the case with the deformation compensation (static compensation) only, the reference trajectory is an acceleration-limited trajectory. For the two other cases, the reference trajectory is the jerk-limited trajectory resulting from the FIR filtering of the acceleration-limited trajectory.

Case 1 - Initial response

The initial response of the load tip is clearly characterized by two different phases. During the motion, the load tip exhibits significant vibrations superimposed to the deformation error pattern. After the motion, the undamped residual vibrations are clearly visible.

Table 3.1: The deformation error comparison in the three considered cases: initial response (case 1), vibration compensation only (case 3) and vibration/deformation compensation (case 4).

Case	w_{max}	Vibration (%)	Deformation (%)
Case 1 - Initial	12.3 mm	100 % (ref.)	100 % (ref.)
Case 3	8.8 mm	5 %	71 %
Case 4	2.3 mm	5 %	18 %

Case 2 - Deformation (static) compensation only

In this case, only the angle compensation technique is used. As described in figure 3.18, the vibration amplitude is increased due to the fact that the compensation is done on the unshaped acceleration profile. Hence, vibrations induces by the translation motion of the TCP are naturally not suppressed (see (3.6)), but worse, the added rotation trajectory of the TCP induces new vibrations. For the test trajectory, the contribution of each motion on the vibration level is clearly additive. This case reflects the fact that the proposed deformation compensation cannot be used without a vibration suppression action.

Case 3 - Vibration compensation only

The jerk-limited profile is used in this case to suppress the vibrations. Figure 3.18 shows that the vibrations are efficiently damped out while the deformation still exists during the motion. The residual vibration amplitude is less than 5% of the initial one. The remaining small vibration amplitude can be related to different factors such as the estimation bias of the natural frequency and the neglect of the damping effect.

Case 4 - Vibration and deformation compensation

This case shows that the proposed two-stages feedforward method is efficient to significantly reduce the vibrations and the deformation. The residual tracking error of the load tip is less than 18% and the residual vibration value is equivalent to the previous case. This value is due to the fact that the flexible beam is too sensitive to the external disturbance.

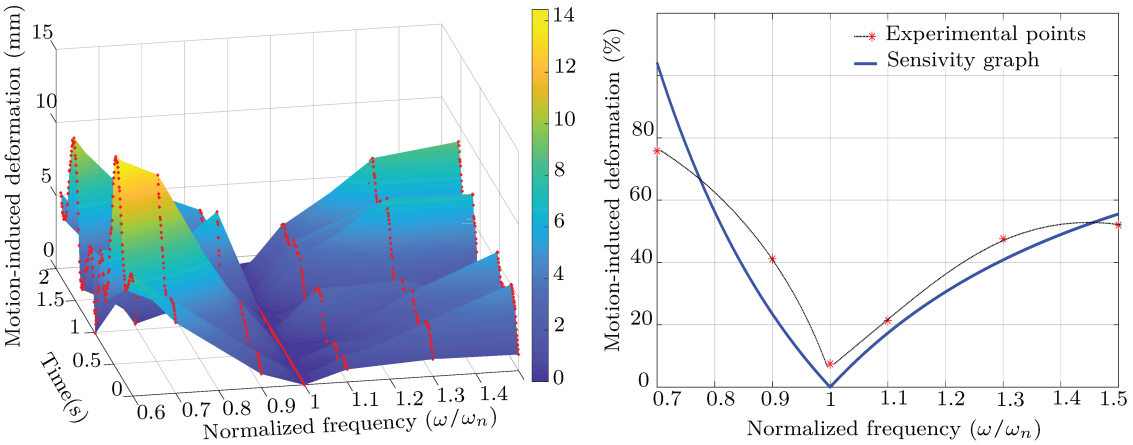

Figure 3.19: Sensitivity of the deformation compensation action in the theoretical study is compared to the experimental graph. The deformation's time-varying amplitudes are collected experimentally as function of variable frequencies.

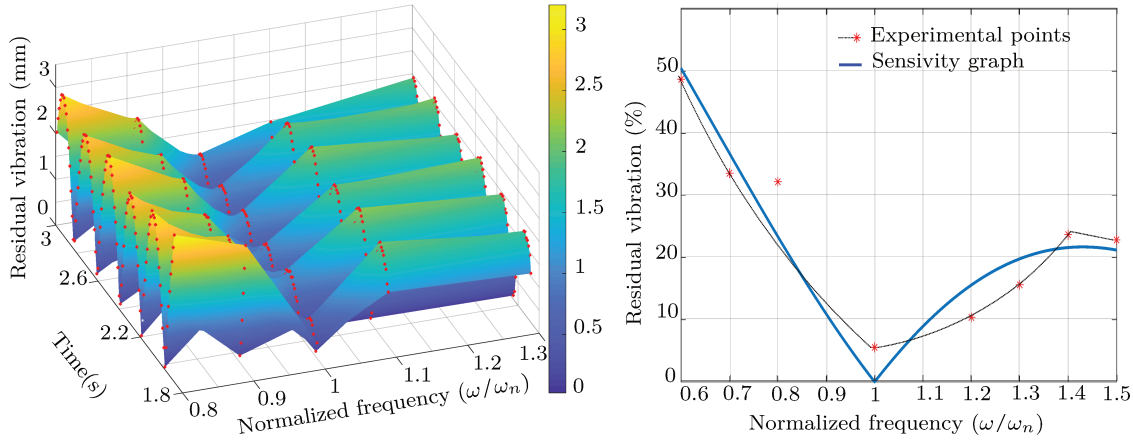

Figure 3.20: Sensitivity of the residual vibration suppression action compared to the experimentally collected points as function of variable frequencies.

3.6.3 Sensitivity analysis

As shown in figure (3.19), the time-varying deformations are proportional to the acceleration profile depicted in figure (3.11). In the case of the ban-bang or trapezoidal acceleration profiles, the deformation's amplitude is maximum just after the switching point at the acceleration maximum value. The experimental sensitivity graph has the same variations as the theoretical graph, a small difference in the percentage allure is due to the non-null initial conditions knowing that the flexible object is too sensitive to other external disturbances. Nevertheless, this feedforward action may guarantees less than 20% of residual elastic deformation over a margin of ($\pm 0.1\ \omega_n$) frequency variation about the nominal value. On the other hand, the vibration are reduced over a large

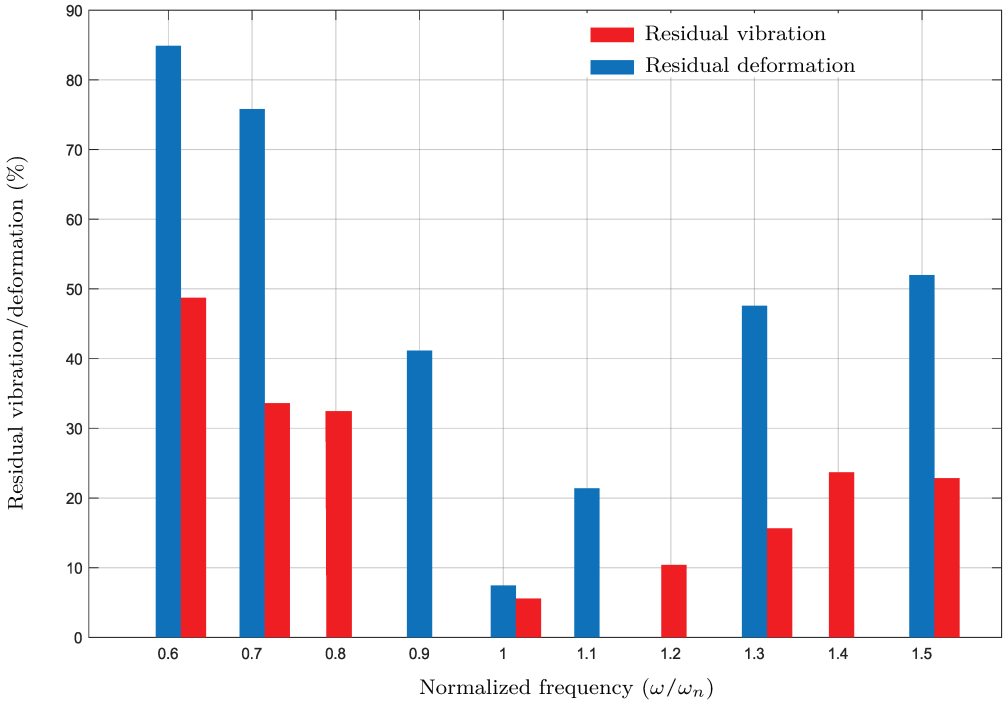

Figure 3.21: The sensitivity of the residual vibration and motion-induced deformation are compared for different frequency values.

range frequencies ($\pm 0.2\ \omega_n$), less than 10% of residual vibration are remained as shown in the experimental tests, see figure (3.20). The sensitivity curve is more or less similar to the one in the theoretical analysis, nevertheless the experimental tests are influenced by the external noise and non-null initial conditions. The residual vibrations depend only on the frequency variation since their amplitude is constant after the motion. One may note the residual vibrations are less sensitive to the variable frequencies compared to the elastic deformation, see figure (3.21). The effectiveness of the deformation reduction action depends mainly on the filtered trajectory. Thus, for a designed trajectory which is based on a poorly identified frequency, the residual motion-induced deformations are important compared to those issued from the nominal filtered trajectory case.

From above, one may note that the proposed control design comes to reinforce the input shaping approach so that the residual flexural motion may be significantly reduced. The feedback vibration control design presented in [27] and [29] are just binding on calculation and measurement, which are generally difficult to implement due to an infeasible fast estimation of flexural motion state. On the other hand, the simplicity and the robustness make the proposed feedforward more advantageous and useful for industrial applications.

3.7 CONCLUSION

In this chapter, the redundancy of the robot is exploited to build a feedforward control to compensate for the deformations of a flexible load during the translational motion of this later with a robot manipulator. The analysis and interpretation of the comparison study between different trajectories, i.e. on the selection of a suitable trajectory, reveals that the chosen trajectory may depend on different factors regarding the kinematic constraints and the desired performances (vibrations reduction) as shown in section 3.1. The shaping filter such as the jerk-limited profile smooths the robot trajectory by eliminating the motion-induced vibration, while the degradation due to the inertial force of the robot end-effector remains along the motion phase. The main contribution of the proposed strategy can be resumed in the combination of a trajectory shaping stage for the vibration suppression, with a trajectory compensation action for the elastic deformation occurring during the motion as demonstrated in section 3.4. The latter action makes use of the robot redundancy via free rotation DOFs in the Cartesian space of the robot manipulator. The effectiveness of the proposed approach is demonstrated analytically and then experimentally on industrial robot, where the precision of the load transfer is guaranteed under high kinematic constraints which is promising for industrial applications.

The sensitivity of the two actions with regard to the estimated vibration frequencies has been derived in section 3.5. The two actions in the proposed feedforward control architecture are built on a simple knowledge of the frequencies vibration. This factor is independent from the the robot dynamic and its low-level control. It has been shown that both filter and compensation actions can tolerate a considerably large variation margin on the frequency estimation which is interesting outcome for real system applications. The rotational action is complementary to the filtered trajectory, its effectiveness is guaranteed as long as the trajectory complies with the required smoothness degree. The results of experimental tests which have been conducted using an industrial robot manipulator and a pure flexible beam are analysed in section 3.6. In the industry, the robot trajectory for a given task should be simple and easy to implement to avoid any malfunction which may endanger its work-space environment especially the security of co-workers. This feedforward approach avoids any implementation complication which may result from numerical optimisation or by using sensors which is the case for most feedback control. In addition, using the redundancy DOFs optimizes the energy consumption and allows the robot to optimize its configuration during the manipulation task. Nevertheless, in some cases when the manipulated objects have no-uniform deformations properties where the deformations are denoted by complex system, the application of input shaping approach is not beneficial.

The manipulation of a flexible load in different directions simultaneously requires an analysis of the resulting three-dimensional motion. In this case, the shaping filter should be considered since the time delay is possibly different from one axis to another which may result in an asynchronous resultant motion. In the next chapter 4, we present a methodology to adapt the accuracy of the task positioning in the case of trajectory-

planning along filter-shaping action for vibrations reduction.

Chapter

4 NULL-PHASE TRACKING WITH VIBRATION CONSTRAINTS

The robotic manipulation on the production lines may require to perform repeatedly positioning tasks with constant velocity, such as assembly operations. The investigation on the feasibility and the consistence of a practical approach such as jerk-limited profiles to enhance the motion and the accuracy of the robotic tasks is covered in the present chapter. The applications of the Finite Impulse Response (FIR) filter with the jerk-limited profile are detailed in chapter 3.

The use of the filter may be necessary to minimize the vibrations due to the robot compliance in purpose to avoid any damage to the manipulated object. As a result, the shaping filter introduces a delay between the original input signal and the filtered signal. The time delay may affect the task precision and limit the dynamic performances. The non null-phase tracking error of the shifted trajectory may degrade the precision for tracking task. Additionally, the time-delay may affect the trajectory tracking if the motion is composed by more than one axis, where the filter parameters are different from one axis to another which will induce an asynchronized motion, see figure (4.1). The present work comes to enhance the feedforward control of the motion-induced vibration presented in chapter 3. For example, to execute a generalized motion profile for flexible load transfer.

In this chapter, a technique to improve the accuracy of multi-axis robot manipulators is addressed. In section 4.1, we give a better insight into the ability of the jerk-limited profile along the time synchronization to reduce the residual vibration and guarantee a precise tracking of the prescribed trajectories. In section 4.2, a proper compensation scheme has been put forward in order to achieve a consistent synchronization between the different motion axes. A comparative study on the generation of jerk-constrained trajectories for multi-axis motion is put forward based on the proposed algorithms in section 4.3.

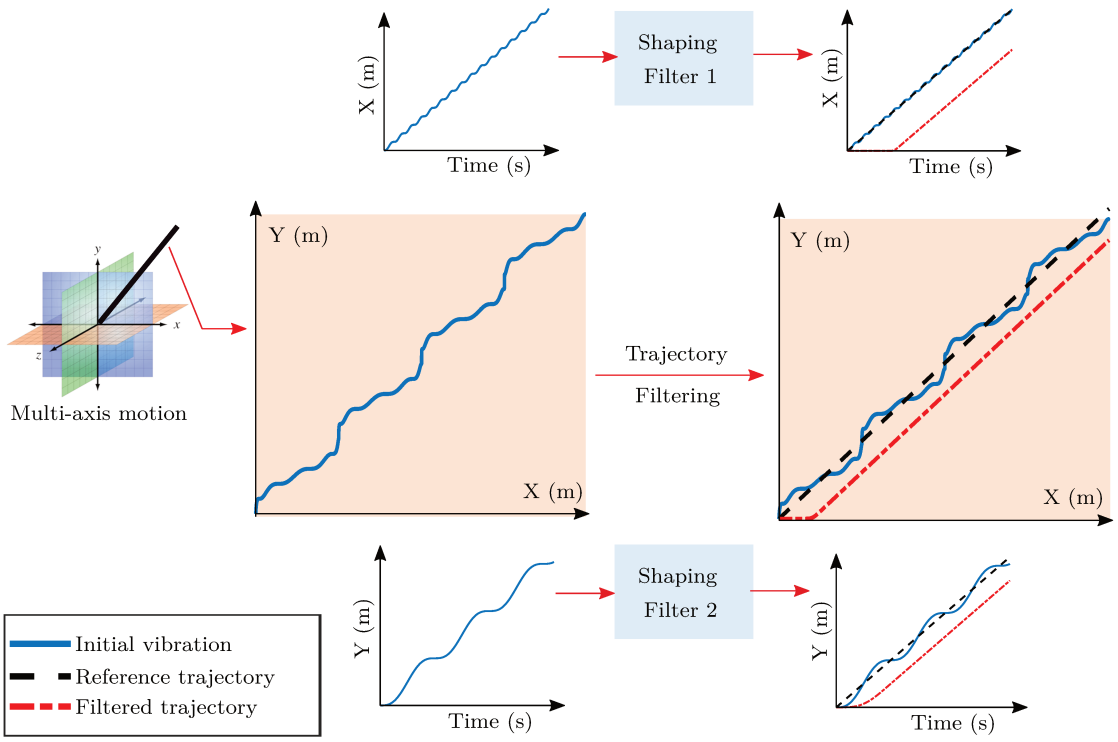

Figure 4.1: Illustration of multi-axis motion: the trajectories of the axis Y with high-frequency vibration mode and the axis X with low-frequency vibration mode are filtered using an adapted shaping filter for each. The time delays in Y and X axis motions induce an asynchronized motion in (XY) plan.

4.1 NULL-PHASE VELOCITY TRACKING

4.1.1 Ramp trajectory tracking

The classical feedforward scheme presented in figure (4.2) allows to get rid of the motion-induced vibrations. Nevertheless, it has an impact on the dynamic performance of the system plant because of the time delay. Null-phase velocity tracking of vibratory systems is proposed to deal with the online filter time compensation specially when the input signal is composed of modulated ramp signals, see for instance the reported works in [169, 170].

Let's consider a ramp trajectory which is depicted by linearly time-dependent signal $r(t) = m_0.t$. This input signal is applied to the dynamic system described by the transfer function $V(s)$, supposed stable, i.e. characterized by n poles p_i with $\mathrm{Re}\{p_i\} < 0$ and verifying the physical causality condition as well, i.e. $zeros(V(s)) < poles(V(s))$ as follows

$$V(s) = \frac{\sum_{i=0}^{m} a_i \cdot s^i}{\sum_{i=0}^{n} b_i \cdot s^i} \tag{4.1}$$

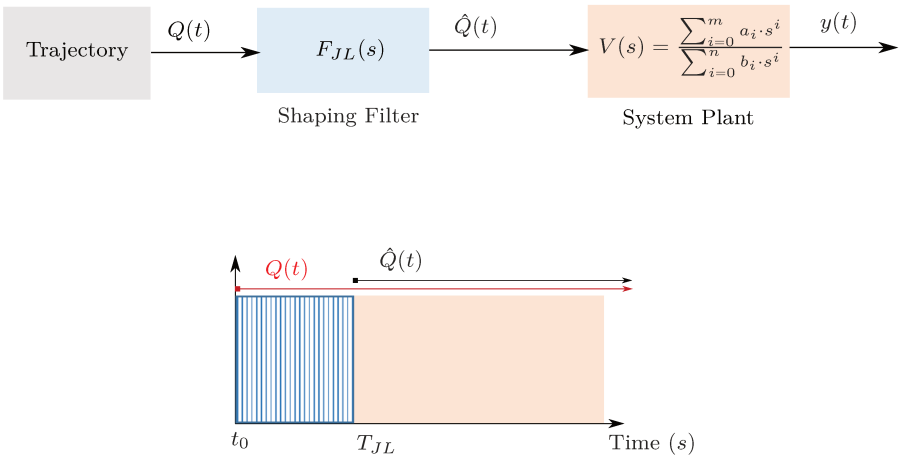

Figure 4.2: Conventional shaping filter structure. The filter output $\hat{Q}(t)$ is shifted from the reference trajectory $Q(t)$ by time delay T_{JL} equal to characteristic time of the considered filter.

where $n, m \in \mathbb{N}^2$ and $m < n$. Under the assumption of initial conditions being null, the system response can be obtained by the Laplace transforming as follows

$$\begin{aligned} Y(s) &= V(s) \cdot R(s) \\ &= \frac{\sum_{i=0}^{m} a_i \cdot s^i}{\sum_{i=0}^{n} b_i \cdot s^i} \cdot \frac{m_0}{s^2} \end{aligned} \tag{4.2}$$

this formulation can be decomposed into three main factorized terms as follows

$$Y(s) = \hat{V}(s) + \frac{m_1}{s^2} + \frac{m_2}{s} \tag{4.3}$$

where $\hat{V}(s)$ contains the terms tied to the poles p_i of $V(s)$, and the two constants m_1 and m_2 are respectively given by

$$\begin{aligned} \frac{m_1}{m_0} &= \lim_{s \to 0} V(s) \\ \frac{m_2}{m_0} &= \lim_{s \to 0} \frac{dV(s)}{ds} \end{aligned} \tag{4.4}$$

By assuming that $V(s)$ has a unit static gain, i.e. $V(s = 0) = 1$, it consequently leads

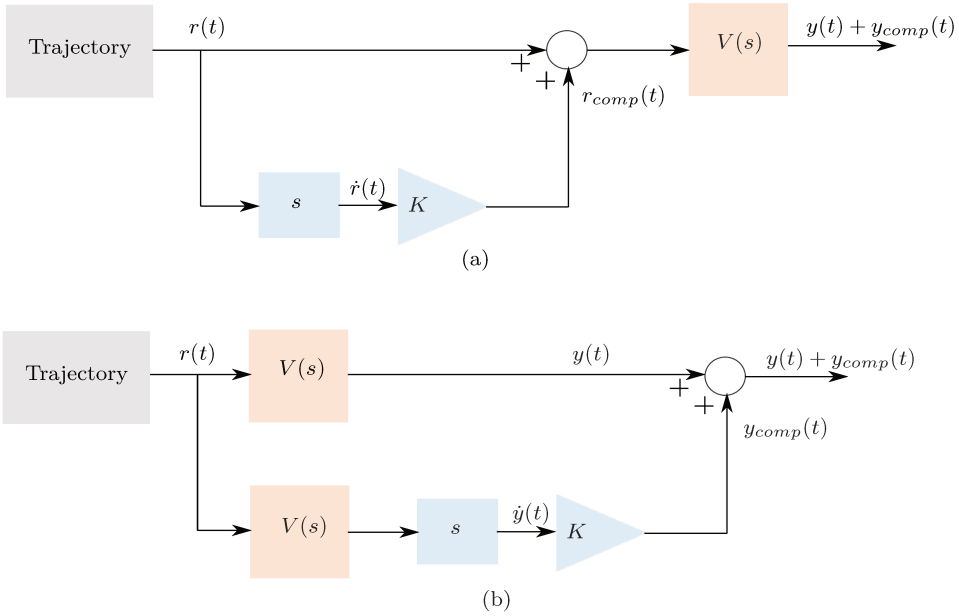

Figure 4.3: Modified feedforward scheme to compensate for the ramp gap. The schemes (a) and (b) are equivalent, since the compensation action can be added to the input or the output. It is defined as $Y_{comp}(s) = V(s) \cdot R_{comp}(s)$.

to $m_1 = m_0$. Finally, the time output signal is given in the following relation by the inverse Laplace transformation of (4.3)

$$y(t) = \hat{v}(t) + m_0.t + m_2 \tag{4.5}$$

since $\hat{v}(t)$ is a stable signal, it will asymptotically vanish in time. The static error between the system output $y(t)$ and the reference input $r(t)$ in this case is equal to m_2

$$\begin{aligned} e &= \lim_{t\to\infty} (y(t) - r(t)) \\ &= \lim_{s\to 0} s \cdot (1 - V(s)) \cdot R(s) \\ &= m_2 \end{aligned} \tag{4.6}$$

therefore this error can be compensated with a constant feedforward action, see figure (4.3).

As a result, the system output follows the input signal accurately after a time response equals to the slowest time constant of the plant $V(s)$, see plots (a) and (b) in figure (4.4). One may note that this action is not causal since it requires the derivative of the input reference $r(t)$. Thus, in case of no available input derivative, this later can be approximated via filtering methods or numerical differentiation algorithms, see for

instance [171, 172]. The gain of the compensator in the feedforward scheme presented in figure (4.3) is given as follows respectively to (4.4)

$$\begin{aligned} K &= -\lim_{s=0} \frac{dV(s)}{ds} \\ &= -\frac{m_2}{m_0} \end{aligned} \tag{4.7}$$

For a given system depicted by global transfer function $V(s)$ which is composed of cascade of n separated subsystems as follows

$$V(s) = \prod_{i=1}^{n} V_i(s) \tag{4.8}$$

by assuming that the static gain of all subsystems is unit, i.e $(\lim_{s\to 0} V_i(s) = 1)$ and from (4.7) and (4.8), the total compensator gain of the system is given by

$$\begin{aligned} K &= -\lim_{s\to 0} \frac{dV(s)}{ds} \\ &= -\lim_{s\to 0} \sum_{i=1}^{n} \left[\frac{dV_i(s)}{ds} \cdot \prod_{j\neq i} V_j(s) \right] \\ &= \sum_{i=1}^{n} K_i \end{aligned} \tag{4.9}$$

The sub-gains of the cascade system are defined as follows

$$\begin{aligned} K_i &= -\lim_{s\to 0} \frac{dV_i(s)}{ds} \\ &= -\frac{m_{2,i}}{m_i} \qquad\qquad , \; i = \overline{1,n} \end{aligned} \tag{4.10}$$

where $\lim_{s\to 0} \prod_{j\neq i} V_i(s) = 1$ since the static gain is supposed equal to unity $(\lim_{s\to 0} V_i(s) = 1)$.

4.1.2 Equivalent FIR filter formulation for null-phase velocity tracking

The ramp profile can be basically obtained by filtering a step function with a continuous filter described by the transfer function

$$F_{JL}(s) = \frac{1}{T_J} \frac{(1 - e^{-T_J s})}{s} \tag{4.11}$$

The filter time corresponds to the jerk period time T_J. The function $F_{JL}(s)$ is nothing than the averaging filter depicted by the convolution of an integrator with a succession of two impulses which is deeply detailed in chapter 3.

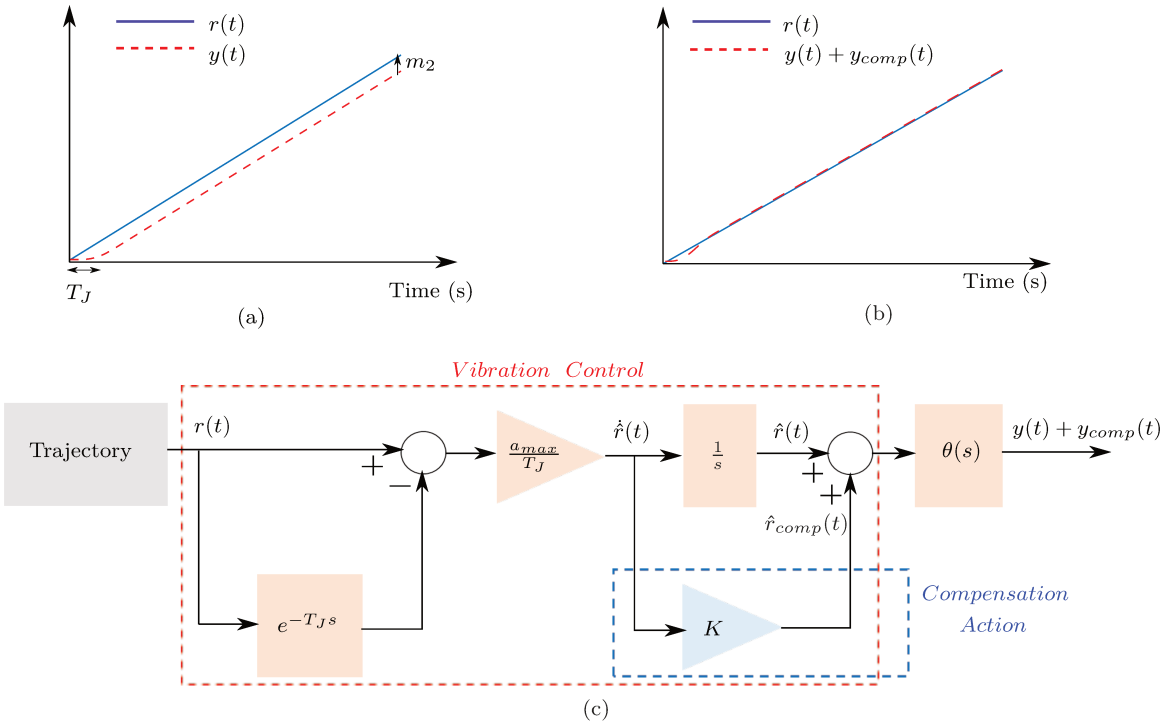

Figure 4.4: The filter introduces a delay which shifts the filtered signal by a constant offset from the input reference signal: (a) the delayed output signal ; (b) the filtered ramp signal with compensation action; (c) The proposed feedforward vibration control with null-velocity compensation action.

Noting T_e the sampling time of the signal and using the backward difference method, the z-transformation of the FIR filter equivalent to (4.11) is given by

$$F(z) = \frac{1}{N_e} \frac{1 - z^{-N_e}}{1 - z^{-1}} \tag{4.12}$$

with $N_e \in N$ is the round integer of T_J/T_e. This FIR filter is equivalent to a moving averaging filter. Noting respectively Y_k and u_k the output and the input value of the filter at time instance kT_e, the filter output is defined as follows

$$Y_k = \frac{1}{N_e} \sum_{i=1}^{N_e} u_{k-i+1} \tag{4.13}$$

As mentioned previously in chapter 3, the convolution of the limited-acceleration profile of maximum amplitude a_{max} with FIR filter depicted by the transfer function $F_{JL}(s)$ in (4.11) will result in the jerk-limited profile, its corresponding function transfer is given by

$$F_{JL}(s) = \frac{a_{max}}{T_J} \frac{(1 - e^{-T_J s})}{s} \tag{4.14}$$

Considering a system submitted to a dominant undamped flexible mode of frequency value ω_n, the cancellation of the residual vibration by the jerk-limited profile is equivalent to the zeros placement at the undamped flexible poles locations, i.e. at $s = \pm j\omega_n$. Applying this principle to the previous jerk shaper given by (4.14), the general solution for the jerk time is given by

$$T_J = \frac{2k\pi}{\omega_n} \tag{4.15}$$

with k being a positive integer. Using this tuning methodology the maximum jerk value will be imposed by the jerk time and the maximum acceleration value.

In case of the zero-phase tracking of the input signal, the feedforward has no effects on the vibration modes since the derivative of the input reference signal is filtered as well, see the control scheme in figure (4.4). Let's consider the filtering shaper in (4.14) and assuming that the system plant is depicted by second order system which is characterized by nominal natural frequency ω_n and damping ratio ξ as follows

$$\theta(s) = \frac{\omega_n^2}{s^2 + 2\xi s + \omega_n^2} \tag{4.16}$$

Thus, to compensate the static error resulting from both systems in (4.14) and (4.16) respectively, the compensator gain K is chosen according to (4.9) as follows

$$\begin{aligned} K &= -\lim_{s\to 0} \frac{dF_{JL}(s)}{ds} - \lim_{s\to 0} \frac{d\theta(s)}{ds} \\ &= \frac{T_J}{2} + \frac{2\xi}{\omega_n} \end{aligned} \tag{4.17}$$

In general, the input reference is a piecewise linear function which can be considered as the combination of sequence of ramp functions as follows

$$\begin{aligned} r(t) &= r_1(t-\tau_1) + r_2(t-\tau_2) + ... + r_n(t-\tau_n) \\ &= \sum_{i=1}^{n} (m_i - m_{i-1})(t-\tau_i) \end{aligned} \tag{4.18}$$

where $m_0 = 0$, m_i is the slope of the input signal, i.e. time velocity, at time instant τ_i, see figure (4.5). Trajectories based on sequence of ramp functions are analyzed in [173]. In general, the filter introduces a delay which may shift the filtered signal by a constant offset from the input signal. In the online-filter shaper, it is necessary to reduce the vibration and at the same time eliminate the static error when the input signal is composed of ramps sequence. This result is still the same for other trajectory profiles. Nevertheless, the important fact is that the critical situation due essentially to the filter delay is the asynchronized motion, this special trajectory is resulted from multi-axis motion with different time delays which is analyzed in the next section.

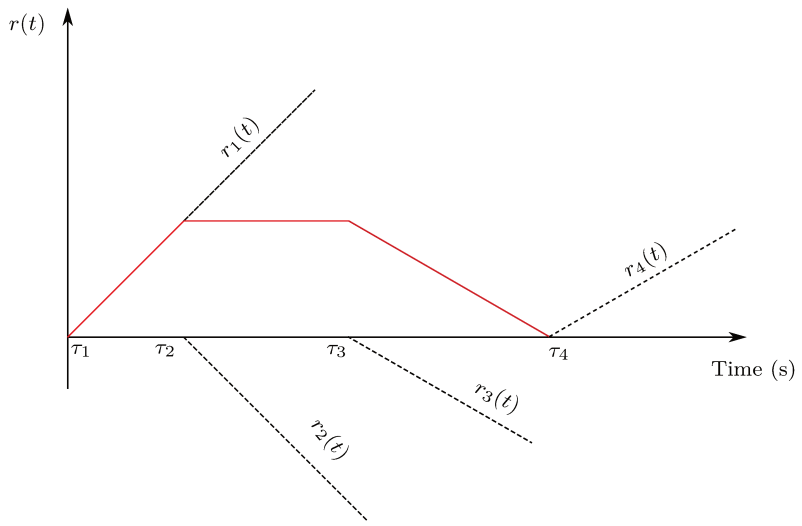

Figure 4.5: Input reference signal composed by set of ramp signals.

4.2 MULTI-AXIS TRAJECTORY GENERATION WITH VIBRATION CONSTRAINTS

In the context of robot manipulators, the trajectory in the work-space is generated from different combinations of the robot motion-axes. Thus, several DOFs are controlled simultaneously to reach a desired position. The global vibration motion at the manipulator TCP is then issued from combined vibration modes which are projected on different axes of the task motion frame. Generally, the dominant vibration modes are kept on each main axis. As solution to reduce these deformations, a set of parameterized filters with different time periods have to be designed on each of axes separately. Although the vibration can be damped out, an other issue may be emerged. The performed trajectory could be completely different from the desired one because the axis motions are not synchronized.

Classically, for better precision it is required that the motion of each involved DOF ends at the same time. Consequently, for a motion involving n DOFs where T_i the duration of the time-response trajectory for the ith axis, the n filtered trajectories have to be adjusted. In this study, two proposed solutions are discussed to reach the motion synchronization for multi-axis manipulator: online and offline solutions.

In order to analyze the possible cases, numerical simulation of a combination of approaches are applied on a 7 DOFs robot manipulator. The robot is supposed to be

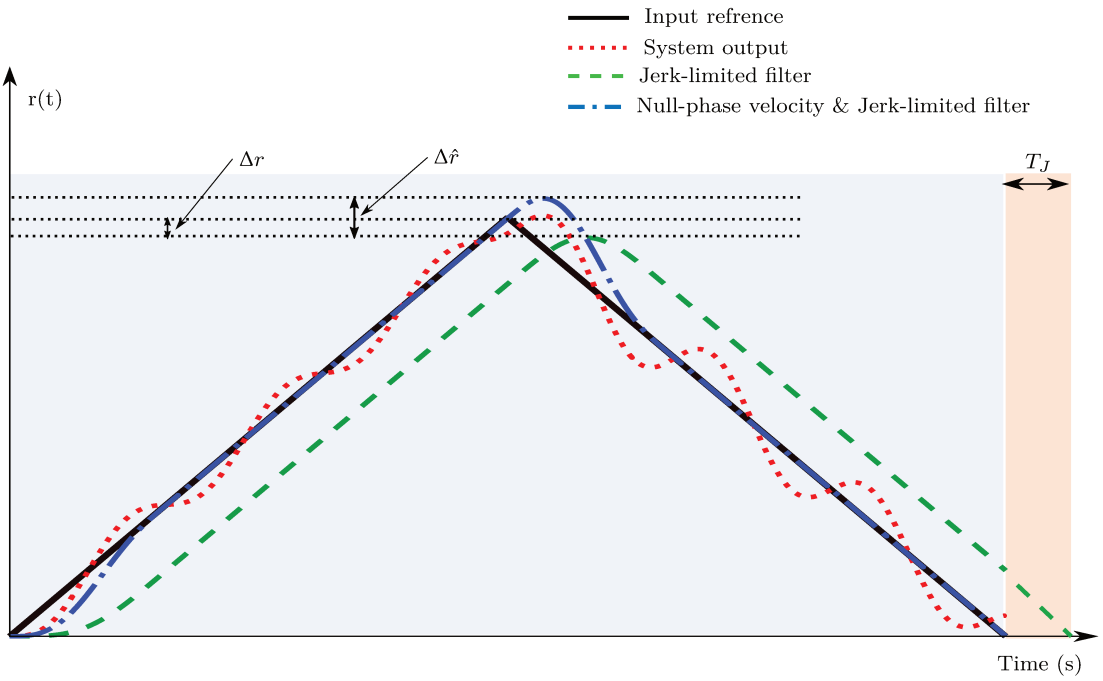

Figure 4.6: Time response of vibration plant given in (4.16) to 2 DOFs ramps sequences input. The filter get ride of the motion-induced vibrations but it delays the system output by T_J. Using the compensation action reduce the gab between the filtered and the input signal, nevertheless an overshot is noticed at the transition point between the first and the second ramp signal which can be referred to by the ratio $\frac{\Delta \hat{r}}{\Delta r}$.

rigid while manipulating flexible load in the motion plan (XY). In the following analysis of the considered example, only the dominating vibration modes on each of the two axes is maintained. The frequencies and the damping ratio used are $\omega_1 = 10\ rad/s$ and $\omega_2 = 52\ rad/s$, $\xi_1 = \xi_2 = 0$, respectively. Thus, the oscillatory behaviour is depicted by second order system for each axis with different frequencies and damping ratios. The end-effector is controlled via the robot controller to follow a desired trajectory which has Bang-Bang profile.

4.2.1 Offline trajectory generation scheme

A simple way to guarantee the motion synchronization of the multiple axes induced-motion is the offline solution. This can be reached by setting $(n-1)$ trajectories to the fixed time constraint T_c given by the slowest DOF as follows

$$\begin{aligned} T_c &= max(T_i) \\ &= max(T_{J,(X)}, T_{J,(Y)}) \end{aligned} \tag{4.19}$$

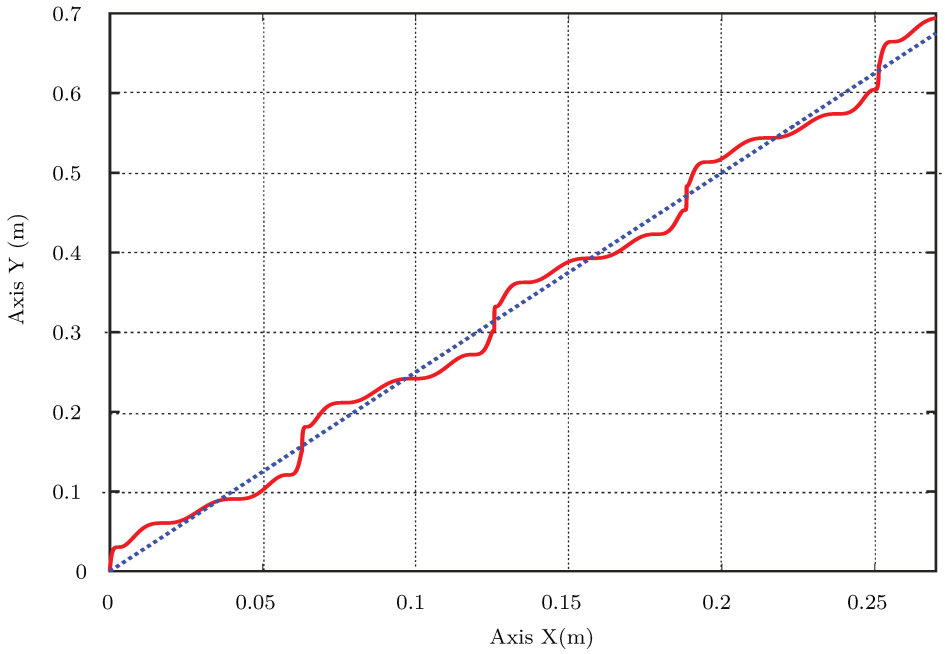

Figure 4.7: The input reference signal in dashed blue compared to the system response for unshaped input in red. Two vibration modes: $w_1 = 10rad/s$ on (X) and $w_2 = 52rad/s$ on (Y).

Here $T_{J,(Y)} < T_{J,(X)}$, from (4.15) we have $T_{J,(X)} \approx 0.62s$ and $T_{J,(Y)} \approx 0.12s$. Thus, we choose $T_c = T_{J,(X)}$. This adjustment can be done in several ways. Here, we propose to take benefits from the filtering strategy to easily compute the fixed-time solution for the jerk-limited profile. The multi-axis synchronisation is done on the slowest axis which can be interpreted as the axis submitted to the lowest natural flexible frequency. This strategy implies following the slowest time response which may restrict the dynamic of the manipulator. Since the planification process along with filtering are executed off-line, the shaper block may be considered in planification stage. Thus, the online trajectory generation is proposed to deal with the time evolution profile on the online trajectory specifications and constraints.

In offline synchronization scheme, the trajectory is pre-designed so that no real time information is needed, only the kinematic constraints are considered, see figure (a) (4.8). The filtering shaper stage is proceed in planification step. One may note that on each axis the filter is implemented with different parameters that depend on the vibration system (frequency and damping ratio). The trajectories synchronization scheme is designed so that the axis with faster response follows the slowest one. That can just be achieved by setting the trajectories to a fixed time constraint given by the slowest DOF. As shown in figure (4.9), the output follows perfectly the input reference signal with zero phase

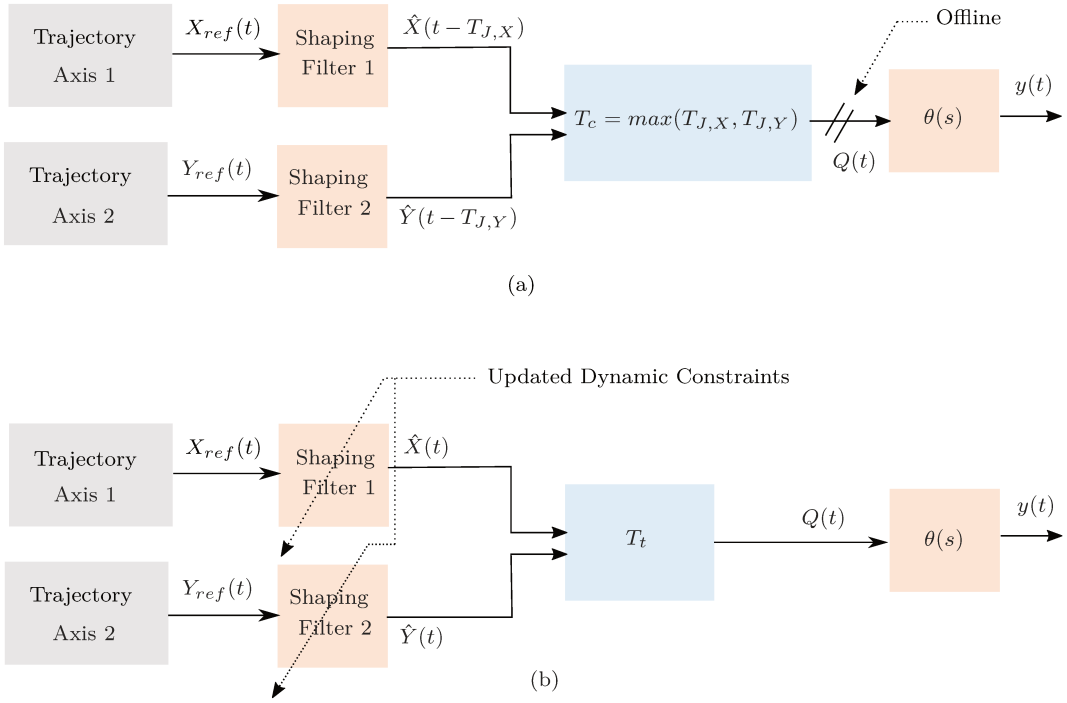

Figure 4.8: Control scheme for trajectory synchronisation: (a) offline solution ;(b) online solution. Where $Q(t)$ represents the resulting motion vector.

tracking.

4.2.2 Online trajectory generation scheme

In this context, the trajectory may change arbitrarily. Thus, the filter scheme should be adapted to meet the expected performance even when the trajectory is not pre-defined, see figure (b) (4.8). In online-filter shaper, it is necessary to reduce the vibration and at the same time eliminate the static error when the input signal is composed of ramps. The time delay resulting from the convolution of the input signal with filter is still critical since the process is performed in real time. The zero-phase tracking of the input signal is required to not influence the dynamic performance of the dynamic system. Thus, the zero-phase input tracking of vibratory systems is intensively studied to deal with the online filter time compensation [170, 173].

Case 1:

The online trajectory generation scheme is an interesting solution since the kinematic constraints on the trajectories are updated in real time. The filter shaper scheme is added on each axis separately according to the vibration mode of each axis, such as the one presented in figure (4.4). The time delay which is caused by the filter shifts the

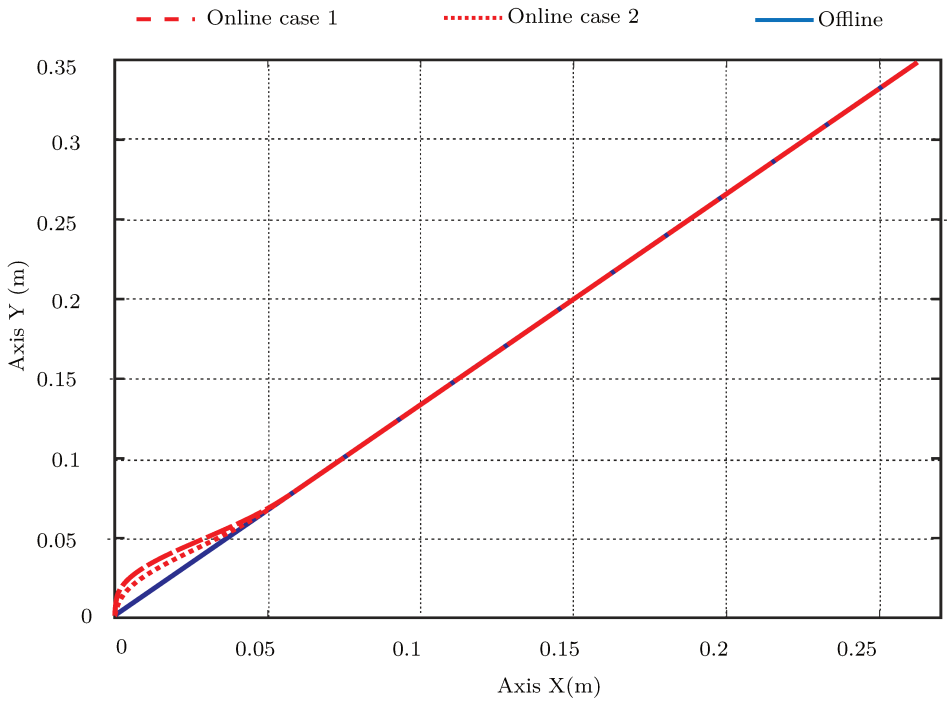

Figure 4.9: The system response for different cases.

reference input and produces eventually a static error. This offset may be eliminated after a transitional time by the feedforward compensation action given as follows

$$T_T = max(T_{J,i}) \tag{4.20}$$

where $T_{J,i}$ is the ith time response of the ith axis. In the present example we have

$$\begin{aligned} T_T &= max(T_{J,(X)}, T_{J,(Y)}) \\ &= T_{J,(X)} \end{aligned} \tag{4.21}$$

Thus the trajectories synchronization is achieved automatically and the output follows the input reference signal perfectly with zero phase tracking after transition time T_T, see figure (4.9).

Case 2:

As mentioned in case 1, the filter and the compensation scheme allows the output signal to follow the input signal with zero phase tracking. Nevertheless, the overshoot amplitude in the transitional time is undesirable specially if the robot task requires a perfect tracking along all points of the prescribed TCP trajectory including transitional phase as well. In order to reduce this overshoot, the compensation feedforward action is not

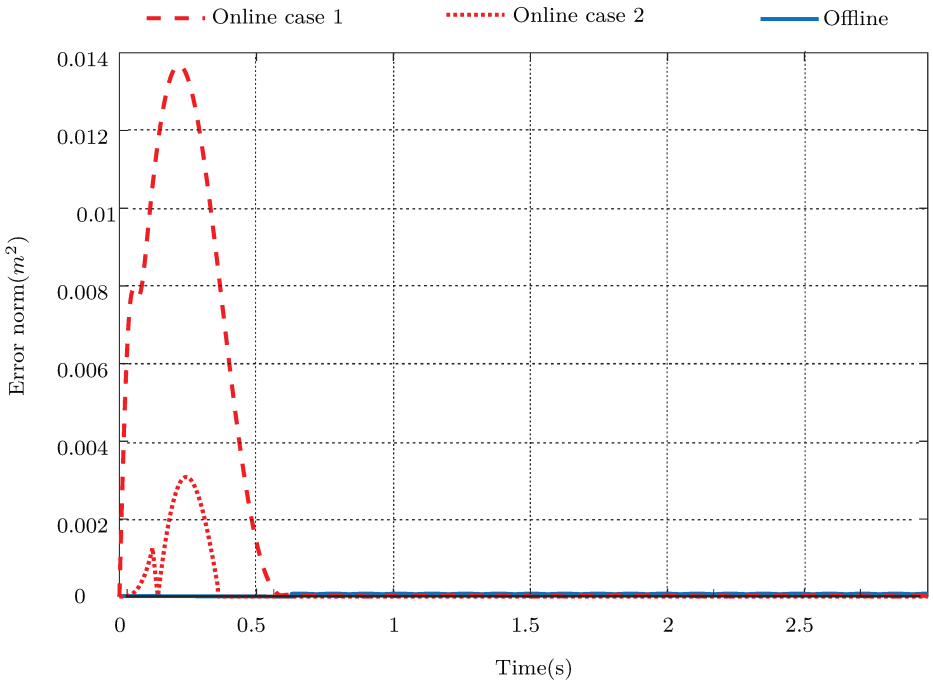

Figure 4.10: Error norm in the three cases.

used for the axis with fast response and is only used on the other slower response axes to follow their input reference after time delay is equal to the smallest transitional time response among all the axes which is formulated as follows

$$T_T = min(T_{J,i}) \tag{4.22}$$

since $T_{J,(X)} < T_{J,(Y)}$, the response on the axis (X) follows the reference trajectory after a time delay equals to $T_{J,(Y)}$. As a result, this proposed solution produces shifted output signal and the zero phase tracking is achieved in case of online trajectory synchronization for the global trajectory. This filter scheme is adapted as well for offline trajectories synchronization. Compared to the case 1, the time delay is smaller and, on the other hand, a small overshoot is noted in the transitional time, see figure (4.9).

4.3 MULTI-AXIS MOTION ANALYSIS

The trajectories synchronization and the nature of the implemented shaper is discussed and resumed in table (4.1). As discussed in the different possible cases, we can deal with the delay by taking into account a simple compensation in the development of the feedforward control. The time response and the robot closed loop controller are designed separately from the trajectory generation. The vibrations are reduced by 95% in all cases

	Offline solution	**Online Case 1**	**Online Case 2**
Synchronization	Offline	Online	Online
Trajectory tracking	Ideal	An overshoot in transitional time ($\|e\| = 0.014m^2$)	A reduced overshoot in transitional time ($\|e\| = 0.003m^2$)
Vibration reduction	Damped out (95%)	Damped out (95%)	Damped out (95%)
Time constraint	Slow (offline)	Fast (no time delay)	Average (time delay T_T in (4.22))

Table 4.1: Comparison study of different possible cases for trajectory synchronization and filtering shaper.

since the synchronization has been done on the filtered trajectories.

On the operational time, the offline planification consumes a considerably time compared to the online solution since three phases are considered in the control design: trajectory planning, adjustment, implementation. On the other hand, the online scheme in case 1 has faster time response where the null-phase velocity tracking is achieved, while in case 2 the response is delayed by a time interval equals to the minimum time response among all the considered motion axes.

Thus, the offline trajectory scheme is preferred in repeated applications where the task is not susceptible to alter the dynamic constraints, otherwise, the online trajectory planning is suggested. On the trajectory tracking performance, the offline adjusted trajectory follows perfectly the prescribed trajectory since the time delay is truncated. Nevertheless, the two proposed solutions in online scheme presented an overshoot in translation phase (less in the case 2) where the error norm is $\|e\|_{case1} = 0.014m^2$ for first case and $\|e\|_{case2} = 0.003m^2$ in case 2, see figures (4.9) and (4.10). This error can be tolerated if it is within the system dynamic constraints. The ratio $(\Delta\hat{r}/\Delta r)$ represented on figure (4.6) can be used to add optimization constraint on the synchronisation scheme, this ratio is less than one in case of filtered trajectory without compensation action (null-phase velocity),

$$\frac{\Delta\hat{r}}{\Delta r} < 1 \tag{4.23}$$

Generally, the different proposed forms of the shaping filters in literature focus on the effectiveness regarding the vibration reduction and the residual vibrations. The experimental tests are performed on simple one axis in one direction motion, but did not treat the case when the motion is generated by n axes with different flexural modes which implies different time delays on each axis. One may note that the shaping filter has a high degree of robustness according to the frequencies missmatch or non-stationarity. The practical application of such strategy was presented for instance in [49]. In practice, the neglected rigidity or the non-linearity of the robot may certainly limit the perfect vibration compensation.

4.4 CONCLUSION

In this chapter, the jerk-limited profile is used to reduce the vibrations of multi-axis manipulator since it is turned to be able to cancel undamped vibrations for flexible dynamic system. In addition, the analysis of its effectiveness in case of multi-axis applications revealed challenging possible scenarios, such as null-phase velocity tracking and trajectory synchronisation. This can be noticed in trajectory which is composed of ramp functions tracking and multi-axis motion planning respectively. To guarantee the vibration reduction as well as the perfect tracking of the prescribed trajectory, a suitable solution is put forward in section 4.1. The motion synchronisation is discussed via different proposed solutions in section 4.2. The main contribution of the present work is to demonstrate that it is possible to use shaping methodology for vibration suppression in online reactive control of synchronized axes. Thus, the main interest is how to adapt the feedforward control to achieve the prescribed trajectory for multi-axis motion. The different scenarios with the proposed solutions focus on how to deal with the synchronization to be feasibly tested on real robots, as long as the dominating modal frequencies values are known on each axis. The results in section 4.2 show that the synchronization should be considered to guarantee the tracking of the trajectory performed by multi-axis manipulator. This control action is integrated to the proposed feedforward control in chapter 3 in order to generalize the proposed approach for multi-axis motion.

In section 4.3, the comparison analysis shows that it is critical to select one solution among the others since they are depended on multiple factors. The task specifications should be considered before any solution selection. Future works may focus on adapting the dynamic constraints with the transient error so that the input trajectory stay within its defined limits.

Chapter

5 CONCLUSIONS

The main contribution of the thesis is to exploit the robot redundancy to enhance the manipulator precision and the robotic manipulation of flexible load. The redundancy resolution is useful and highly advantageous since it reinforces the optimal functionality of the robotic task to overcome its accuracy-positioning limitation.

In robotic manipulation task, many factors should be considered to achieve a precise positioning operation. In the case of mobile manipulator which is handling task of transporting a load, the deformation is caused by one or a combination of the followings: robot flexible structure, mobile platform and flexible load. In chapter 1, the induced deformations due to the mechanical conception of the robot and the load are presented. The deformations can be additive while passing from one sub-system to another. The manipulator inaccuracy is generally caused by the transmission/reduction components in the joint gearbox. On the other hand, the mobile platform is likely to deteriorate the dynamic precision because of the discontinuous structure of its Mecanum wheels. The mostly identified errors are the slippage error and those which are related to the angular navigation. In a point-to-point motion, the flexible load can be deformed under the actuated force of the robot dynamics, which may cause a degradation of its shape and eventually the load positioning is deflected. Nevertheless, the errors issued in robotic manipulation task are mostly systematic and can be reduced using motion control algorithms.

The actuated torques of flexible robot manipulators are the main source for the exciting force of the flexural motion. In chapter 2, the redundancy resolution integrates the optimization problem under dynamic constraints on vibration reduction to resolve the robot trajectory. The null-space motions are exploited to select optimum joints torque in the design of the proposed feedback control. In positioning task, this solution allows the manipulator to maintain the nominal trajectory with minimum motion-induced vi-

brations. The flexural motion is transformed to a free-damped vibratory system which vanishes quickly after the system time response. The redundancy resolution used in the proposed approach helps to linearize the robot plant on which the control scheme is conducted using the linear control theory. Since the robustness of the control relies on accurate dynamic modeling either via measurement and/or numerical estimation.

The accumulated deformations from the mobile platform until the robot TCP are added to the load deformations in aim to reduce all errors at once. In chapter 3, a control approach is proposed for robotic manipulation of deformable objects to reduce the motion-induced deformations. This solution guarantees both an accurate robotic manipulation and safe collaborative environment including the positioning accuracy, the object quality and the optimal execution time. The two stages feedforward-based approach combines the trajectory shaping technique for vibrations reduction and a corrective action for elastic deformations compensation which are caused by the inertial force of the robot dynamics. The latter exploits the redundancy of the robot, meaning the free Cartesian rotation DOFs in this case, to mitigate the flexural motion of the flexible load. The sensitivity with regard to frequencies variation has been derived. The results show that for a given task, a large variation margin on the frequency estimation is tolerated. Thus, the proposed solution is simple and easy to implement in the robot controller which is promising for industrial applications. The shaping filter induces a time delay which may deviate the filtered trajectory from its reference. In chapter 4, a compensation feedforward scheme is added in order to achieve a consistent synchronization of an asynchronized multi-axis motion. The null-phase tracking error is achieved along the motion direction according to the task specifications. Online and offline solutions are proposed for the possible scenarios.

Future works focus on potential developments of the present works to take advantage of the redundancy DOFs in order to enhance the performances of the robotic manipulation process. First, the sensitivity to system parameters should be considered to define a reliable work-space in the case of the feedforward control which is based on the robot's dynamic model. Then, the implementation of the feedback control solution on redundant flexible manipulators can be then conducted in the low-level control-loop of the robot plant. Additional sub-tasks can be considered on promise of improving the kinematic and/or dynamic performances of flexible redundant manipulators since the analysis of the self-motions satisfying the vibration reduction revealed an additional redundancy DOFs in chapter 2. For example to minimize the energy which drives the robot joints. On the other hand, the proposed feedforward scheme is suitable for robotic manipulation in industrial applications to compensate for the deformations of a flexible load during the translational motion. The outcome of this work is to design a control approach so that the manipulators are precise while being fast with low costs. The coming works focus mainly on the generalization of the methodology for translational and rotational motion of the flexible load to mitigate the torsional and the flexion deformations. The dynamic constraints with the transient error should be adapted so that the input trajectory stay within its defined limits for better synchronised motions in the case of multi-axis motion. The load transporting or assembly tests in an industrial context are envisaged to make

use of the proposed work. The mobile platform may offer more redundancy DOFs for the robotic manipulation task. The frequency of the induced error from its Mecanum wheels should be analyzed to avoid the aggravation of the load deformation. In meanwhile, the additional DOFs can be exploited in this case to manage and coordinate the robot motion (robotic platform and robot manipulator). For example to avoid static and/or dynamic obstacle such as in the context of the industry 4.0 where the Human-robot shared the same environment, and in which the robot can maintain performing its task while offering flexible and enough room to make it easy for the co-workers to move around freely and safely.

Chapter

A Résumé étendu de la thèse

A.1 INTRODUCTION

A.1.1 Solutions de manipulation robotique

Depuis son introduction à l'ère technologique, le robot envahit rapidement tous les secteurs d'activité pour répondre aux besoins de la vie humaine, comme c'est le cas pour l'industrie manufacturière, l'ingénierie spatiale, la santé, etc. Les processus industriels ainsi que les exigences de leurs applications, telles que la production et la fiabilité optimales en termes de temps, nécessitent des systèmes dynamiques et notamment des robots manipulateurs dotés d'un haut niveau de dextérité pour fonctionner dans des environnements sophistiqués.

L'interaction homme-robot est le principal défi de cette nouvelle ère industrielle, c'est-à-dire l'industrie 4.0 [1]. Le développement actuel de robots manipulateurs collaboratifs dédiés à l'interaction avec l'homme révèle des scénarios opérationnels pour lesquels l'homme et les robots partagent le même espace de travail. Soit dans le contexte industriel, soit dans les domaines de l'assistance personnelle. De nombreuses normes et chartes ont été introduites depuis, pour garantir la sécurité des travailleurs et les normes de qualité [2].

La manipulation robotique est l'un des procédés les plus utilisés dans l'industrie manufacturière afin d'améliorer le retour sur investissement de la production, voir figure (A.1). Ainsi, les solutions pour la manipulation mobile (c'est-à-dire un ou deux bras manipulateurs sur une base mobile) trouvent un intérêt particulier. Il existe de nombreux types de robots différents sur le marché, et le meilleur choix peut être basé sur les spécifications des tâches ainsi que sur le coût.

Suivant les principales contributions qu'elle entend apporter (voir figure (A.2)).

Figure A.1: Contexte industriel d'un robot mobile manipulant un pare-chocs de voiture souple.

A.1.2 Structure du manuscrit

- **Chapitre 2** introduit l'utilisation de la résolution de redondance pour l'amélioration de la précision dynamique d'un robot manipulateur à structure flexible. Tout d'abord, le couplage dynamique entre le mouvement de flexion et les DDL (Degrés De Liberté) de contrôle du robot est analysée pour quantifier l'erreur dynamique. La solution de redondance permet d'amortir les vibrations dynamiques tout en suivant précisément la trajectoire nominale. Cette solution révèle des configurations optimales où l'énergie du robot est minimisée puisque la contrainte d'optimisation du couple est prise en compte dans la résolution de la redondance.

- **Chapitre 3** quantifie toutes les sources de déformations du robot manipulateur mobile et de la charge flexible au point d'extrémité de l'objet manipulé. La déformation élastique et les vibrations résiduelles sont contrôlées par une approche de planification de trajectoire utilisant un schéma d'une action anticipatrice qui est la combinaison d'un filtre de lissage et d'une résolution de redondance du robot. La robustesse de l'approche est retenue et discutée dans le cadre d'une manipulation

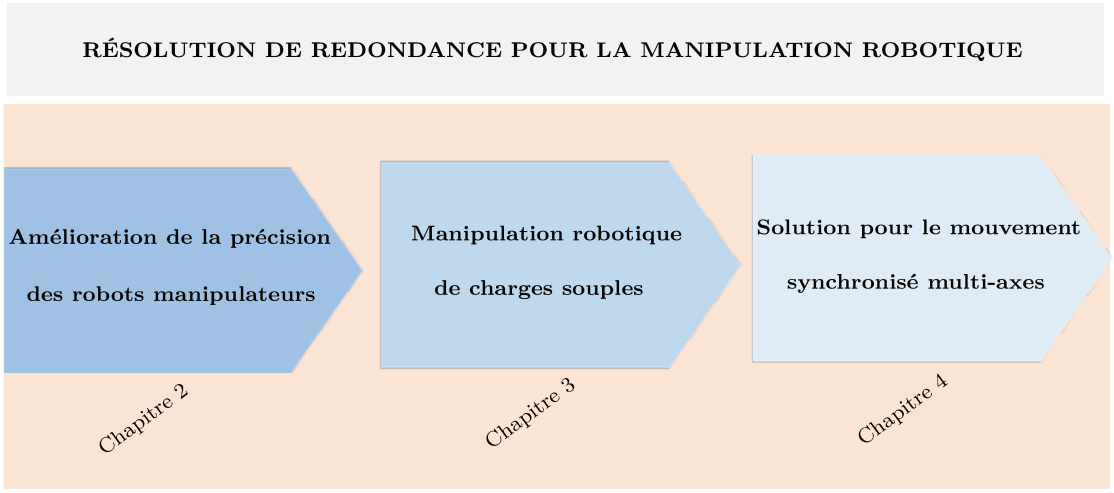

Figure A.2: Organisation de la thèse.

robotique précise pour des applications industrielles.

- **chapitre** 4 se concentre sur les problèmes de dégradation de la trajectoire pour des mouvements multi-axes où le retard du filtre de mise en forme induit un mouvement asynchrone. Le schéma de l'action anticipatrice est ajusté en ajoutant une action de compensation sur les trajectoires filtrées. Les principales catégories de mouvement synchronisé sont proposées en fonction de l'erreur de transition et de la nature de la planification des trajectoires, c'est-à-dire un schéma en ligne ou hors ligne.

A.2 L'IMPRÉCISION DANS LA MANIPULATION ROBOTIQUE

Les sources d'imprécision sont multiples, elles peuvent être regroupées en deux catégories différentes : les erreurs dues à la conception mécanique et les erreurs dues au contrôle utilisé. La déformation d'un manipulateur mobile pourrait être traitée séparément, en supposant que le manipulateur est rigidement attaché à un robot mobile, ce qui est le cas généralement considéré dans la pratique. Par la suite, il s'agira donc de présenter les différents potentiels facteurs qui peuvent affecter la précision des tâches robotiques : la structure flexible du manipulateur de robot, la plate-forme mobile et la charge flexible.

Conception des articulations

Articulations	Couple	Raideur
1 & 2	200 N	20000 N/m
3 & 4	85 N	12000 N/m
5 & 6 & 7	35 N	6000 N/m

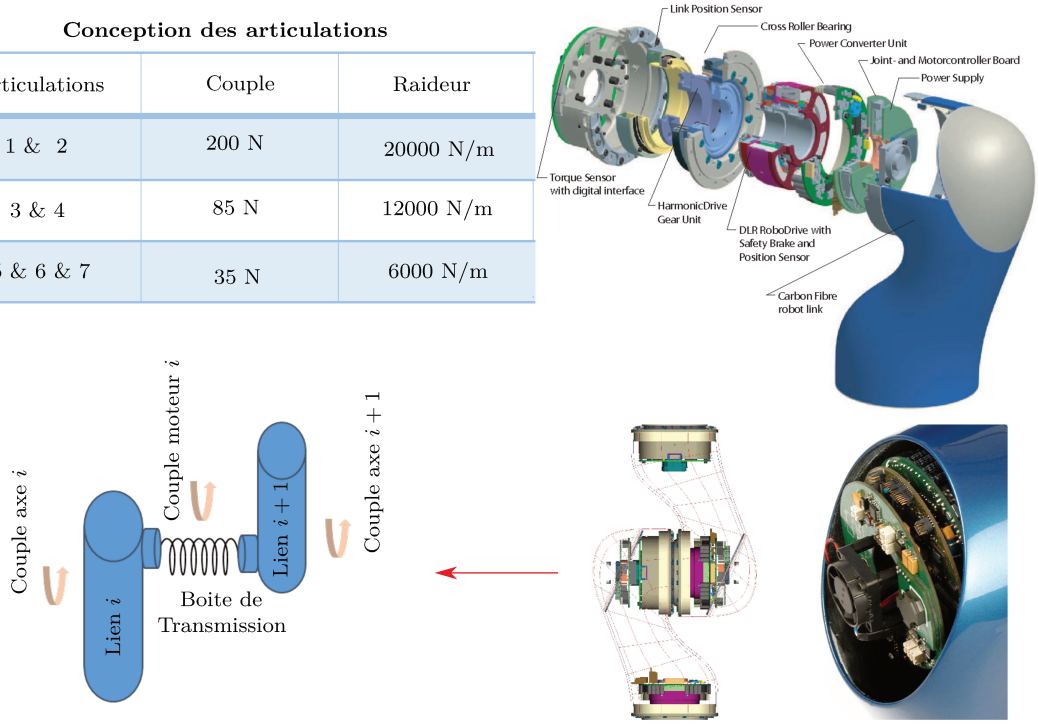

Figure A.3: Conception de l'articulation mécanique du manipulateur léger DLR.

A.2.1 Robots manipulateurs flexibles

La vision robotique du futur a accordé plus d'attention aux manipulateurs flexibles, qui ont une structure légère, un faible coût, un rapport charge/masse élevé et une faible consommation d'énergie, ainsi que la capacité d'effectuer une tâche donnée à grande vitesse. En plus de la sécurité de l'interaction Homme-Robot, la vision de la robotique du futur s'intéresse aux manipulateurs flexibles. Les remarquables avantages des manipulateurs flexibles précédemment exposés en font la génération de manipulateurs robotiques appropriée pour l'industrie, par rapport aux manipulateurs rigides classiques. Le robot manipulateur est constitué d'une série de corps reliés par des articulations. Cependant, la présence des structures flexibles induit un comportement oscillatoire à l'extrémité du manipulateur, d'où la détérioration de la précision et la dégradation des performances. Cette erreur dépend à la fois de la conformité du robot et de la force appliquée extérieurement au point central d'outil (TCP : Tool Center Point). La déformation est variable dans le temps et diffère principalement dans l'espace de travail en raison des changements de configuration du manipulateur. Donc le mouvement du TCP est influencé par des mouvements rigides et de flexion qui sont dynamiquement couplés.

Dans le cas du manipulateur à articulations souples, le robot est caractérisé par des corps rigides et des articulations souples. L'élasticité de la transmission du moteur à l'articulation peut être représentée par un ensemble de systèmes simples de paires ressort-

amortisseur, où le ressort est modélisé comme torsionnel pour l'articulation en rotation et linéaire pour la translation [3, 4, 5]. L'hypothèse sur laquelle repose l'élasticité linéaire est due aux petites déformations limitées dans l'articulation où les contributions de la dynamique non linéaire sont négligées. Les composantes de transmission/réduction du mouvement rendent l'articulation mécaniquement souple, voir la figure (A.3). Elle est de préférence utilisée pour se conformer au contact de l'environnement physique pour des interactions souples. Par exemple, dans un contexte visant à assurer l'entière sécurité de la collaboration Homme-Robot [2]. On peut noter que les articulations souples sont soumises à une contrainte de stockage d'énergie due à la transformation de l'énergie cinétique en énergie potentielle entre l'inertie dynamique du robot et les articulations souples. De nombreuses tâches robotiques requièrent des couples d'articulation considérablement développés, qui excitent principalement la structure flexible de l'articulation, entraînant des vibrations dynamiques au niveau de l'effecteur final.

Concernant les liens flexibles, leur fabrication est réalisée à partir de matériaux légers et résistants, supposés avoir des propriétés uniformes. Cette structure particulière a un impact énorme sur l'utilisation d'énergie, puisque concevoir un robot léger de ce type requiert moins d'énergie que pour un robot à structure rigide. La vitesse du robot augmente ainsi que le rapport charge utile/masse [8, 9]. De ce fait, les manipulateurs avec des corps flexibles attirent de nombreuses applications dans des domaines variés. Par exemple, les robots dotés de longs bras flexibles sont les meilleurs candidats dans les applications spatiales ont une longue portée dans le but d'assister les astronautes. Dans un environnement de faible gravité, le robot peut aider à collecter des débris spatiaux, à entretenir la station spatiale et à assurer le processus d'approvisionnement [10, 11]. Pour cela, le manipulateur flexible est monté sur des engins spatiaux en flottaison libre afin d'accroître sa maniabilité [12]. Dans le domaine médical, la sécurité des opérations est garantie grâce à la conformité du robot et à la réduction de son inertie.

A.2.2 Robot mobile

Les robots mobiles conventionnels, avec une ou deux paires de roues actionnées, ont une manœuvrabilité limitée dans leur exécution de tâches sous certaines contraintes cinématiques, comme l'évitement d'obstacles. D'autre part, les plates-formes mobiles omnidirectionnelles offrent davantage de possibilités cinématiques à l'espace de travail du robot grâce à la construction mécanique spéciale de ses roues [19]. Par rapport aux roues conventionnelles, les roues omnidirectionnelles sont actionnées indépendamment. Elles ont été inventées par Ilon en 1975 [20]. Les rouleaux courbés sont disposés autour de la circonférence de chaque roue. La disposition de chaque axe de rouleau doit être inclinée de 45^o par rapport à l'axe de la roue concernée. Ainsi, la plate-forme omnidirectionnelle a trois DDLs dans le plan de mouvement horizontal, ce qui lui permet de se déplacer instantanément dans n'importe quelle direction par la simple combinaison de la vitesse des roues sans les diriger du tout. En plus de la redondance de mouvement, la plateforme robotique omnidirectionnelle permet de gagner du temps et de consommer moins d'énergie [19].

Le mouvement rigide de la base mobile est susceptible de détériorer la précision dy-

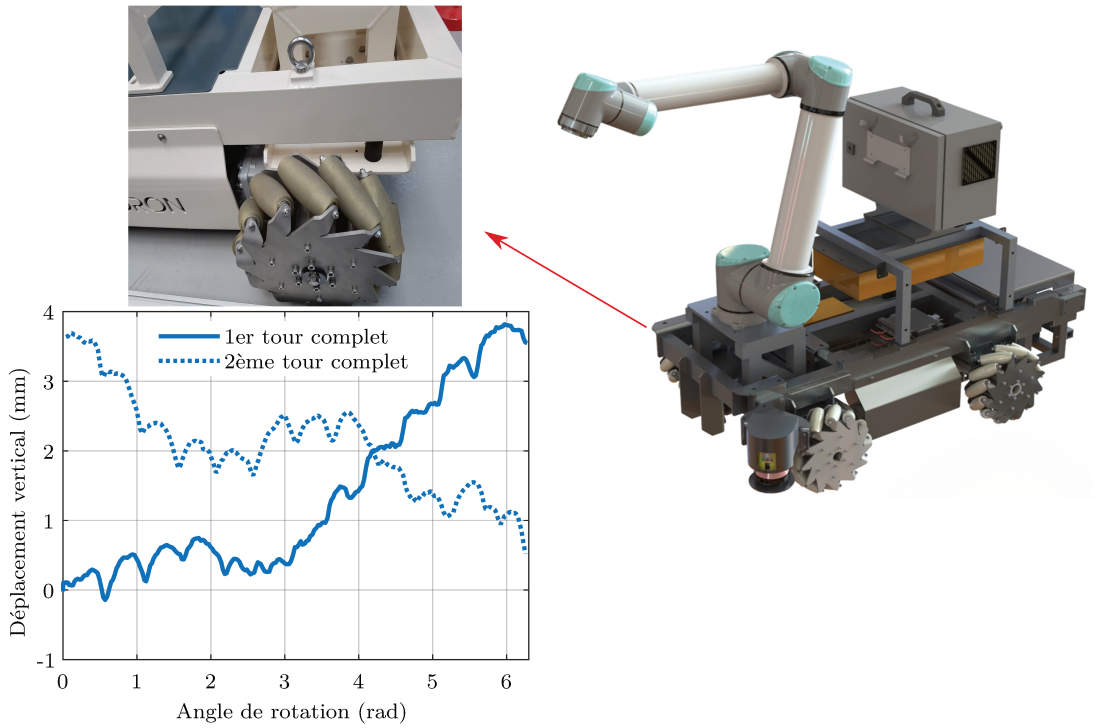

Figure A.4: Plate-forme mobile TC200 : 12 rouleaux sur chaque roue. La quantification des erreurs est mesurée pour 20 % de la puissance maximale. L'amplitude de la déviation verticale due aux roues (c'est-à-dire l'écart entre les rouleaux intérieurs et les rouleaux extérieurs) est inférieure d'environ 1 mm à celle qui provient de la surface du sol ($4mm$).

namique de l'effecteur final du manipulateur, notamment en provoquant des vibrations, voir figure (A.4). En raison de la structure incurvée des rouleaux, elle n'est pas adapté à l'exécution de mouvements fluides. Le point de contact entre la roue et le sol est trop petit, de sorte qu'il varie de façon discontinue d'un rouleau à l'autre pendant le mouvement. Ainsi, la rotation séquentielle de la roue induit des vibrations périodiques le long du mouvement, ce qui peut limiter les performances de l'algorithme de navigation [21]. La composante verticale de l'erreur induite par le mouvement est critique pour les opérations des robots mobiles. Par conséquent, elle peut entraîner une instabilité et des déformations de l'outil ou de la charge transférée à l'effecteur final du robot manipulateur. Différents facteurs sont liés à l'apparition de ces déformations pendant le mouvement de la plate-forme mobile [24]. Celle-ci est principalement influencée par la vitesse angulaire, l'alignement des roues avec l'axe vertical du corps de la plate-forme, la forme géométrique, y compris l'écart dû au point de contact discontinu, la structure flexible du corps de la plate-forme. On peut noter que le facteur le plus important est la surface de contact puisque la plate-forme mobile est très sensible aux irrégularités du sol [23]. Cette erreur est fortement appréciable lors du mouvement de la plate-forme, voir figure (A.4).

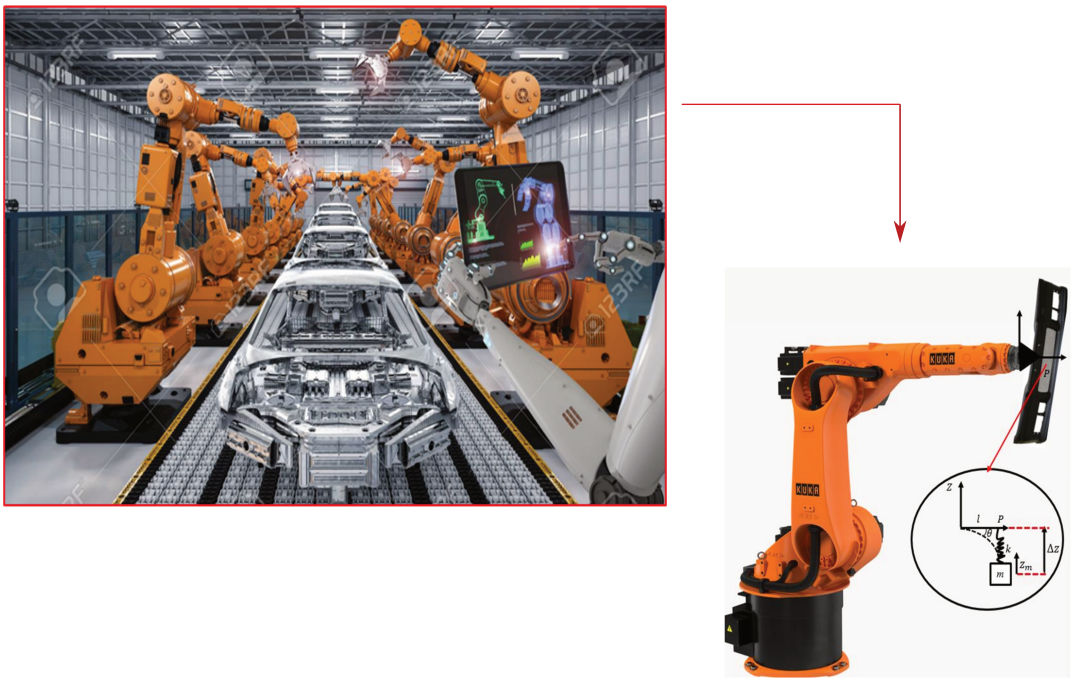

Figure A.5: Exemple de manipulation d'objets déformables "pare-chocs de voiture", les vibrations induites par le mouvement peuvent être présentées par un système oscillatoire incluant les modes de vibration.

A.2.3 Charge flexible

Dans un contexte de manipulation, l'intervention des travailleurs est limitée en raison de la question de la sécurité ou d'autres contraintes. Par exemple, la manipulation de conteneurs en acier fondu ou de toute sorte de liquides dangereux. Par conséquent, le robot est chargé de manipuler différents types de charges qui ont une structure corporelle rigide ou flexible. La manipulation de tels objets déformables peut être trouvée dans les industries automobile et aérospatiale pour des opérations d'assemblage, comme dans le cas des câbles ou des pare-chocs de voiture, voir la figure (A.5). Cela peut être également le cas dans des activités de la vie quotidienne, par exemple pour le pliage des vêtements. Mais le robot n'est pas qualifié pour manipuler des charges flexibles en utilisant des algorithmes qui sont développés pour la manipulation de corps rigides, la contrainte de déformation doit donc être prise en compte dans le but d'ajuster le processus de préhension et de transport notamment. Ainsi, le robot peut atteindre la pose souhaitée qui correspond à la pointe de la charge ou à tout autre point de référence sur la structure de son corps. Cela inclut l'orientation pour un angle donné ou la pose pour une courbure spécifique.

Une manipulation robotique spécifique doit être abordée en cas de charges déform-

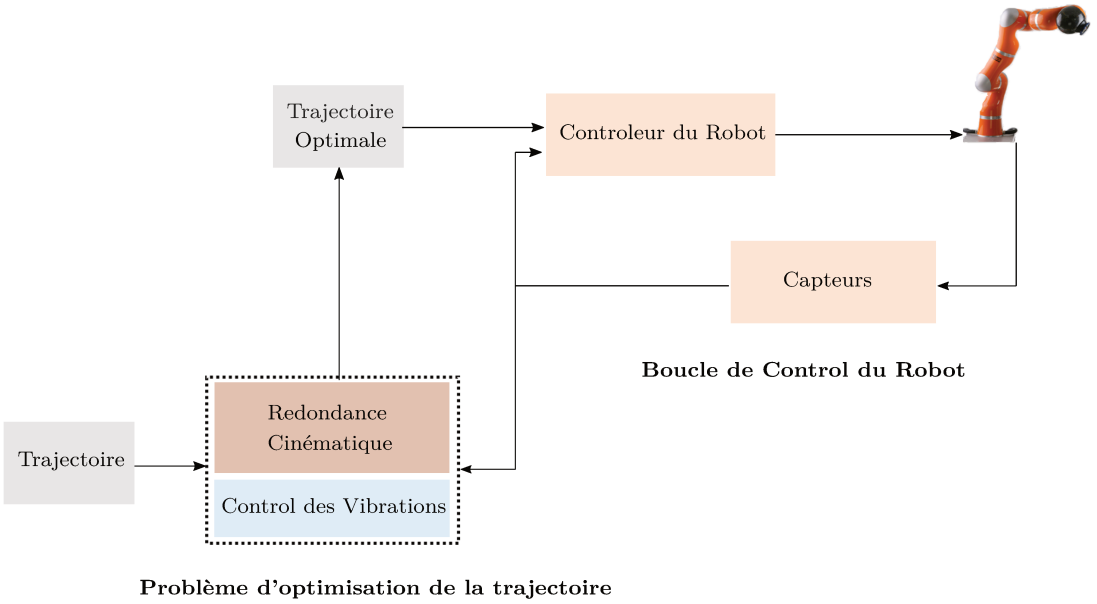

Figure A.6: Contrôle des vibrations via la résolution de la redondance.

ables. La structure de la charge peut être déformée sous l'effet de forces externes ou de forces provenant de la dynamique du robot lui-même où la force actionnée est appliquée. Par conséquent, une dégradation variable dans le temps de sa forme par rapport à la forme d'origine peut se produire. On peut noter que tous les objets déformés ne peuvent pas retrouver leur forme initiale, cette caractéristique peut distinguer les objets déformables en trois modèles principaux. D'une part, les objets soumis à une déformation dimensionnelle en fonction de leurs propriétés physiques, comme les objets déformables linéaires tels que les poutres et les cordes. D'autre part, les objets soumis à une déformation bidimensionnelle, si leur dégradation se produit dans un plan, soit sur le contour, soit sur la surface. Par exemple, le mouvement du liquide en cas de transport linéaire d'un récipient rempli de liquide. Enfin, les objets soumis à une déformation tridimensionnelle, comme dans le cas de la manipulation d'un morceau de viande où les déformations sont constatées dans les trois directions de la charge. Comme toutes les autres structures flexibles, la charge flexible est un système sous-actionné qui peut contenir un nombre infini de DDLs [26]. Outre le contrôle du positionnement et de l'orientation de la charge, la déformation indésirable doit être raisonnablement contenue en limitant l'amplitude des vibrations [27, 28].

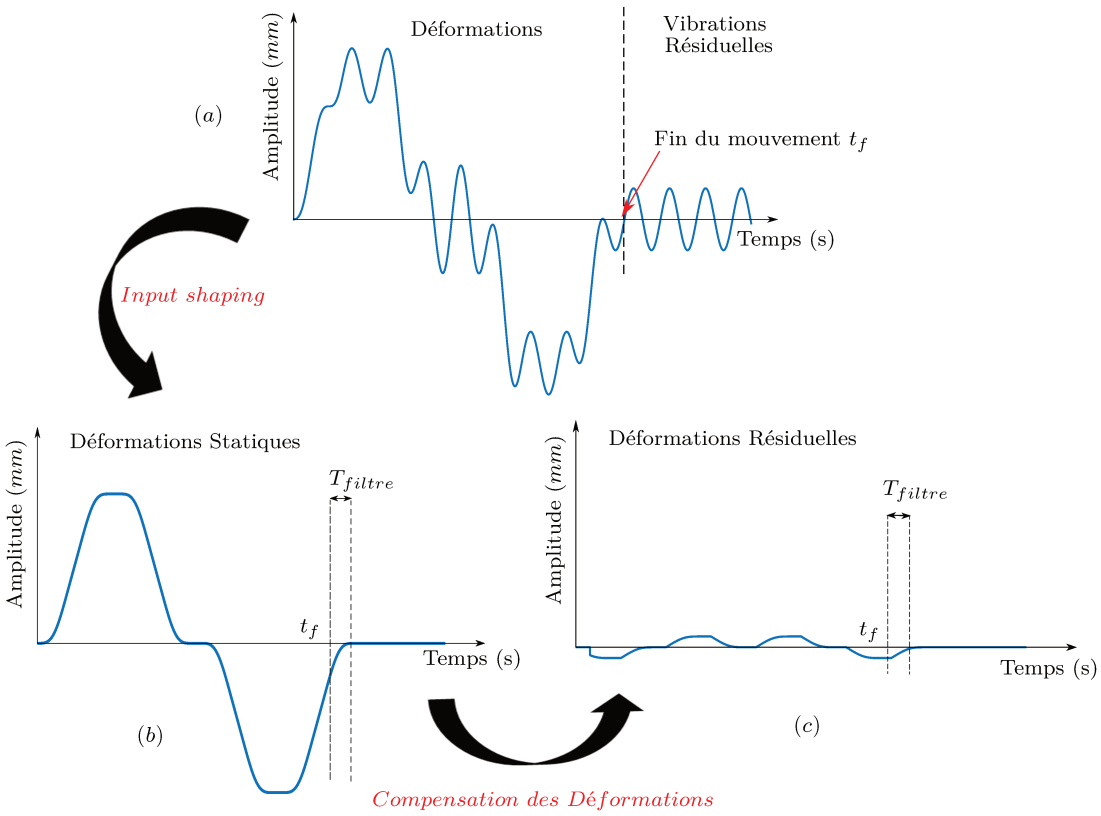

Figure A.7: Déformations : a) déformations et vibrations initiales. (b) déformations avec trajectoire de mise en forme pour la compensation des vibrations. (c) déformations résiduelles avec mise en forme de la trajectoire et de compensations pour des déformations. Avec T_{filtre} qui représente le délai dû au filtre de mise en forme.

A.3 CONTRIBUTIONS DE LA THÈSE

A.3.1 Contrôle des vibrations d'un robot manipulateur flexible et redondant en exploitant les capacités de redondance

Ce travail aborde la réduction des vibrations et l'amélioration de la précision des tâches pour un manipulateur, en utilisant la résolution de la redondance. La force excitante du mouvement de flexion qui est induite par le mouvement du manipulateur provoque une déviation non désirée au niveau de l'effecteur. Sur la base d'un modèle élasto-statique du robot collaboratif qui est cinématiquement redondant, le mouvement inhérent à la fonction de redondance est exploité pour amortir la vibration tout en maintenant la position de l'effecteur final. Afin d'exploiter tous les degrés de liberté dans l'espace nul, un concept de contrôle de rétroaction basé sur l'optimisation du couple a été introduit en utilisant une méthode analytique pour la résolution de la redondance, voir figure (A.6).

A.3.2 Génération de trajectoires de robot pour un transfert de charge flexible sous des contraintes de réduction des déformations

Dans cette étude, nous abordons le problème de la réduction des déformations élastiques et des vibrations résiduelles des charges flexibles lorsqu'elles sont manipulées par un robot manipulateur. Lors de la manipulation d'une charge de faible rigidité, comme un pare-chocs dans l'industrie automobile, de grandes déformations et vibrations peuvent être induites par le mouvement du robot. Ces déformations auront des effets néfastes sur le temps de stabilisation, sur la précision et sur l'intégrité du processus opérationnel dans un environnement contraint. Les méthodes de mise en forme de la trajectoire, c'est-à-dire le filtre de lissage ou la méthode de mise en forme de l'entrée sont des solutions bien connues pour la suppression des vibrations résiduelles d'un mouvement. Cependant, l'utilisation de la technique de mise en forme de la trajectoire seule peut ne pas suffire à supprimer les déformations élastiques statiques pendant la phase de transfert de l'objet souple. Ainsi, la principale contribution de ce travail est de proposer une approche en deux étapes, basée sur l'anticipation, qui combine la technique de mise en forme de la trajectoire pour la réduction des vibrations, avec une trajectoire de compensation des déformations. Cette dernière exploite l'espace de rotation du manipulateur pour atténuer le mouvement de flexion de la charge flexible, voir la figure (A.7).

A.3.3 Suivi de trajectoire avec contraintes de vibrations pour les mouvements multi-axes synchronisés

Dans le cadre de la planification des trajectoires, nous proposons une technique visant à améliorer la précision des manipulateurs de robots pour les mouvements composés multi-axes. Comme mentionné précédemment, la manipulation de charges flexibles et/ou la structure flexible inhérente du manipulateur induisent des vibrations indésirables au niveau de la charge/effecteur final qui entraînent une imprécision du mouvement. Le cas abordé dans cette thèse donne un meilleur aperçu de la capacité du profil limité aux secousses le long de la synchronisation temporelle à réduire la vibration résiduelle et à garantir un suivi précis des trajectoires prescrites. Pour l'action de filtrage en ligne, un système de compensation approprié a été mis en place afin d'obtenir une synchronisation cohérente entre les différentes trajectoires des axes du manipulateur. L'efficacité et la faisabilité de différentes approches pour les applications robotiques industrielles sont évaluées.

A.4 CONCLUSIONS & PERSPECTIVES

La principale contribution de la présente thèse est d'exploiter la redondance du robot pour améliorer la précision du manipulateur et la manipulation robotique d'une charge flexible. La résolution de la redondance est utile et très avantageuse car elle renforce la fonctionnalité optimale de la tâche robotique pour surmonter les limites de sa précision de positionnement.

Dans les tâches de manipulation robotique, de nombreux facteurs doivent être pris en compte pour réaliser une opération précise. Dans le cas d'un manipulateur mobile qui effectue une tâche de transport d'une charge, la déformation est causée par l'un des éléments suivants ou par une combinaison de ceux-ci : structure flexible du robot, plate-forme mobile et charge flexible. Les déformations dues à la conception mécanique du robot et de la charge sont présentées en chapitre 1. Les déformations peuvent être additives lors du passage d'un sous-système à un autre. L'imprécision du manipulateur est généralement causée par les éléments de transmission/réduction dans la boîte de vitesse de l'articulation. D'autre part, la plate-forme mobile est susceptible de détériorer la précision dynamique en raison de la structure incurvée de ses roues omnidirectionnelles. Les erreurs les plus souvent identifiées sont l'erreur de glissement et celles qui sont liées à la navigation angulaire. Dans un mouvement point-à-point, la charge flexible peut être déformée sous la force d'actionnement du robot, ce qui peut entraîner une dégradation de sa forme et, finalement, la déviation du positionnement de la charge. Néanmoins, les erreurs commises dans les tâches de manipulation robotique sont pour la plupart systématiques et peuvent être réduites en utilisant des algorithmes de contrôle de mouvement.

Les couples actionnés des manipulateurs de robots flexibles sont la source principale de la force excitante du mouvement de flexion. Dans le chapitre 2, la résolution de redondance intègre le problème d'optimisation sous des contraintes dynamiques de réduction des vibrations pour résoudre la trajectoire du robot. Les mouvements dans l'espace du noyau sont exploités pour sélectionner le couple optimal des articulations dans la conception de la commande de rétroaction proposée. Dans la tâche de positionnement, cette solution permet au manipulateur de maintenir la trajectoire nominale avec un minimum de vibrations induites par le mouvement. Le mouvement de flexion est transformé en un système vibratoire libre et amorti qui disparaît rapidement après la réponse du système. La résolution de redondance utilisée dans l'approche proposée permet de linéariser la boucle de contrôle du robot où le schéma de commande est réalisé en utilisant la théorie de la commande linéaire. Étant donné que la robustesse de la commande repose sur une modélisation dynamique précise, soit par mesure soit par estimation numérique, la sensibilité aux paramètres du système doit être prise en compte pour définir un espace de travail fiable.

Les déformations accumulées depuis la plate-forme mobile jusqu'au TCP du manipulateur sont ajoutées aux déformations de la charge afin de réduire toutes les erreurs en même temps. Dans le chapitre 3, une approche de contrôle est proposée pour la manipulation robotique d'objets déformables afin de réduire les déformations induites par le mouvement. Cette solution garantit à la fois une manipulation robotique précise et un environnement collaboratif sûr, c'est-à-dire la précision du positionnement, la qualité de l'objet et le temps d'exécution optimal. L'approche est basée sur l'anticipation en deux étapes et combine la technique de mise en forme de la trajectoire pour la réduction des vibrations et une action corrective pour la compensation des déformations élastiques qui sont causées par la force d'inertie de l'effecteur du robot. Cette dernière exploite la redondance du robot, c'est-à-dire les DDLs en rotation libre dans l'espace Cartisien, pour atténuer le mouvement de flexion de la charge flexible. La sensibilité en ce qui

concerne la variation des fréquences a été dérivée. Les résultats montrent que pour une tâche donnée, une grande marge de variation sur l'estimation des fréquences est tolérée. Ainsi, la solution proposée est simple et facile à mettre en œuvre, ce qui est prometteur pour des applications industrielles. Le filtre de mise en forme induit un délai qui peut dévier la trajectoire filtrée de sa référence. Dans le chapitre 4, un schéma de compensation est ajouté afin d'obtenir une synchronisation cohérente d'un mouvement multi-axes asynchronisé. L'erreur de poursuite à phase nulle est obtenue le long de la direction du mouvement selon les spécifications de la tâche. Des solutions en ligne et hors ligne sont proposées pour des scénarios possibles.

Les travaux futurs se concentrent sur la mise en œuvre de la solution de contrôle du retour d'états sur un manipulateur flexible et redondant. Des sous-tâches supplémentaires peuvent être envisagées, car elles promettent d'améliorer les performances cinématiques et/ou dynamiques des manipulateurs flexibles redondants. En effet, l'analyse des mouvements propres satisfaisant la réduction des vibrations a révélé des DDLs de redondance supplémentaire. D'autre part, le schéma d'anticipation est adapté à la manipulation robotique en applications industrielles pour compenser les déformations d'une charge flexible pendant le mouvement en translation. Les travaux à venir se concentrent sur la généralisation de la méthodologie pour le mouvement de translation et de rotation afin d'atténuer les déformations en torsion et en flexion. Les contraintes dynamiques avec l'erreur transitoire doivent être adaptées de manière à ce que la trajectoire de référence reste dans ses limites définies pour des mouvements mieux synchronisés.

Bibliography

[1] Saturno, Maicon, et al. "Proposal of an automation solutions architecture for Industry 4.0." 24th International Conference on Production Research, Poznan, Poland. 2017.

[2] Bounouar, Mouad, et al. "L'ergonomie, la robotique collaborative et le génie industriel: Vers une conception pluridisciplinaire des systèmes Humains-Robots ."Actes du 55ème Congrès de la SELF, L'activité et ses frontières, 2020.

[3] Fichera F., Grossard M., "On the modeling and identification of stiffness in cable-based mechanical transmissions for robot manipulators." Mechanism and Machine Theory, vol. 108, pp. 176-190, February 2017.

[4] Guo, Chuangqiang, et al. "A vibration suppression method for flexible joints manipulator based on trajectory optimization." 2016 IEEE International Conference on Mechatronics and Automation. IEEE, 2016.

[5] Spong, M. W. "Modeling and control of elastic joint robots." Mathematical and Computer Modelling 12.7 (1989): 912.

[6] Moberg, Stig. "Modeling and control of flexible manipulators." Diss. Linköping University Electronic Press, 2010.

[7] Li, Haijie, and Xuping Zhang. "A Method for Modeling Flexible Manipulators: Transfer Matrix Method with Finite Segments." International Journal of Computer and Information Engineering 10.6 (2016): 1086-1093.

[8] Benosman, Mouhacine, and G. Le Vey. "Control of flexible manipulators: A survey." Robotica 22.5 (2004): 533-545.

[9] Dwivedy, Santosha Kumar, and Peter Eberhard. "Dynamic analysis of flexible manipulators, a literature review." Mechanism and machine theory 41.7 (2006): 749-777.

[10] Sellmaier, Florian, et al. "On-orbit servicing missions: Challenges and solutions for spacecraft operations." SpaceOps 2010 Conference Delivering on the Dream Hosted by NASA Marshall Space Flight Center and Organized by AIAA. 2010.

[11] Aghili, Farhad. "Optimal control of a space manipulator for detumbling of a target satellite." 2009 IEEE international conference on robotics and automation. IEEE, 2009.

[12] Yihuan, L. I. A. O., Li Daokui, and T. A. N. G. Guojin. "Motion planning for vibration reducing of free-floating redundant manipulators based on hybrid optimization approach." Chinese Journal of Aeronautics 24.4 (2011): 533-540.

[13] Mordfin, Theodore G., and Sivakumar SK Tadikonda. "Truth models for articulating flexible multibody dynamic systems." Journal of Guidance, Control, and Dynamics 23.5 (2000): 805-811.

[14] Wang, Congqing, and Linfeng Wu. "Chaotic vibration prediction of a free-floating flexible redundant space manipulator." Shock and Vibration 2016 (2016).

[15] Parks, T. R., and H. A. Pak. "Effect of payload on the dynamics of a flexible manipulator—modeling for control." (1991): 409-418.

[16] Tu, Q., and J. Rastegar. "Effects of payload on the vibrational excitation of robot manipulators during motion." ASME Conf. Mach Elements Mach Dyn. 1994.

[17] Gao, Xin, et al. "Research on Joint Torque Optimization Method of Redundant Space Manipulators with Vibration Suppression." ITM Web of Conferences. Vol. 12. EDP Sciences, 2017.

[18] De Luca, Alessandro, et al. "Control problems in underactuated manipulators." 2001 IEEE/ASME International Conference on Advanced Intelligent Mechatronics. Proceedings (Cat. No. 01TH8556). Vol. 2. IEEE, 2001.

[19] Tătar, Mihai Olimpiu, et al. "Design and development of an autonomous omnidirectional mobile robot with Mecanum wheels." 2014 IEEE International Conference on Automation, Quality and Testing, Robotics. IEEE, 2014.

[20] Ilon, Bengt Erland. "Wheels for a course stable selfpropelling vehicle movable in any desired direction on the ground or some other base." U.S. Patent No. 3,876,255. 8 Apr. 1975.

[21] Xie, Li, et al. "Heavy-duty omni-directional Mecanum-wheeled robot for autonomous navigation: System development and simulation realization." 2015 IEEE International Conference on Mechatronics (ICM). IEEE, 2015.

[22] Li, Yunwang, et al. "Modeling and kinematics simulation of a Mecanum wheel platform in RecurDyn." Journal of Robotics 2018 (2018).

[23] Luo, Ren C., and Yueh-Shiuan Tsai. "On-line adaptive control for minimizing slippage error while mobile platform and manipulator operate simultaneously for robotics mobile manipulation." IECON 2015-41st Annual Conference of the IEEE Industrial Electronics Society. IEEE, 2015.

[24] Park, Young Kyun, et al. "Analysis of factors related to vertical vibration of continuous alternate wheels for omnidirectional mobile robots." Intelligent Service Robotics 9.3 (2016): 207-216.

[25] Doroftei, Ioan, Victor Grosu, and Veaceslav Spinu. "Omnidirectional mobile robot-design and implementation." INTECH Open Access Publisher, 2007.

[26] Tanner, Herbert G., and Kostas J. Kyriakopoulos. "A manipulated deformable object as an underactuated mechanical system." Robot Manipulation of Deformable Objects. Springer, London, 2000. 175-196.

[27] Tanner, Herbert G. "Mobile manipulation of flexible objects under deformation constraints." IEEE transactions on robotics 22.1 (2006): 179-184.

[28] Tanner, Herbert G., Savvas G. Loizou, and Kostas J. Kyriakopoulos. "Nonholonomic navigation and control of cooperating mobile manipulators." IEEE Transactions on robotics and automation 19.1 (2003): 53-64.

[29] Jiang, Zhao-Hui, and Masashi Kohno. "Robotic manipulation of flexible objects based on vibration control using force sensors." IEEE International Conference on Systems, Man and Cybernetics. Vol. 4. IEEE, 2002.

[30] Wada, Takahiro, et al. "Robust manipulation of deformable objects by a simple PID feedback." Proceedings 2001 ICRA. IEEE International Conference on Robotics and Automation (Cat. No. 01CH37164). Vol. 1. IEEE, 2001.

[31] Jasim, Ibrahim F., Peter W. Plapper, and Holger Voos. "Model-Free Robust Adaptive Control for flexible rubber objects manipulation." 2015 IEEE 20th Conference on Emerging Technologies Factory Automation (ETFA). IEEE, 2015.

[32] Luo, Yanhong, and Bradley J. Nelson. "Fusing force and vision feedback for manipulating deformable objects." Journal of Robotic Systems 18.3 (2001): 103-117.

[33] Alvarez, Nahum, and Kimitoshi Yamazaki. "An interactive simulator for deformable linear objects manipulation planning." 2016 IEEE International Conference on Simulation, Modeling, and Programming for Autonomous Robots (SIMPAR). IEEE, 2016.

[34] Singer, Neil C., and Warren P. Seering. "Preshaping command inputs to reduce system vibration." (1990): 76-82.

[35] Singhose, William. "Command shaping for flexible systems: A review of the first 50 years." International journal of precision engineering and manufacturing 10.4 (2009): 153-168.

[36] M. T. Ho and Y. W. Tu, “PID controller design for a flexible-link manipulator,” Proc. IEEE Conf. on Decision and Control, Spain, pp. 6841-6846, Dec. 2005.

[37] J. Kim and E. A. Croft, “Full-state tracking control for flexible joint robots with singular perturbation techniques,” IEEE Transactions on Control Systems Technology, vol. 27, no. 1, pp. 63–73, Oct 2017.

[38] A. De Luca, S. Panzieri and G. Ulivi, "Stable inversion control for flexible link manipulators", IEEE Int. Conference on Robotics and Automation, Leuven, Belgium (May, 1998) pp. 799-801.

[39] Lizarraga, I., Etxebarria, V., and Sanz, A., “Slidingmode adaptive control for flexible-link manipulators using a composite design,” Cybern. Syst., Vol. 36, No. 5, pp. 471–490 (2005).

[40] K. Lochan and B. Roy, “Control of two-link 2-dof robot manipulator using fuzzy logic techniques: A review,” in Proceedings of Fourth International Conference on Soft Computing for Problem Solving. Springer, 2015, pp. 499–511.

[41] M.W.Vandegrift,F.L.Lewis,andS.Q.Zhu,“Flexible-linkrobotarm control by a feedback linearization/singular perturbation approach,” J. Robot. Syst., vol. 11, no. 7, pp. 591–603, 1994.

[42] Arisoy, A., Gokasan, M., Bogosyan, O.S.."Partial feedback linearization control of a single flexible link robot manipulator", Proceedings of the 2nd the IEEE International Conf.on Recent Advances in Space Technologies Session Papers, RAST2005 in İstanbul, 2005, June 9-11.

[43] F.SchnelleandP.Eberhard,"Adaptivenonlinearmodelpredictivecontrol design of a flexible-link manipulator with uncertain parameters," Acta Mech. Sinica, vol. 33, no. 3, pp. 529–542, May 2017.

[44] J. C. Cambera, V. Feliu-Batlle, "Input-state feedback linearization control of a single-link flexible robot arm moving under gravity and joint friction", Robotics and Autonomous Systems, Vol. 88, pp. 24-36, 2017.

[45] M. Baroudi, M. Saad, W. Ghie, "State-feedback and Linear Quadratic Regulator Applied to a Single-link Flexible Manipulator". In: IEEE Int. Conf. Robotics and Biomimetics (ROBIO), 2009, p. 1381.

[46] Bayo E, Papadopoulos P, Stubbe J, et al. "Inverse dynamics and kinematics of multi-link elastic robots: an iterative frequency domain approach". Int J Robot Res, 1989; 8(6): 49–62.

[47] S. C. P. Gomes, V. S. da Rosa, and B. de Carvalho Albertini, “Active control to flexible manipulators,” IEEE/ASME Transactions on Mechatronics, vol. 11, no. 1, pp. 75–83, 2006.

[48] Sahinkaya, MN. . "Input shaping for vibration-free positioning of flexible systems". Journal of Systems and Control Engineering, 2001, 215.5, 467–481.

[49] Béarée Richard. "New Damped-Jerk trajectory for vibration reduction". Control Engineering Practice, 2014, 28, 112–120.

[50] Biagiotti, Luigi, et al. . "Optimal trajectories for vibration reduction based on exponential filters". IEEE Transactions on Control Systems Technology, 2015, 24.2, 609–622.

[51] Cole MOT and Wongratanaphisan T. "A direct method of adaptive FIR input shaping for motion control with zero residual vibration". IEEE/ASME T Mech 2013; 18(1): 316–327.

[52] J. Malzahn, A. S. Phung, F.Hoffmann, and T. Bertram, "Vibration control of a multi-flexible-link robot arm under gravity," IEEE International Conference on Robotics and Biomimetics, pp. 1249–1254, 2011.

[53] D Newman, J Vaughan. "Concurrent design of linear control with input shaping for a two-link flexible manipulator arm" IFAC-PapersOnLine, 51 (14) (2018), pp. 66-71.

[54] N. M. Tahir, S. M. Hassan, Z. Mohamed, A. G. Ibrahim, "Output Based input Shaping for Optimal Control of Single Link Flexible Manipulator", International Journal on Smart Sensing Intelligent Systems, Vol. 10, Issue 2, 2017, pp. 367-386.

[55] E, Trapero JR, Díaz IM, et al. "Adaptive input shaping for single-link flexible manipulators using an algebraic identification". Control Engineering Practice,2012, 20(2): 138-147.

[56] Phan V, Goo N and Park H. "Vibration suppression of a flexible robot manipulator with a lightweight piezocomposite actuator". Int J Control Autom 2009; 7(2):243–251.

[57] Xinyu, wang, et al. "Obstacle avoidance for kinematically redundant robot". IFAC-PapersOnLine, 2015, 48.28, 490–495.

[58] Khatib, Oussama. "A unified approach for motion and force control of robot manipulators: The operational space formulation". IEEE Journal on Robotics and Automation, 1987, 3.53, 43–53.

[59] Sadeghian, Hamid, et al. "Dynamic multi-priority control in redundant robotic systems". Robotica, 2013, 31.7, 1155–1167.

[60] Nakanishi, Jun, et al."Operational space control: A theoretical and empirical comparison". The International Journal of Robotics Research, 2008, 27.6, 737–757.

[61] Yue, Shigang, et al."Point-to-point trajectory planning of flexible redundant robot manipulators using genetic algorithms". Robotica, 2002, 20.3, 269–280.

[62] Nguyen, Luong A, et al."Dynamic control of flexible, kinematically redundant robot manipulators". IEEE Transactions on Robotics and Automation, 1992, 8.6, 759–767.

[63] Bian, Yushu, et al."Study on vibration reduction and mobility improvement for the flexible manipulator via redundancy resolution". Nonlinear Dynamics, 2011, 65.4, 359–368.

[64] Hirano, Daichi, et al. "Simultaneous control for endpoint motion and vibration suppression of a space robot based on simple dynamic model". IEEE International Conference on Robotics and Automation (ICRA), 2014, 6631–6637.

[65] Sasaki, Koji and Murakami, Toshiyuki."Vibration suppression control of redundant manipulator with flexible structure by considering nullspace motion". IEEJ Transactions on Industry Applications, 2007, 127, 1043–1049.

[66] Hishinuma, Toshimitsu and Nenchev, Dragomir N. "Singularity-consistent vibration suppression control with a redundant manipulator mounted on a flexible base". 2006 IEEE/RSJ International Conference on Intelligent Robots and Systems, 2006, 3237–3242.

[67] M. Sayahkarajy, Z. Mohamed and A. Faudzi, “Review of modelling and control of flexible-link manipulators,” Journal of Systems and Control Engineering, Apr. 2016.

[68] E. A. Alandoli, M. Sulaiman, and M. Rashid, “A Review Study on Flexible Link Manipulators,” J. Telecommun. Electron. Comput. Eng. Fig., vol. 8, no. 2, pp. 93–97, 2016.

[69] B. Siciliano and O. Khatib, Springer handbook of robotics. Springer, 2016.

[70] Subudhi B and Morris AS. "Dynamic modelling, simulation and control of a manipulator with flexible links and joints". Robot Auton Syst 2002; 41(4): 257–270.

[71] H. Gao, W. He, C. Zhou, and C. Sun, “Neural network control of a twolink flexible robotic manipulator using assumed mode method,” IEEE Transactions on Industrial Informatics, pp. 1–1, 2018.

[72] P. Kalra and A.M. Sharan. "Accurate modeling of flexible manipulators using finite element analysis". Mechanism and Machine Theory, 26:299–313, 1991.

[73] R. Vidoni, A. Gasparetto, and L. Scalera, “3-D ERLS based dynamic formulation for flexible-link robots: theoretical and numerical comparison between the Finite Element Method and the Component Mode Synthesis approaches,” International Journal of Mechanics and Control, 2018.

[74] Theodore, R.and Ghosal,A.,‘Comparison of the assumed modes and finite element models for flexible multi link manipulators’, The International Journal of Robotics Research 14(2), 1995, 91–111.

[75] T. Yoshikama and K. Hosoda. "Modeling of flexible manipulators using virtual rigid links and passive joints". The International Journal of Robotics Research, 15(3):290–299, 1996.

[76] D. Subedi, I. Tyapin and G. Hovland, "Modeling and Analysis of Flexible Bodies Using Lumped Parameter Method," 2020 IEEE 11th International Conference on Mechanical and Intelligent Manufacturing Technologies (ICMIMT), Cape town, South Africa, 2020, pp. 161-166.

[77] Giorgio and Del Vescovo I. Giorgio and D. Del Vescovo, “Non-linear lumped-parameter modeling of planar multi-link manipulators with highly flexible arms”, Robotics 7:4 (2018), 60.

[78] Zhu G, Ge SS, Lee TH. Simulation studies of tip tracking control of a single-link flexible robot based on a lumped model. Robotica. 1999;17:71–78.

[79] K.Lochan,B.K.Roy,andB.Subudhi,“SMCcontrolledchaotic trajectory tracking of two-link flexible manipulator with PID slidingsurface,”IFAC-PapersOnLine,vol.49,no.1,pp.219–224, 2016.

[80] Bian, Yushu and Gao, Zhihui. "Impact vibration attenuation for a flexible robotic manipulator through transfer and dissipation of energy". Shock and Vibration, 2013, 24.4, 665–680.

[81] B. Siciliano and O. Khatib, Springer handbook of robotics "chapter 13: Robots with Flexible Elements". Springer, 2016.

[82] Dulęba, I., Opałka, M."A comparison of Jacobian-based methods of inverse kinematics for serial robot manipulators". Int. J. Appl. Math. Comput. Sci. 2013, 23(2), 373–382.

[83] B. Nemec and L. Zlajpah, “Null-space velocity control with dynamicallyconsistentpseudo-inverse,”Robotica18,513–518 (2000).

[84] Park J, Choi Y, Chung WK, Youm Y "Multiple tasks kinematics using weighted pseudo-inverse for kinematically redundant manipulators". In: Proceedings. IEEE international conference on robotics and automation, Seoul, 2001, pp 4041–4047.

[85] Chang and Dubey, Chang, T. and Dubey, R."A weighted least-norm solution based scheme for avoiding joints limits for redundant manipulators. IEEE Trans. on Robotics and Automation, 1995, 11(2):286– 292.

[86] G. Marani, Jinhyun Kim, Junku Yuh, and Wan Kyun Chung."A realtime approach for singularity avoidance in resolved motion rate control of robotic manipulators". In IEEE Int. Conf. on Robotics and Automation ICRA, 2002.

[87] Da Graça Marcos M., Machado J.T. Azevedo-Perdicoulis T.-P., "A multi-objective approach for the motion planning of redundant manipulators", Applied Soft Computing, 2012, pp.589-599.

[88] F. Fahimi, H. Ashrafiuon, and C. Nataraj, “An improved inverse kinematic and velocity solution for spatial hyper-redundant robots,” IEEE Trans. on Robotics and Automation, vol. 18, no. 1, Feb. 2002, pp. 103– 107.

[89] K. Kazerounian and A. Nedungadi. Redundancy resolution of serial manipulators based on robot dynamics. Mechanism and Machine Theory, 1988, 23:295-303.

[90] Khatib, O., "Redundant Manipulators and Kinematic Singularities: The Operational Space Approach," Sixth CISM-IFToMMSymposium on Theory and Practice of Robots and Manipulators, 1986. 9-12.

[91] Ghosal, A., and Desa, S. "Dynamical Resolution of Redundancy for Robot Manipulators". Transactions of the ASME, Journal of Mechanical Design, 1993, 115.3, 592-–598.

[92] Henrich, D. and Wörn."Robot Manipulation of Deformable Objects", Advanced Manufacturing Series, Springer–Verlag, 2000, Berlin.

[93] Hou, Yew Cheong, Khairul Salleh Mohamed Sahari, and Dickson Neoh Tze How. "A review on modeling of flexible deformable object for dexterous robotic manipulation." International Journal of Advanced Robotic Systems 16.3 (2019).

[94] Sanchez, Jose, et al. "Robotic manipulation and sensing of deformable objects in domestic and industrial applications: a survey." The International Journal of Robotics Research 37.7 (2018): 688-716.

[95] Svinin, Mikhail, et al. "Motion Planning Strategies and Human Performance in the Manipulation of Underactuated Flexible Objects." 2018 IEEE International Conference on Systems, Man, and Cybernetics (SMC). IEEE, 2018.

[96] Pan, Zherong, and Dinesh Manocha. "Motion planning for fluid manipulation using simplified dynamics." 2016 IEEE/RSJ International Conference on Intelligent Robots and Systems (IROS). IEEE, 2016.

[97] Li, Yinxiao, et al. "Regrasping and unfolding of garments using predictive thin shell modeling." 2015 IEEE International Conference on Robotics and Automation (ICRA). IEEE, 2015.

[98] Li, Yinxiao, et al. "Model-driven feedforward prediction for manipulation of deformable objects." IEEE Transactions on Automation Science and Engineering 15.4 (2018).

[99] Huang, Sandy H., et al. "Leveraging appearance priors in non-rigid registration, with application to manipulation of deformable objects." 2015 IEEE/RSJ International Conference on Intelligent Robots and Systems (IROS). IEEE, 2015.

[100] Stückler, Jörg, et al. "Towards robust mobility, flexible object manipulation, and intuitive multimodal interaction for domestic service robots." Robot Soccer World Cup. Springer, Berlin, Heidelberg, 2011.

[101] Svinin, Mikhail, Igor Goncharenko, and Shigeyuki Hosoe. "Motion planning of human-like movements in the manipulation of flexible objects." Advances in Robot Control. Springer, Berlin, Heidelberg, 2006. 263-291.

[102] Aribowo, Wisnu, et al. "Input shaping control to suppress sloshing on liquid container transfer using multi-joint robot arm." 2010 IEEE/RSJ International Conference on Intelligent Robots and Systems. IEEE, 2010.

[103] Aribowo, Wisnu, Takahito Yamashita, and Kazuhiko Terashima. "Integrated trajectory planning and sloshing suppression for three-dimensional motion of liquid container transfer robot arm." Journal of Robotics 2015 (2015).

[104] Henrich, D. and Wörn. Chapter 3 "Planning and Control Strategies". Book: "Robot Manipulation of Deformable Objects", Advanced Manufacturing Series, Springer–Verlag, 2000, Berlin.

[105] Fernandez, Sebastian Rendon, Adei Olabi, and Olivier Gibaru. "Multi-Surface Admittance Control Approach applied on Robotic Assembly of Large-Scale parts in Aerospace Manufacturing." 2019 19th International Conference on Advanced Robotics (ICAR). IEEE, 2019.

[106] Dai, Changsheng, et al. "Robotic manipulation of deformable cells for orientation control." IEEE Transactions on Robotics 36.1 (2019): 271-283.

[107] Yamakawa, Yuji, Akio Namiki, and Masatoshi Ishikawa. "Motion planning for dynamic folding of a cloth with two high-speed robot hands and two high-speed sliders." 2011 IEEE International Conference on Robotics and Automation. IEEE, 2011.

[108] Yamakawa, Yuji, Akio Namiki, and Masatoshi Ishikawa. "Simple model and deformation control of a flexible rope using constant, high-speed motion of a robot arm." 2012 IEEE International Conference on Robotics and Automation. IEEE, 2012.

[109] Fanson, Richard, and Alexandru Patriciu. "Model based deformable object manipulation using linear robust output regulation." 2010 IEEE/RSJ International Conference on Intelligent Robots and Systems. IEEE, 2010.

[110] Yue, Shigang, and Dominik Henrich. "Manipulating deformable linear objects: fuzzy-based active vibration damping skill." Journal of Intelligent and Robotic Systems 46.3 (2006): 201-219.

[111] Wada, Takahiro, et al. "Modeling of hysteresis in deformation of rodlike objects toward their manipulation." Proceedings. 2000 IEEE/RSJ International Conference on Intelligent Robots and Systems (IROS 2000)(Cat. No. 00CH37113). Vol. 1. IEEE, 2000.

[112] Ding, Feng, et al. "Vibration damping in manipulation of deformable linear objects using sliding mode control." Advanced Robotics 28.3 (2014): 157-172.

[113] Donner, Philine, et al. "Cooperative dynamic manipulation of unknown flexible objects." International Journal of Social Robotics 9.4 (2017): 575-599.

[114] Yoshida, Eiichi, et al. "Simulation-based optimal motion planning for deformable object." 2015 IEEE International Workshop on Advanced Robotics and its Social Impacts (ARSO). IEEE, 2015.

[115] Sun, Dong, Yunhui Liu, and James K. Mills. "Cooperative control of a two-manipulator system handling a general flexible object." Proceedings of the 1997 IEEE/RSJ International Conference on Intelligent Robot and Systems. Innovative Robotics for Real-World Applications. IROS'97. Vol. 1. IEEE, 1997.

[116] Kawaharazuka, Kento, et al. "Dynamic manipulation of flexible objects with torque sequence using a deep neural network." 2019 International Conference on Robotics and Automation (ICRA). IEEE, 2019.

[117] Cherubini, Andrea, et al. "Towards vision-based manipulation of plastic materials." 2018 IEEE/RSJ International Conference on Intelligent Robots and Systems (IROS). IEEE, 2018.

[118] Chi, Cheng, and Dmitry Berenson. "Occlusion-robust deformable object tracking without physics simulation." 2019 IEEE/RSJ International Conference on Intelligent Robots and Systems (IROS). IEEE, 2019.

[119] Yan, Mengyuan, et al. "Self-Supervised Learning of State Estimation for Manipulating Deformable Linear Objects." IEEE Robotics and Automation Letters 5.2 (2020): 2372-2379.

[120] McConachie, Dale, et al. "Learning When to Trust a Dynamics Model for Planning in Reduced State Spaces." IEEE Robotics and Automation Letters 5.2 (2020): 3540-3547.

[121] Kicki, Piotr, Michał Bednarek, and Krzysztof Walas. "Measuring bending angle and hallucinating shape of elongated deformable objects." 2018 IEEE-RAS 18th International Conference on Humanoid Robots (Humanoids). IEEE, 2018.

[122] Howard, Ayanna M., and George A. Bekey. "Intelligent learning for deformable object manipulation." Autonomous Robots 9.1 (2000): 51-58.

[123] Hu, Zhe, Peigen Sun, and Jia Pan. "Three-dimensional deformable object manipulation using fast online Gaussian process regression." IEEE Robotics and Automation Letters 3.2 (2018): 979-986.

[124] Bednarek, Michał, and Krzysztof Walas. "Comparative Assessment of Reinforcement Learning Algorithms in the Taskof Robotic Manipulation of Deformable Linear Objects." 2019 4th International Conference on Robotics and Automation Engineering (ICRAE). IEEE, 2019.

[125] Han, Haifeng, Gavin Paul, and Takamitsu Matsubara. "Model-based reinforcement learning approach for deformable linear object manipulation." 2017 13th IEEE Conference on Automation Science and Engineering (CASE). IEEE, 2017.

[126] Hu, Zhe, et al. "3-D deformable object manipulation using deep neural networks." IEEE Robotics and Automation Letters 4.4 (2019): 4255-4261.

[127] Hou, Yew Cheong, Khairul Salleh Mohamed Sahari, and Dickson Neoh Tze How. "Modeling of flexible deformable object for robotic manipulation." 2016 IEEE International Symposium on Robotics and Intelligent Sensors (IRIS). IEEE, 2016.

[128] Tan, Qingyang, et al. "Realtime simulation of thin-shell deformable materials using CNN-based mesh embedding." IEEE Robotics and Automation Letters 5.2 (2020): 2325-2332.

[129] Caldwell, Timothy M., Dave Coleman, and Nikolaus Correll. "Robotic manipulation for identification of flexible objects." Experimental Robotics. Springer, Cham, 2016.

[130] Bodenhagen, Leon, et al. "An adaptable robot vision system performing manipulation actions with flexible objects." IEEE transactions on automation science and engineering 11.3 (2014): 749-765.

[131] Costanzo, Marco, et al. "Motion Planning and Reactive Control Algorithms for Object Manipulation in Uncertain Conditions." Robotics 7.4 (2018): 76.

[132] Frank, Barbara, et al. "Learning object deformation models for robot motion planning." Robotics and Autonomous Systems 62.8 (2014): 1153-1174.

[133] Biagiotti, Luigi, and Claudio Melchiorri. Trajectory planning for automatic machines and robots. Springer Science Business Media, 2008.

[134] Matsuno, Takayuki, and Toshio Fukuda. "Manipulation of flexible rope using topological model based on sensor information." 2006 IEEE/RSJ International Conference on Intelligent Robots and Systems. IEEE, 2006.

[135] Wang, He, and Taku Komura. "Manipulation of flexible objects by geodesic control." Computer Graphics Forum. Vol. 31. No. 2pt2. Oxford, UK: Blackwell Publishing Ltd, 2012.

[136] Kapsalas, C. N., et al. "An ARX-based method for the vibration control of flexible beams manipulated by industrial robots." Robotics and Computer-Integrated Manufacturing 52 (2018): 76-91.

[137] Ito, Koichiro, Yuji Yamakawa, and Masatoshi Ishikawa. "Winding manipulator based on high-speed visual feedback control." 2017 IEEE Conference on Control Technology and Applications (CCTA). IEEE, 2017.

[138] Singhose, William, and L. Pao. "A comparison of input shaping and time-optimal flexible-body control." Control Engineering Practice 5.4 (1997): 459-467.

[139] Moriello, Lorenzo, et al. "Manipulating liquids with robots: A sloshing-free solution." Control Engineering Practice 78 (2018): 129-141.

[140] Chen, Suei Jen, Bjorn Hein, and Heinz Worn. "Using acceleration compensation to reduce liquid surface oscillation during a high speed transfer." Proceedings 2007 IEEE International Conference on Robotics and Automation. IEEE, 2007.

[141] Feddema, John T., et al. "Control for slosh-free motion of an open container." IEEE Control Systems Magazine 17.1 (1997): 29-36.

[142] Ata, ATEF A. "Optimal trajectory planning of manipulators: a review." Journal of Engineering Science and technology 2.1 (2007): 32-54.

[143] Constantinescu, Daniela, and Elizabeth A. Croft. "Smooth and time-optimal trajectory planning for industrial manipulators along specified paths." Journal of robotic systems 17.5 (2000): 233-249.

[144] Boryga, M., and A. Graboś. "Planning of manipulator motion trajectory with higher-degree polynomials use." Mechanism and machine theory 44.7 (2009): 1400-1419.

[145] Xiao, Yongqiang, Zhijiang Du, and Wei Dong. "Smooth and near time-optimal trajectory planning of industrial robots for online applications." Industrial Robot: An International Journal (2012).

[146] Guan, Yishen, et al. "On robotic trajectory planning using polynomial interpolations." 2005 IEEE International Conference on Robotics and Biomimetics-ROBIO. IEEE, 2005.

[147] Perumaal, Saravana, and Natarajan Jawahar. "Synchronized trigonometric S-curve trajectory for jerk-bounded time-optimal pick and place operation." International Journal of Robotics and Automation 27.4 (2012): 385.

[148] Simon, Dan, and Can Isik. "A trigonometric trajectory generator for robotic arms." International Journal of Control 57.3 (1993): 505-517.

[149] Simon, Dan, and Can Isik. "Optimal trigonometric robot joint trajectories." Robotica 9.4 (1991): 379-386.

[150] Nguyen, Kim Doang, I-Ming Chen, and Teck-Chew Ng. "Planning algorithms for s-curve trajectories." 2007 IEEE/ASME international conference on advanced intelligent mechatronics. IEEE, 2007.

[151] Chen, Chaobin, Haichen Qin, and Zhouping Yin. "Trajectory planning for omnidirectional mobile robot based on Bezier curve, trigonometric function and polynomial." International Conference on Intelligent Robotics and Applications. Springer, Berlin, Heidelberg, 2012.

[152] Visioli, Antonio. "Trajectory planning of robot manipulators by using algebraic and trigonometric splines." Robotica 18.6 (2000): 611-631.

[153] Chiddarwar, Shital S., and N. Ramesh Babu. "Optimal trajectory planning for industrial robot along a specified path with payload constraint using trigonometric splines." International Journal of Automation and Control 6.1 (2012): 39-65.

[154] Gasparetto, Alessandro, and V. Zanotto. "A new method for smooth trajectory planning of robot manipulators." Mechanism and machine theory 42.4 (2007): 455-471.

[155] Saravanan, R., S. Ramabalan, and C. Balamurugan. "Evolutionary optimal trajectory planning for industrial robot with payload constraints." The International Journal of Advanced Manufacturing Technology 38.11-12 (2008): 1213-1226.

[156] Gasparetto, Alessandro, and Vanni Zanotto. "Optimal trajectory planning for industrial robots." Advances in Engineering Software 41.4 (2010): 548-556.

[157] Lanzutti, Albano. "Smooth Trajectory Planning Algorithms for Industrial Robots: An Experimental Evaluation." Annals of the Faculty of Engineering Hunedoara 9.1 (2011): 127.

[158] Ali, Sari Abdo, Khalil Azha Mohd Annuar, and Muhammad Fahmi Miskon. "Trajectory planning for exoskeleton robot by using cubic and quintic polynomial equation." International Journal of Applied Engineering Research 11.13 (2016): 7943-7946.

[159] Piazzi, Aurelio, and Antonio Visioli. "Global minimum-jerk trajectory planning of robot manipulators." IEEE transactions on industrial electronics 47.1 (2000): 140-149.

[160] Gosselin, C. M., and A. Hadj-Messaoud. "Automatic planning of smooth trajectories for pick-and-place operations." (1993): 450-456.

[161] Chettibi, Taha. "Smooth point-to-point trajectory planning for robot manipulators by using radial basis functions." Robotica 37.3 (2019): 539-559.

[162] Gasparetto, Alessandro, et al. "Path planning and trajectory planning algorithms: A general overview." Motion and operation planning of robotic systems. Springer, Cham, 2015. 3-27.

[163] Saravanan, R., S. Ramabalan, and C. Balamurugan. "Evolutionary optimal trajectory planning for industrial robot with payload constraints." The International Journal of Advanced Manufacturing Technology 38.11-12 (2008): 1213-1226.

[164] Béarée, Richard. Prise en compte des phénomènes vibratoires dans la génération de commande des machines-outils à dynamique élevée. Diss. Paris, ENSAM, 2005.

[165] Biagiotti, Luigi, and Claudio Melchiorri. Trajectory planning for automatic machines and robots. Springer Science Business Media, 2008.

[166] Biagiotti, Luigi, and Claudio Melchiorri. "FIR filters for online trajectory planning with time-and frequency-domain specifications." Control Engineering Practice 20.12 (2012): 1385-1399.

[167] Béarée, Richard, and Adel Olabi. "Dissociated jerk-limited trajectory applied to time-varying vibration reduction." Robotics and Computer-Integrated Manufacturing 29.2 (2013): 444-453.

[168] Besset, Pierre, and Richard Béarée. "FIR filter-based online jerk-constrained trajectory generation." Control Engineering Practice 66 (2017): 169-180.

[169] Peng, D-W., T. Singh, and M. Milano. "Zero-phase velocity tracking of vibratory systems." Control Engineering Practice 40 (2015): 93-101.

[170] Kamel, Amine, Friedrich Lange, and Gerd Hirzinger. "New aspects of input shaping control to damp oscillations of a compliant force sensor." 2008 IEEE International Conference on Robotics and Automation. IEEE, 2008.

[171] Brock, Stefan. "Influence of filters for numerical differentiation on parameter tuning of PI speed controllers." Przeglad Elektrotechniczny 5.2018 (2018): 60-64.

[172] Brunot, Mathieu. "Comparison of Numerical Differentiation Techniques for Aircraft Identification." Journal of Aerospace Engineering 32.5 (2019): 06019002.

[173] Biagiotti, Luigi, and Claudio Melchiorri. "Zero-phase velocity tracking of vibratory systems with actuation constraints." Control Engineering Practice 87 (2019): 1-16.